University of Cape Town

Department of Mechanical Engineering

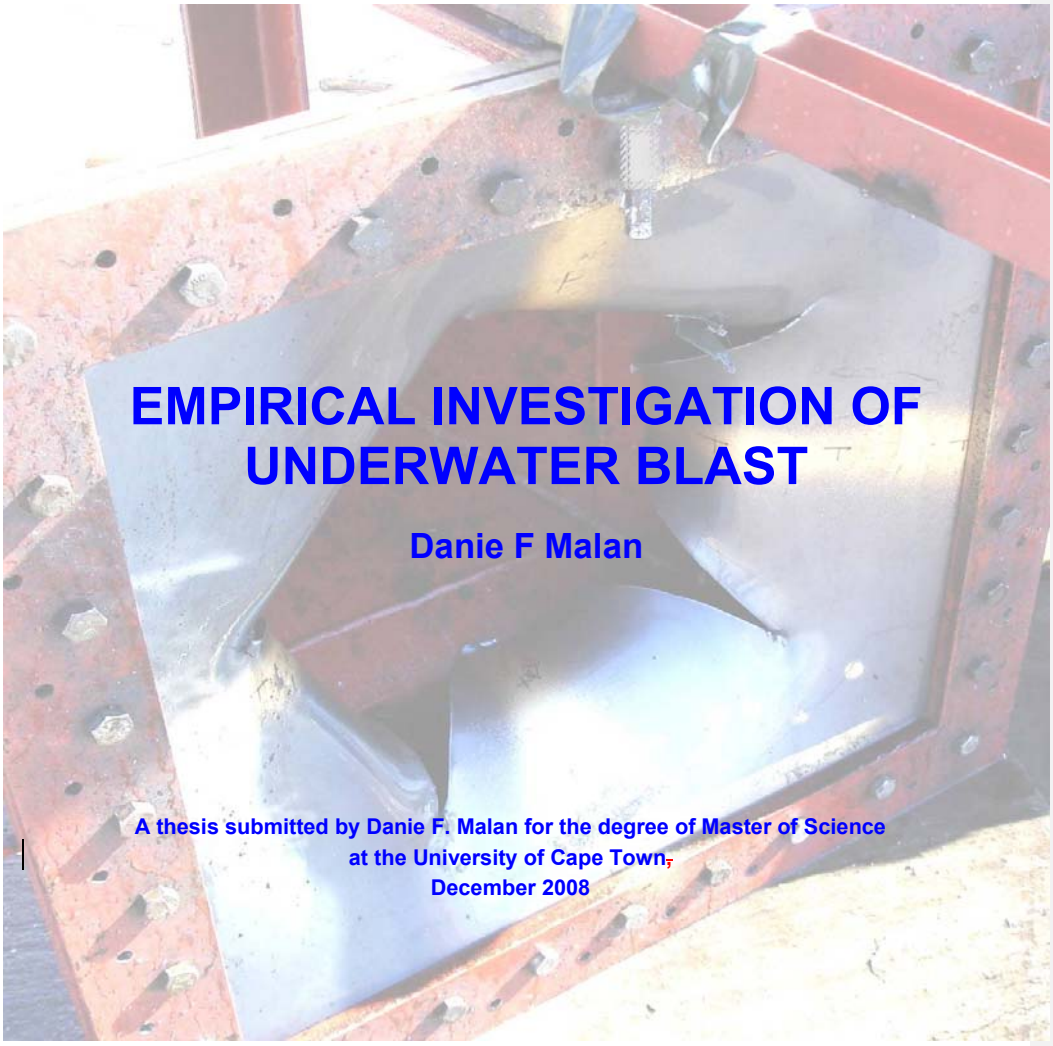

EMPIRICAL INVESTIGATION OF UNDERWATER BLAST

Danie F Malan

A thesis submitted by Danie F. Malan for the degree of Master of Science
at the University of Cape Town,
December 2008

BISRU

BLAST IMPACT AND SURVIVABILITY RESEARCH UNIT

ACKNOWLEDGEMENTS

Prof Gerald Nurick of BISRU

for his encouragement, mentorship, support and patience

Mr Andre Roux

for his encouragement and assistance during field testing

CSIR

for financial support that enabled this dissertation

Lt Col Fielies du Toit and his Team

for performing the demolition work with great enthusiasm

BISRU, in particular Dr Genevieve Langdon, Mr Vic Balden,
Dr Steeve Chung and Mr Gareth Erfort
for their technical assistance and encouragement

Dr Frikkie Mostert

for useful discussions, comments and guidance

STATEMENT

All material contained in this dissertation has never been presented for the award of any other degree, diploma or such qualification at any institution.

I understand the meaning of plagiarism and declare that, to the best of my knowledge and belief, this dissertation contains no material previously written or published by another person, except where due reference and acknowledgement is made.

Danie F. Malan

SYNOPSIS

Background

Most demolition practitioners seem to accept that an explosive charge is placed in direct contact with the target surface. Placing the charge in this way may be very convenient, but from an under water demolition point of view, this may not be the most effective placement. It should be noted that an underwater charge can be used in two distinctly different types of application against a target – a large charge at a distance from the target (eg a torpedo) or a small charge in direct contact (eg demolition charge or limpet mine). In the first type of application a very large charge is detonated at a relatively large offset distance (typically 500kg at 10 meters or more). This type of application relies on extensive damage to and subsequent disruption of equipment on board a ship. The second type of application involves a small charge (typically 10 to 50kg) in direct contact with the target. The effect of this type of application is very localised and very severe, causing flooding and/or local structural failure.

The work of this dissertation focuses on the second type of application which is a relatively small charge in contact or at very close offset distance (as opposed to a large charge at a large distance).

It is often stated by experienced users in underwater explosions, that the damage caused by an underwater explosion is greater when the close proximity charge is physically slightly offset from the target surface. At the same time, none of these users could offer any specific rule or guideline that can be used to determine the optimum offset distance for any given charge or target. Most demolition users believe that a contact charge is the best way. In addition, they follow a rule of thumb: “If in doubt, double the charge”.

An important tendency of modern demolition work is to achieve better results with a smaller charge by improving the efficiency of the application. This implies either a better result with the same charge mass or the required effect with a smaller charge mass. If the demolition objective is well defined, the mass of explosive can be minimised. This would save cost and, in case of man-carried munition, save effort by the carrier.

The principles, phenomena and effects of demolition in an air environment are very different from demolition under water. A principle difference is that a submerged detonation creates a pulsating gas bubble. Such a bubble is absent in an explosion in air. This thesis is focused on underwater detonations.

It is well known that about half of the energy of an underwater detonation is transferred to the gas bubble (see Figure A), therefore it is fair to assume that the gas bubble associated with an underwater detonation should cause significant damage to a target (over and above the effect of the shock impulse). This “significant damage” is a term that is usually used in a casual way and is hardly ever quantified.

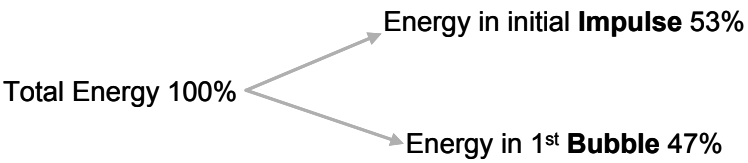

** source: Swisdak [11] and others*

Figure A: Detonation energy split between Shock Impulse and Bubble

A contentious issue is the definition of “better results”. It is important to keep in mind that “better results” is very dependant on the specific application. Generally, blowing a hole in a wall or ship hull usually is a required result in which case a larger hole (greater area) would be considered a better result. In contrast, demolition work such as clearing of underwater obstructions would require cutting or shattering of the target and not holing at all.

The question "What is the best result" and an implied question "What is the optimum offset distance for a given charge" prompted the work that is reported in this dissertation.

The work in this dissertation would focus on

a) detonation under water

b) small distance between charge and target,

c) holing of the target (as opposed to shattering or cutting)

Rationale

All forces that act on a submerged target surface originate from two characteristics of a submerged detonation – the initial pressure shock wave, followed by the effect of the expanding gaseous detonation products. The shock wave is characterised by very high pressure and very short duration (typical in the order of micro seconds). The expanding gas bubble that follows after the shock impulse grows and collapses (in the order of milliseconds). The collapse of the gas bubble causes a second pressure impulse, albeit of substantially lower amplitude.

During detonation the shock wave travels through the explosive at VOD (velocity of detonation) until it reaches the boundary of the explosive. As soon as the shock wave enters the water it gradually slows to the acoustic speed of sound in water. In water the shock wave is followed by the spherical expanding bubble of gas from the decomposed explosive material. The maximum velocity of the periphery of the growing gas bubble travels at less than half the acoustic speed of sound in water. This implies that the shock impulse reaches the target a relatively long time before the effect of the expanding bubble reaches the target.

If the detonation occurs close to the target (within maximum bubble radius), the development of the gas bubble is proportionately impeded by the presence of the target surface. Assuming that some water exists between the detonating charge and the target surface, the bubble should develop to at least a certain degree (ie impeded towards the target but not suppressed).

Whether the gas bubble develops partly or fully, the shock impulse due to the detonation reaches the target relatively long before the boundary of the expanding gas bubble. This difference in time of arrival of the two (approximate) halves of the explosive energy is illustrated in Figure B. The vertical axis represents the distance from the detonation and the horizontal axis represents the time from detonation until the time that the gas bubble has developed fully. The target in the figure is shown at a distance slightly less than the maximum bubble radius from the detonation. Note that the shock wave reaches the target surface long before the surface of the expanding bubble ($T_{shock} << T_{bubble}$).

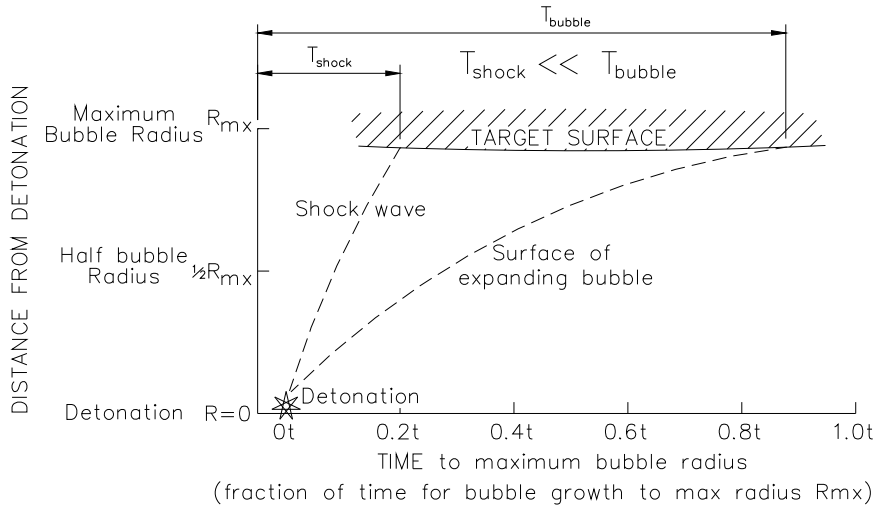

Figure B: Shock wave reaches the target long before the expanding bubble

The pressure impulse (integral of pressure over duration) is widely used to quantify/define/measure the ~~energy/~~strength of a pressure pulse. The target is breached when the local dynamic strain exceeds the threshold value of the material under impact. This occurs typically due to the initial pressure impulse. If the effect of the bubble can be applied such that the initial strain (rupturing) of the target is maintained longer, the hole should be larger. By definition then, the efficiency of the charge is increased. The difference in time of arrival, as illustrated in Figure B, could enable optimisation of the offset distance for maximum hole-size.

The initial pressure impulse is attenuated by any water that may be between the detonating charge and the target surface. Therefore the initial pressure impulse is most effective when in direct contact with the target. As the distance between the detonation and the target surface increases, the effect of the shock impulse decreases due to increased attenuation

and losses. The holing of the target progressively diminishes accordingly and a distance is reached where the target is not breached (holed) because the shock impulse has become too weak. Beyond this distance only plastic deformation occurs.

The damage potential of the gas bubble is an opposite function of distance from the target. The development of the gas bubble is impeded close to the target. As the distance from the target increases, the gas bubble can develop more fully and therefore (presumably) contribute more to the damage of the target. The gas bubble is formed at the moment of the detonation and grows spherically into the surrounding water at a predictable rate, to a predictable size and then collapses onto itself, creating another pressure impulse. This cycle can repeat itself a number of times, in diminishing magnitude.

If it can be proven that the gas bubble contributes to enlarging the hole in the target, and that the bubble needs to have a non-zero offset distance in order to have maximum effect on the target, then it follows that it should be possible to find an optimum (non-zero) offset distance in which the combined effect is larger than having the charge in direct contact with the target.

This thesis is an attempt to prove (or disprove) that such a non-zero optimum offset distance exists.

LAYOUT OF THIS DISSERTATION

Chapter 1

The first chapter describes the aim of this thesis and elaborates on some of the history that lead up to this work.

Chapter 2

The second chapter presents the principle literature review. It discusses all related published information that could be found.

Chapter 3

This chapter discusses the principles and phenomena associated with an underwater detonation.

The hypothesis upon which the work for this thesis is based is stated, explained and discussed.

Chapter 4

The fourth chapter is an analysis of what is required to prove (or disprove) the hypothesis as stated in chapter 3.

The planning and preparation for the field work is discussed.

Chapter 5

This chapter describes the actual field work and presents the results as obtained in the field work.

Chapter 6

In chapter 6 the results of the field work are analysed and discussed at length.

Appendices

The Appendices contain all reference information that may be needed to clarify specific aspects mentioned in the text of the dissertation.

TABLE OF CONTENTS

FIGURES

TABLES

ABBREVIATIONS AND ACRONYMS

BISRU	Blast Impact and Survivability Research Unit
CSIR	Council for Scientific and Industrial Research
COD	Core Offset Distance (mm)
CODR	Core Offset Distance Ratio (dimensionless)
D	depth below surface (m)
D_e	Effective diameter (diameter of sphere, representing mass of the charge)
E	Energy (Joule or Nm)
FOI	Scandinavian Research Institute
ft	feet
g	gram
h	thickness
Hz	Hertz
I	Impulse (Ns)
I_A	Impulse per unit area (Ns/m^2)
m	metre
mm	millimetre
MPa	Mega Pascal
NEC	Nett Explosive Content (gram or kg)
NSWC	Naval Surface Weapons Centre (USA)
OD	Offset Distance (mm)
ODR	Offset Distance Ratio (dimensionless)
PE4, HBX, RDX, TNT, HNS	Formulations of explosives
psi	pounds per square inch
R, S, r, s	distance (m)
R_e	Effective Radius (= $D_e/2$)
R_{mx}	Maximum Radius (typically maximum radius of expanded gas bubble)
SF	Shock Factor (dimensionless)
sec	seconds
t	time
t_R	Time to reach maximum radius (sec)

UCT	University of Cape Town
UNDEX	Underwater Explosion (used as a generic term)
v	velocity (m/s)
VOD	Velocity of detonation (m/s)
vs	versus
W	equivalent TNT mass (kg)
x_a	Inverse mass number
ε	strain (m/m)
η	coupling factor
θ	Decay constant (sec)
ρ	density (kg/m^3)

1 CHAPTER 1: BACKGROUND AND AIM OF THIS THESIS

1.1 Background

It has long been known that a submerged explosion causes significantly more damage to objects (targets) in the water than the same mass of explosive in air. This is due to two principle characteristics that ~~is~~ are absent in detonations in air – firstly the water is incompressible and secondly the underwater detonation products (gas) is trapped inside an expanding gas bubble that contains significant destructive energy.

An explosive charge is usually placed tight against the target or is shaped to fit the contours of the target. This appears to be most sensible because the transfer of the detonation shock energy from the charge to the target is direct, be it in air or in water.

In both instances the gaseous product formed due to the decomposition of the explosive material expands at a very high rate. In air this volume of gas continues to expand until it dissipates into the free air. In water this volume of gas behaves quite differently. The gas bubble in water expands at a rapid rate, pushing water outward along the boundary of the spherical gas bubble. At a predictable diameter, the static pressure of the surrounding water overcomes the pressure inside the gas bubble and forces the bubble to collapse onto itself, releasing a second shock wave into the water.

An ~~anomaly~~ incongruity seems to exist – the charge needs to be against the target in order to maximise the effect of the shock impulse (representing one half of the detonation energy, see Figure A, page 5). At the same time, the bubble needs to be in free water to ensure full development and, by implication, full utilisation of the second half of the detonation energy.

This MSc was initiated in order to find an answer to this question: what is the optimum offset distance for an underwater charge to maximise holing of air backed underwater target.

1.2 Aim of the thesis

Establish some kind of guide regarding the following questions:

a) Is a given charge more effective when offset rather than in contact with the target?

b) If so, what is the optimum offset distance?

c) Is it possible/reliable to scale this optimum distance as function of charge mass and of target thickness.

1.3 Activities

Overview

A brief overview of the physical field testing is given here in order to assist the reader.

After designing the field trials and the test equipment, a series of exploratory detonations was conducted. The results of these first tests were of little use due to deformation of the

test housing. The results of these tests are not used in the dissertation. They are described (for information only), in Appendix D.

After the exploratory tests on 3mm plate, the test housing was reinforced and a new set of tests was performed. This set of tests is named "Group 1". This test series (also on 3mm plates) started with a large offset distance and the offset distance was reduced for each subsequent detonation. The result of this group of tests was not useful because only plastic deformation occurred. Holing (breeching) of the target panel is a required result for the purpose of this dissertation (reason: the size of the hole needs to be maximised).

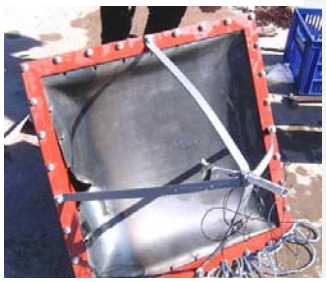

Image from Group 1 tests

The Group 2 tests on 3mm plate followed, with the main emphasis on detonating the same charge at same offset distance in different orientations (eg near the surface, deeply submerged, face up, face down etc.). This was an effort in trying to physically separate the effect of the shock impulse from the effects of the bubble. This effort proved that it was not practical to try and separate these two effects by physical orientation of the test housing

Arrangements from Group 2

Group 3 tests consisted of four test series (named 3a, 3b, 3c and 3d), each performed on a separate day. Each of these series started at zero offset (contact), increasing the offset distance until holing (breeching) of the target ceased. Plate thickness was 3mm.

Examples from Group 3

Group 4 test was a single series of tests on a thinner test panel (1.2mm instead of 3mm). As with the previous tests, detonation started at zero offset (contact), increasing the offset distance until holing (breeching) of the target ceased.

Examples from Group 4

Basic Requirement

The basic requirement of the testing was to subject an air-backed target surface (steel sheet) to an underwater blast. A test-housing (see Figure 1-1~~Figure 1-1~~~~Figure 1-1~~ and Figure 4-1~~Figure 4-1~~~~Figure 4-1~~) was designed and constructed for these tests. A replaceable faceplate was clamped to the test housing and subjected to a controlled underwater blast (30g of PE4 was manually detonated). The faceplate was then removed and analysed.

Specific variables were controlled in order to isolate the effect of specific parameters.

Three variable parameters were addressed:

(i) Distance between charge and target surface ('offset distance')

(ii) Depth below water surface

(iii) Orientation of the test piece (face up/down/sideways)

Parameters that remained constant were:

(i) Mass, shape and orientation of the charge

(ii) Initiation geometry

(iii) Thickness, size, material and fixing of the faceplate

The initial field testing was *aimed at separating the effect of the shock impulse from the effect of the bubble*. It was reasoned that, after the shock impulse, the *collapsing* gas bubble was the major contributor to the damage on the target. The collapse of the bubble occurred a long time *after* the shock impulse has passed the target. This was another reason why it was thought that the effect of the shock impulse and the gas bubble could be separated using the technique as shown in Figure 1-1~~Figure 1-1~~~~Figure 1-1~~.

During the initial testing, the orientation of the submerged target was changed from facing up and facing down, very near the surface (forced venting of the bubble) and submerged deeper than the bubble diameter. The reasoning was that near the surface, facing up, the bubble could not develop due to venting. In this way, it was thought, the effect of the bubble could be eliminated. This is illustrated in Figure 1-1~~Figure 1-1~~~~Figure 1-1~~.

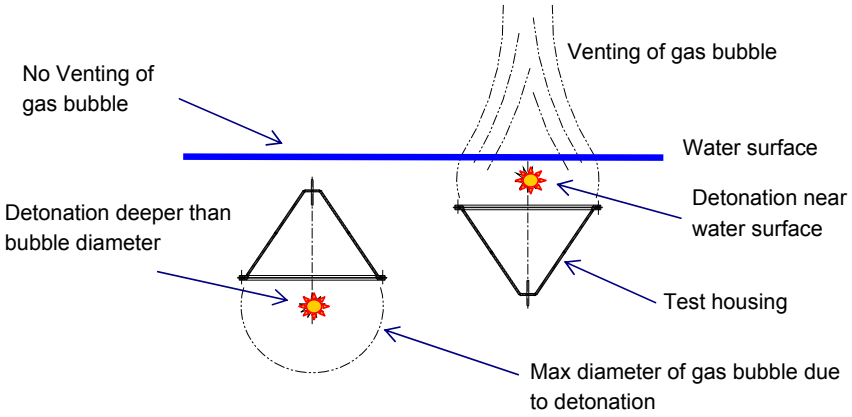

Figure 1-1: Detonation when fully submerged vs near water surface

The same charge size and offset distance was used with the target submerged, facing down, to ensure that the bubble would fully develop and contribute its full effect to the damage of the target. In this way, it was reasoned, the combined effect of the impulse plus bubble could be compared to the effect of the shock impulse alone.

Surprisingly, the resultant damage to the target was very similar for the two cases, indicating that this technique cannot be used to clearly distinguish between the effect of the shock wave and the added effect of bubble.

This indicated that there was an important effect that was linked to the initial stages of the development of the gas bubble.

After re-considering and re-planning the field testing, it was decided to investigate the combined effect of shock and bubble (ie not separating the effects). An attempt shall also be made to find the reason why it is difficult to demonstrate the damage due to shock impulse and damage due to bubble separately as attempted in Figure 1-1~~Figure 1-1~~~~Figure 1-1~~.

2 CHAPTER 2: LITERATURE STUDY

This chapter is a review of literature that is of general relevance to this dissertation.

Chapter 2 is divided into three subsections. The first subsection is a review of publications representing the historical progress in the field of underwater detonation research.

The second subsection mentions the publications that are generally regarded as defining work in the field of underwater detonation research. These publications are referred to and discussed in more detail throughout the dissertation.

The third subsection briefly discusses the papers and publications that are directly relevant to this dissertation. Detail discussion of these publications can be found in Chapter 3.

2.1 History of related research

A new dimension in naval warfare started when it was realised that explosions under water was possible and that such explosions caused exceptional damage to submerged structures. Keil [1] reports that systematic explosion tests against ships started in 1860. Scientific studies of the phenomena of an underwater explosion commenced many years later. This relatively late start of systematic scientific studies (relative to progress in other disciplines related to explosives) was due to three important technical constraints – the initial absence of instruments that could reliably measure the peak pressure and duration of the shock impulse, the absence of photographic equipment that could capture images at a sufficiently high rate and the late arrival of computer capability for the mathematical simulation of the phenomena.

Research on most aspects of underwater explosions was generally funded by military or governmental institutions. The result was that publications on many aspects of the research work was treated as classified information and subsequently such publications were either never published or released for publication many years later.

Von Neumann and Shapiro [2] as well as Keil [1] refers to work that was done by Hilliar at the British Admiralty as early as 1919. The title of Hilliar's work "*Experiments on the Pressure Wave thrown out by Submarine Explosions*" indicates that the work is focused on the shock wave. Analysis of the bubble is not presented. Benjamin and Ellis [3] refer to the "implosion mechanism" demonstrated by Rayleigh in 1917.

The First World War accelerated the research into underwater explosions. By 1940 the pressure-time curve of an underwater explosion could be measured Penney [4] and the development of the theory of the gas bubble started in 1941 Aarons [5].

G.I. Taylor was a very well known researcher at the time during and after the Second World War. His contribution towards many scientific disciplines, amongst others UNDEX, is collated in an autobiography by Batchelor [6]. Taylor and his fellow researchers is said to have realised that knowledge of blast waves propagating under water was just as meagre as blast waves in air (ca 1940). He is described as having an uncanny knack to explain seemingly complex phenomena by apt assumptions and simple mathematics. It is interesting to note that he and fellow scientists in 1950, Penney and Taylor [7], made no mention of the defining publication by Cole [8] during a (published) discussion on underwater detonation. A number of Taylor's papers were perused during the research for this dissertation, yet none of these papers related specifically to underwater detonations.

Since 1940 the phenomena associated with an underwater explosion have been

extensively studied and by 1948 the main features were well understood. When a charge of high explosive is detonated under water, the explosive is immediately converted to gas under very high pressure. Part of the explosive energy is transmitted into the surrounding water as a shock wave moving at very high velocity. The shock wave is followed by the much slower boundary of expanding gaseous combustion products that forms an expanding bubble. The expansion of the gas bubble continues until the pressure inside the bubble drops to equal and slightly below the hydrostatic pressure of the surrounding water. At this point the excess pressure outside the expanded gas bubble causes it to contract and collapse onto itself.

The theory and mathematical representation of the major phenomena approached maturity after 1945. The research effort of the Second World War maintained momentum after the war. A defining publication in book form was released in 1948 by Cole [8]. This book is based on research done by various groups between 1941 and 1946. It addresses all aspects of an underwater explosion in both empirical as well as mathematical terms. A large proportion of the mathematical relations were developed from first principles. The research teams that contributed to this book laid a foundation that has withstood the test of time. Modern research confirmed their work as intrinsically sound and can only manage to refine the basic mathematical relations presented by them. Cole's work is discussed in more detail later in this dissertation.

Von Neumann and Shapiro [2] discussed the principal phenomena which are expected to be of importance in the underwater explosion of a nuclear bomb (equivalent to 22000 tons TNT). A comment by [2] may be important in this dissertation:

> "If the pressure pulse lasts longer than the natural period of the target, the blast acts essentially as a static pressure and therefore the peak pressure alone is relevant - otherwise the duration of the pulse and indeed the detailed structure of the pressure-time curve must also be considered."

Measuring the peak pressure was difficult in 1954, as stated in a publication by Arons [9]. He noted that the sensitivity of the recording instruments was such that it was necessary to use increasingly larger size tourmaline gauges with increasing distance from the charge in order to maintain adequate signal strength. A second restriction was that the rise time of the sensors were too slow. A slow response time would cause the sensor to register a peak value that is less than the true peak value. The time that the shock wave took to travel through the thickness of the sensing element caused a slope in the recorded rise time of the shock wave pressure. As the sensors became physically smaller, the recorded rise time became shorter, yielding a more realistic representation of the actual pressure profile of the shock wave.

Snay [10] presented a paper at a symposium of hydrodynamics in 1957. The paper was a survey of recent findings at that time about various topics related to underwater explosions. The characteristics of the shock wave when travelling over long distance was treated, the shape of a migrating (rising) bubble, the spray dome and reloading of an air backed plate was presented. He noted that very little was known about the mechanism of the forming of spray plumes (a column of water rising above the surface following a detonation at shallow depth). In research of later years this phenomenon is explained by the toroidal collapse of the bubble.

From 1960 onwards there was a marked increase in the number of papers related to underwater explosions and associated shock wave and bubble phenomena. The publications dated 1960 to 1965 seem to focus on the measurement of the peak pressure

and phenomena associated with the shock wave. Mathematical modelling of underwater explosion phenomena, especially the collapse of the bubble started to appear in the later years.

It is interesting that practically all publications up to 1965 originate from USA. Publications from European researchers started to appear from 1966. At the same time, the focus of the publications started to move away from physical measurement and concentrated more on mathematical aspects.

Keil [1] published a paper in 1961 on the various phases of an underwater explosion and the effect on target ships. At the time of his work, finite element mathematical analysis was not available. Useful nomograms from the U.S. Naval Ordnance Laboratory are included in this publication. Similar nomograms are presented in an extensive technical report by the NSWC [11] (see example in Figure 2-1~~Figure 2-1~~~~Figure 2-1~~)

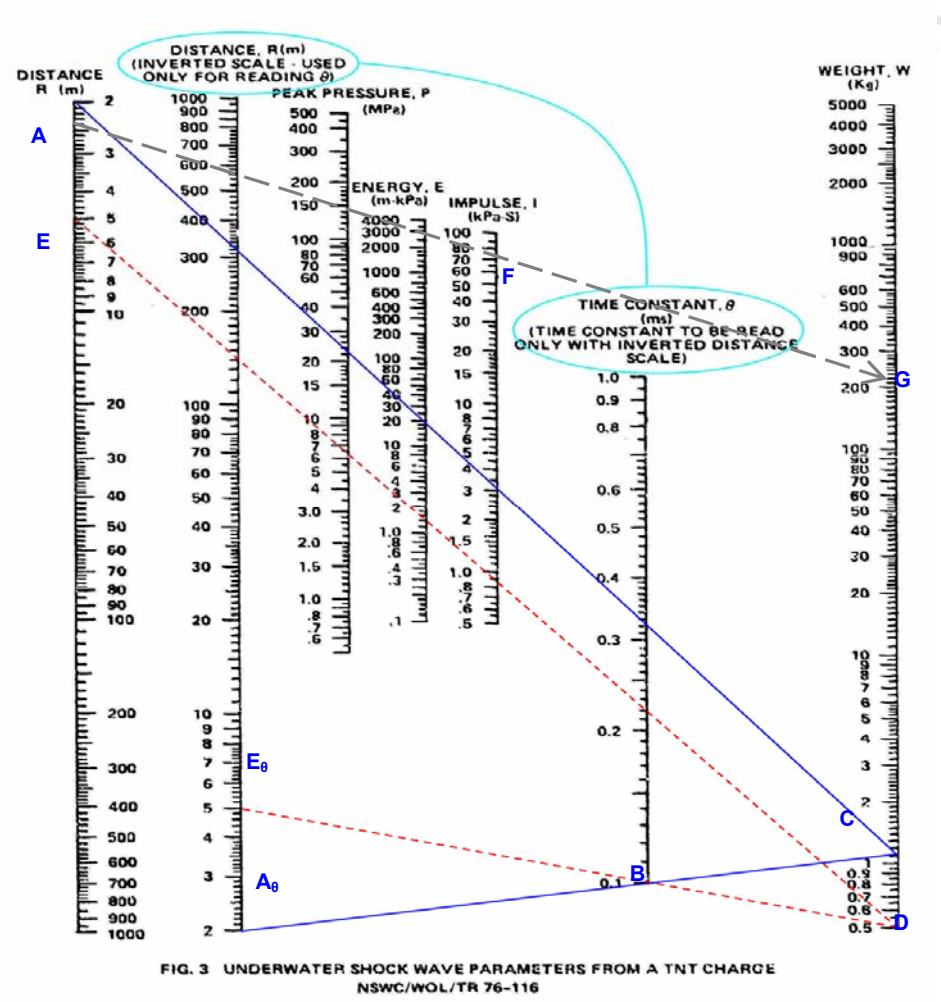

Figure 2-1: A typical Nomogram from Swisdak [11]

Using such a nomogram is very simple – a straight line between a given value on any two parameter axis would render the associated values for the other parameters. It should be noted that the time constant (θ) is associated with an inverted scale, as indicated on the nomogram. Note that the time constant is given in milliseconds.

The nomogram has important limitations for small charges and small offset distances (such as used in this dissertation). The smallest offset distance indicated is 2 meters (annotated *A* and A_θ). The bottom end of the θ scale (annotation *B*) dictates that the corresponding smallest charge usable on this nomogram is 1.1 kg TNT (see *C* on solid line in Figure 2-1~~Figure 2-1~~~~Figure 2-1~~). If the smallest charge of 500g TNT (annotation *D*) is used, the corresponding smallest offset distance is 5m (see dashed line, E_θ).

Hunter [12] explored the collapse of a cavity in water. He investigated the collapse of a bubble and the subsequent formation of a shock wave. Notable is the fact that he treated the collapse of the bubble as symmetrical (i.e. remains a spherical shape).

In 1965 Marsh et al [13] investigated the rise time of pulses from explosive sources in sea water. He found that the non-acoustic behaviour was consistent with the empirical peak pressure and rise-time scaling laws published by Arons [9] in 1954.

Benjamin and Ellis [3] investigated the development and collapse of cavitation bubbles. Their physical measurements were done with the "free-fall" device that effectively eliminated the effect of gravity on the bubble. This is the first paper found that investigates the damaging effect of a collapsing bubble in the close proximity of a solid surface, commonly known as cavitation damage.

A number of papers were published around 1970 that measured energy density levels and frequency spectra as a function of depth, comparing the measured values to theoretical predictions.

A publication in 1975 was edited by Swisdak [11]. It was a compilation of contributions by various researchers from the NSWC (Naval Surface Weapons Centre, USA). It offers very useful reference material. Interestingly the unit system used is metric, although the publication originated in the USA. Clearly it was aimed at an international audience. It addresses all aspects and phenomena associated with underwater explosions in considerable detail. A host of tabulated values and nomograms indicate the depth of the work by the contributors. Many tables and nomograms with advanced information such as similitude constants and coefficients for various high explosives and underwater shock wave and bubble energy equivalent weight ratios for multi component high explosives.

Bjorno and Levin [14] investigated the validity of measurements at small scale in lieu of large (full scale) testing. They conclude that small scale (laboratory) underwater explosion tests give valid useful results and may be used instead of traditional full scale tests in a number of fields.

From 1965 until 1995 very few papers were published that addressed underwater explosions as such. It is possible that most researchers during that period considered this aspect to be sufficiently covered. Most papers addressed cavitation and collapsing of bubbles of very small size.

While all this underwater work was undertaken, research into air blast effects were also progressing swiftly. Menkes and Opat [15] defined three Modes of deformation by blast loading. Olson et al [16] investigated air blast effects on square clamped plates by comparing experimental and numerical work. Three different failure modes were defined, as

illustrated in Figure 2-2~~Figure 2-2~~~~Figure 2-2~~.

Mode I: Large inelastic (ie plastic) deformation
Mode II: Tearing (tensile failure) in outer fibres at the support edge
Mode III: Transverse shear failure at the support

The authors note that the mode of failure is related to the magnitude of the impulse. The maximum midpoint deflection in Mode II failure occurred at an impulse of 21 to 25 Ns. When the impulses are increased to greater than 25 Ns, the failure tended to approach Mode III. It should be noted that the above values are given for uniform loading of the panel. Uniform loading is achieved when the offset distance is relatively large and the spherical front of the shock impulse reaching the target approaches a plane front.

All work in this dissertation is localised loading due to the very small offset distance. This causes Mode I type failure and in addition may cause radial tearing from the position where the detonation occurs.

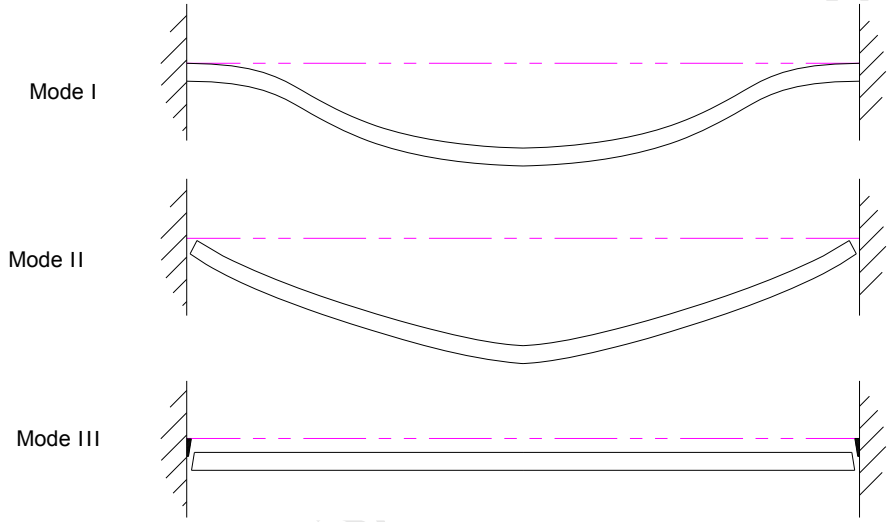

Figure 2-2: Three failure modes

The number of publications increased very rapidly after 1995. Underwater explosions became very well represented and an increasing number of publications concerned the mathematical simulation of the underwater explosion and the effect on nearby structures.

The increase in the number of publications is interesting. For the 60 years before 1995, a total of 42 papers are listed in the bibliography (less than one per year). For the period 1995 until 2007 (twelve years), a total of 83 publications are listed (~7 per year). The last four years (2004-2008) is represented by 44 publications (~11 per year). Some very important factors should be borne in mind when looking at the numbers of publications: the relaxation in global military/defence relations (declassification of research material) on the subject of underwater explosions and the effect thereof. This was for a long time being regarded as classified information by many research institutes (being funded by a defence related

source). Another important factor was the increasing ease of access to technical information (eg internet) and the increase in computing power (mathematical simulation).

Most of the later papers concerned the simulation of the effect of an underwater detonation on a simplified mathematical model, either cylindrical or plane. Examples are Shin and Hooker [17] and Jiang and Olson [18]. The results are generally presented in dimensionless form. In many cases it is clear that the work is based on specific real life requirements such as the stiffening the hull of a submarine or ship. Steel is the material most commonly investigated.

The diversity of topics increased in proportion to the increase in number of papers. Papers based on finite element simulations with associated practical experimental proof became the norm. Through the years research progressed from proving/improving the basic mathematical expressions derived by early researchers to practical applications and case studies. Some of the later work is related to the explosion response of composite materials.

Composite material applied in sandwich panels is a modern technology that is increasingly used in the construction of lightweight structures. The typical sandwich panel is constructed by using two skins (either synthetic material or natural metal) separated by and bonded to a relatively thick core of softer material (synthetic or natural) usually in an expanded form (honeycomb or aerated). Presently the composite panels are more expensive than steel panels of similar strength. This tends to restrict the use of composites to items/products in which the advantages of light weight and strength is more important than the cost of the structure.

The advantages of composite material include light weight combined with high structural strength. The most common application is in smaller high speed vessels (eg ferries), torpedoes, small submarines and URVs (Underwater Remotely controlled Vehicles). The cost of the construction material in these products is small, relative to the overall project cost. In larger constructions the cost of construction material is relatively much more dominant and therefore large ships and large structures (eg oil drilling platforms) are built from steel.

Construction in composite sandwich offers the designer an infinite number of combinations of material, physical composition and construction technique. In addition, sandwich panels may exhibit very non-linear response to blast impact. This poses a major challenge in that, compared to single skin panels, the mathematical representation of sandwich panels become very complicated. The author includes a brief review of a representative publication on composite material.

A paper by Librescu et al [19] is representative of impact related work on composite panels. He states that to his (2006) knowledge "*…the specialised literature addressing the dynamic response of sandwich structures to underwater and in-air explosions is rather scanty"* and that his work was *"…likely to fill a gap in the specialised literature on this topic".*

He states that most of the work in this field is aimed at determining the pertinent factors that characterises the impact strength, resistance to fatigue, energy absorption and many other characteristics. He lists a number of authors that were instrumental in the development of highly encompassing models of sandwich and multilayer composite structures. He states that a complexity associated with mathematical simulation of composite structures arises from the fact that the determination of the pressure-time history induced by an under-water explosion acting on a sandwich panel involves more complex analysis than is the case with monolithic panels. When developing a mathematical model, specific assumptions need to

be made. Examples are the relative strength of the core and skin layers, the shear and axial strength in each axis individually, the strength of bonding (skin to core) and the symmetry (or not) of the characteristics and response of the front and back skin.

-:-

The work for this dissertation is related to the effects on a monolithic steel panel subject to a near-field (near contact) underwater explosion. This definition limits the number of papers that are directly relevant. Although the principles from many papers are useful and important to this dissertation, no publication was found that investigated any form of maximising holing of an air backed target as a function of progressive increase in offset distance.

Hammond [20] investigated the limitations of approximating a spherical charge (detonated from the centre) by using a cylindrical charge detonated from one end. He found that the similitude equations are valid within a limited range. Beyond this range the pressure wave becomes dissipated and the approximation becomes invalid. At very close range the invalidity of the approximation is due to the transient characteristics of the developing shock wave.

A defining publication by Cooper [21] was published in 1996. It comprises a number of sections, each dealing with a specific aspect related to explosives engineering. This publication is a good reference for most aspects related to underwater detonations. It covers chemistry, thermodynamics, fluid dynamics, mechanics and a host of other technologies related to explosive engineering.

In a paper on their investigation related to demolition of charges under water (1995), Chung and Brett [22] presented results of an experimental study visualising the effects of underwater explosions on scaled, submerged cylindrical objects. They state that the relative roles of the underwater shock wave, flow and bubble in the damage process were not clear. Significant structural damage to the cylinder occurred with the passage of the shock wave. During this period, the bubble of detonation products failed to expand sufficiently to contact the cylinder. They state that some evidence is available to suggest that the principal damage mechanism can be attributed to shock wave interaction and not water flow effects. This paper was followed by another similar paper a year later by Chung and Kinsey [23]. They show that the transmitted and reflected shock wave is strongly affected by the degree of matching of impedance between water and a solid medium. The greater the difference in impedance, the greater the amount of energy that is absorbed by the solid.

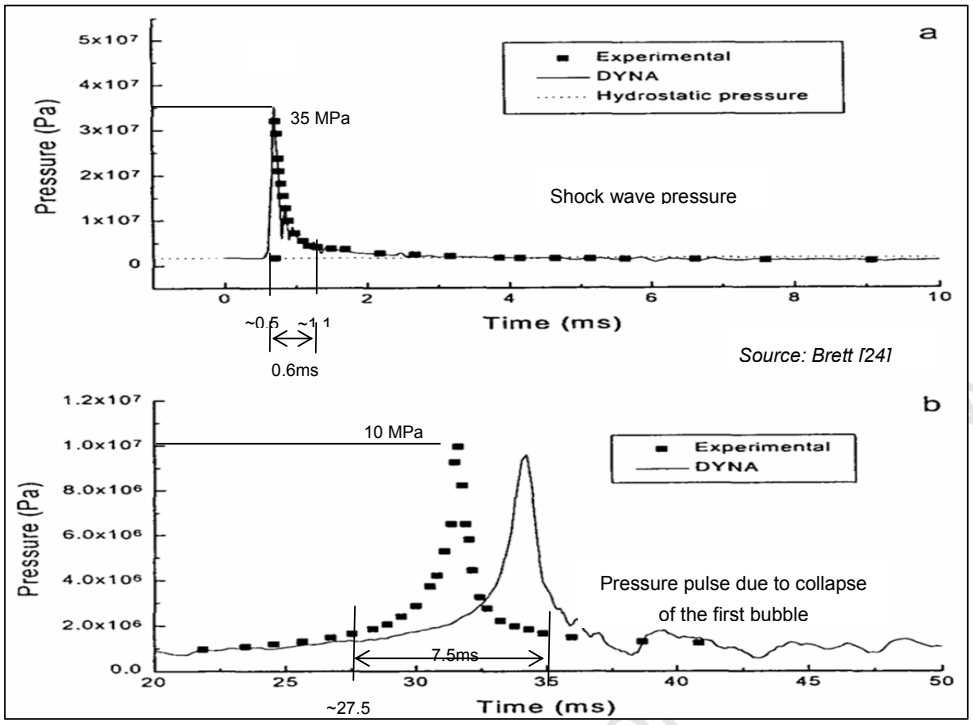

Figure 2-3: Comparing measured data with simulated results by Brett [24]

Brett [24] investigated the use of specific numerical code (DYNA) to model the physical processes associated with an underwater explosion (see Figure 2-3~~Figure 2-3~~~~Figure 2-3~~). He found good quantitative agreement for many of these features and states that, in spite of a number of limitations, finite element analysis can be used to model important aspects of underwater explosions

Murata [25] (1999) showed by experiment that the peak pressure of the bubble pulse is about 15–31% of the peak pressure of the shock wave, but the impulse (integral of pressure as function of time) of the bubble pulse is about 1.5–2.5 times larger than that of the shock wave, within the measured scaled distance range. This is due to the fact that the duration of bubble pulse is about ten times longer than that of shock impulse.

As a matter of interest, consider a number of values from a different paper [24] as shown in Figure 2-3~~Figure 2-3~~~~Figure 2-3~~:- the peak pressure from the first bubble collapse (~10 MPa) is 29% of the peak pressure of the shock pulse (~35 MPa). The duration of the pressure pulse due to the first bubble collapse (~7.5ms) is 12.5 times the duration of the shock pulse (~0.6ms).

An illustration that Murata presents (see Figure 2-4~~Figure 2-4~~~~Figure 2-4~~) indicates that, in the near-field (ie detonation close to the target), the deformation effect of first bubble pulse is much more important than that of shock wave. A statement to this effect was not found in any other reference. Some conditions under which he found this particular distribution of

strain may have been different from the conditions applicable to other authors.

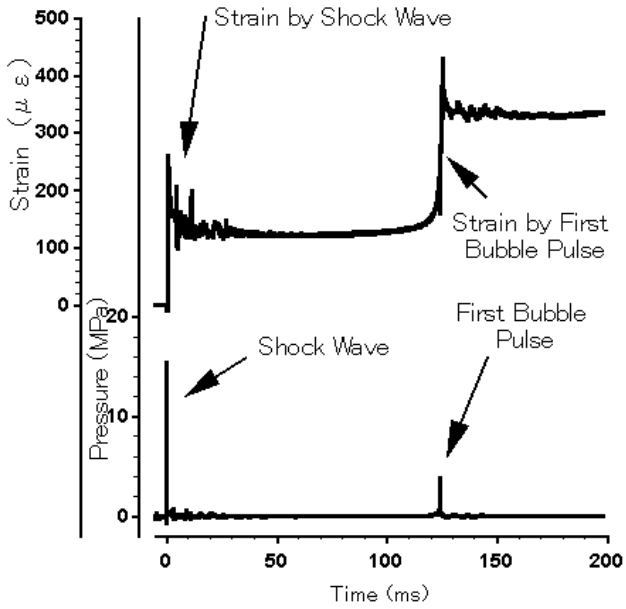

Source: Murata [25]

Figure 2-4: Strain due to the first bubble pulse relative to strain due to the shock wave

Reid [26] published a paper in 1996 that discussed the effect of an underwater shock wave on a ship, more particularly shock testing of newly built ships (ie non-destructive tests). Of interest to the present dissertation is his comment that the incompressible water flow that develops *ahead* of the expanding gas bubble is capable of quite high loading pressures due to its momentum and also acts for a longer period of time than the shockwave. Note: this seems to contradict the statements by Chung et al [22] and [23]. He states that it is possible, under certain circumstances, that 60% or more of the energy involved in plastic deformation damage comes from the early bubble expansion and only 40% from the shock wave. Reid distinguishes between bubble pulse damage and bubble collapse damage, ~~but is not clear whether~~and he refers to the bubble pulse as the ~~pulse due to expansion of the bubble or the~~ pulse due to the implosion of the bubble.

Ramajeyathilagam et al [27] conducted experimental and numerical investigations on clamped rectangular air backed plates subjected to underwater explosion loading. Experiments were conducted using a box model set-up with a 310x250mm air-backed target plate. Plastic deformation of the plates was measured for different charge weights and standoff distances. Numerical analysis was carried out for various test conditions and the results are compared with experimental results. His experimental arrangement was very similar to the setup of the current thesis. **However, he reported on plastic deformation only. No results indicating penetration of the target plate was reported in his paper**.

In his dissertation for a PhD in 2000, Hammond [28] noted that (at that time) a significant amount of work still needed to be undertaken before fluid-structure interactions can be

adequately simulated by Finite Element methods. His thesis included experimental and mathematical work. His prime concern was plastic/elastic deformation of air backed structures due to detonations at relatively large offset distances (far-field).

Brett et al [29] in 2000 described the application of small-scale experiments incorporating cylindrical steel targets instrumented with accelerometers and underwater pressure transducers to investigate the response of the targets to loading from the separate shock wave and bubble collapse events. The author states that their interpretation of the data demonstrated the dominance of bubble collapse loading. The maximum standoff distance of the charge was 1.2 times the bubble diameter. This standoff distance is relatively smaller than that used by most other authors, but still much larger than the offset distances used in the present dissertation.

The work by Zhang et al [30] and [31] is a typical example of the FEM simulation of the three dimensional toroidal collapse of bubbles and associated jet forming. The description "toroidal" stems from the effect that one boundary (usually the lower boundary) of the collapsing bubble tends to form a jet of water that distorts the spherical shape.

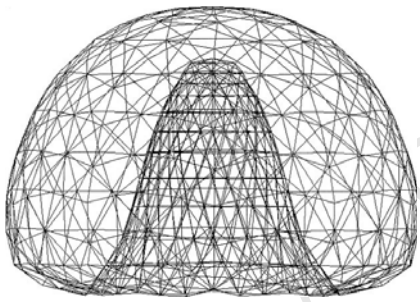

Source: Zhang [30]

Figure 2-5: Simulation of a typical torodal shape of a collapsing bubble

Rajendran and Narasimhan [32] developed a damage prediction model relating the input shock energy, the contour of deformation, the material properties and the thickness of the structural material. This model assumed rigid plastic membrane stretching and neglected the energy dissipated in localised dimpling and cracking during the dynamic deformation process. A case study illustrated correlation with Keil's empirical model and the approach they followed. The results were in good agreement with each other and the experimental observation.

In work that investigates the effect of stiffeners on the onset of tearing, Langdon et al [33] showed that addition of stiffener(s) reduced permanent displacement for a given impulse. However, local increase in stiffness along the stiffener edges can cause premature rupture of the plates (along the stiffened area). Once tearing was initiated, the permanent stiffener displacement magnitudes plateau as additional input energy is absorbed by the tearing mechanism. Results suggest that stiffening of plates does not reduce tearing, it may actually cause tearing to be initiated earlier. The stiffeners seem to restrict the plate to deform plastically, causing tearing to occur at an impulse that would cause plastic deformation in the un-stiffened plate.

Although the work was done in air medium, the difference in response of the different

stiffening configurations is of significance to this thesis. The reason is that a real-life target is stiffened on the air side of the hull plating, ie not simple flat plating. Therefore tearing is likely to be initiated earlier (at lower loading) when the plate is supported by a stiffener at the point of loading. This effect can be seen in Figure 2-6~~Figure 2-6~~~~Figure 2-6~~ that was taken from [34], in which the same author reported on work done on an air backed target in water.

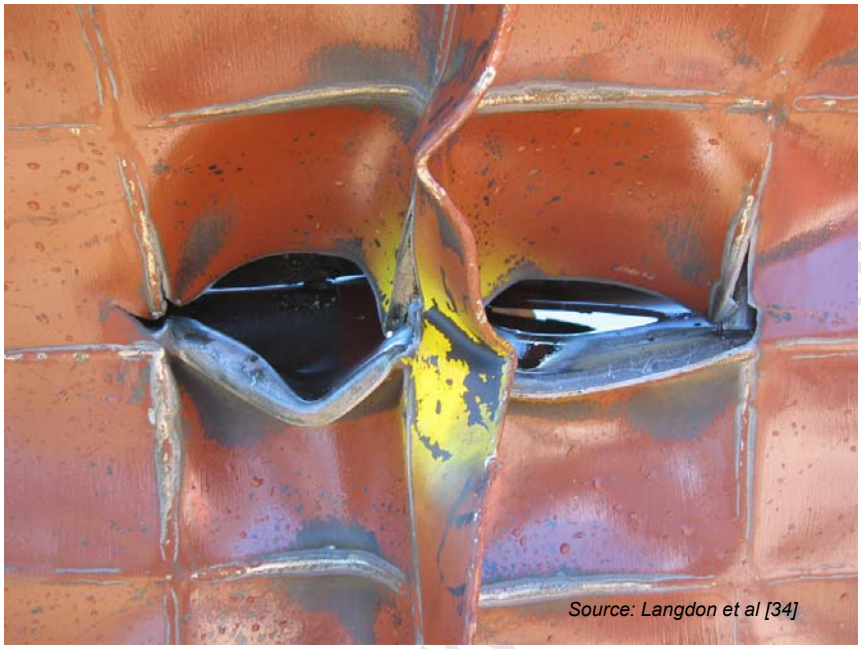

Figure 2-6: Tearing along stiffeners on an air backed target

The work by Church et al [35] is very significant and useful in the present study. Their investigation concerned the relative contribution to holing and damage of the gas loading (detonation products) relative to the contribution of the water loading associated with the bubble. They used high speed photography to determine the rate of hole growth versus time for two sizes of charge and target plate. The practical experiment was correlated by FEM simulation. They concluded that the contribution to target damage by the water loading (due to expanding bubble) could be in the order of 31%. The dramatic effect of the water loading is explained by them in that, although the velocity of the water is small in the axial direction of the plate, its density is much greater than the detonation products. This results in a substantial increase in the overall loading as is illustrated in Figure 2-7~~Figure 2-7~~~~Figure 2-7~~. It illustrates the simulated hole at 5ms after detonation due to the gaseous loading compared to the gaseous plus water loading.

Source: Church [35]

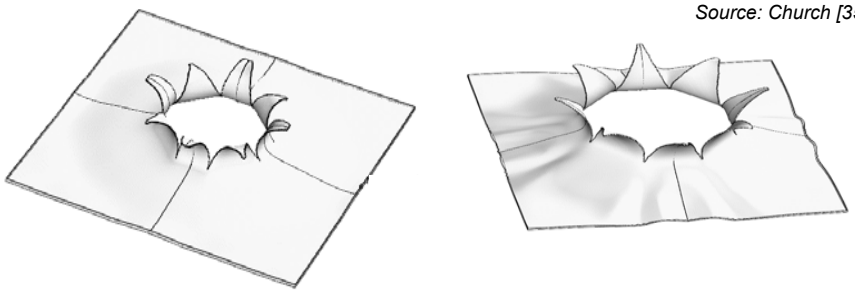

Result of Gaseous loading

Result of Gaseous plus Water loading

Figure 2-7: Simulated hole size after 5ms

The Maritime Platforms Sciences Laboratory in Melbourne, Australia built an experimental facility in a large quarry filled with fresh water. This unique facility is described in a paper by Brett et al [37]. The facility is large enough to allow detonation of charges up to 5kg and is equipped with advanced high speed photographic equipment. The authors describe the challenges and solutions of this facility. Protecting sensitive equipment and ensuring clear water are mentioned as major challenges. The potential of this facility is demonstrated by imaging and analysis of the detonation of a 0.5 kg explosive charge.

Figure 2-8: The experimental facility in Melbourne [37]

The work by Slater et al [36] that was published in 2005 contains an excellent graphic presentation of the growth and collapse cycles of a gas bubble (Figure 2-9~~Figure 2-9~~~~Figure 2-9~~). The target (a submerged hollow cylinder, wall thickness 3mm) was not penetrated by the blast. The 1.1g RDX detonator used as detonating charge clearly was too weak to penetrate the cylinder wall, even at the smallest standoff distance of 20% of the maximum bubble radius.

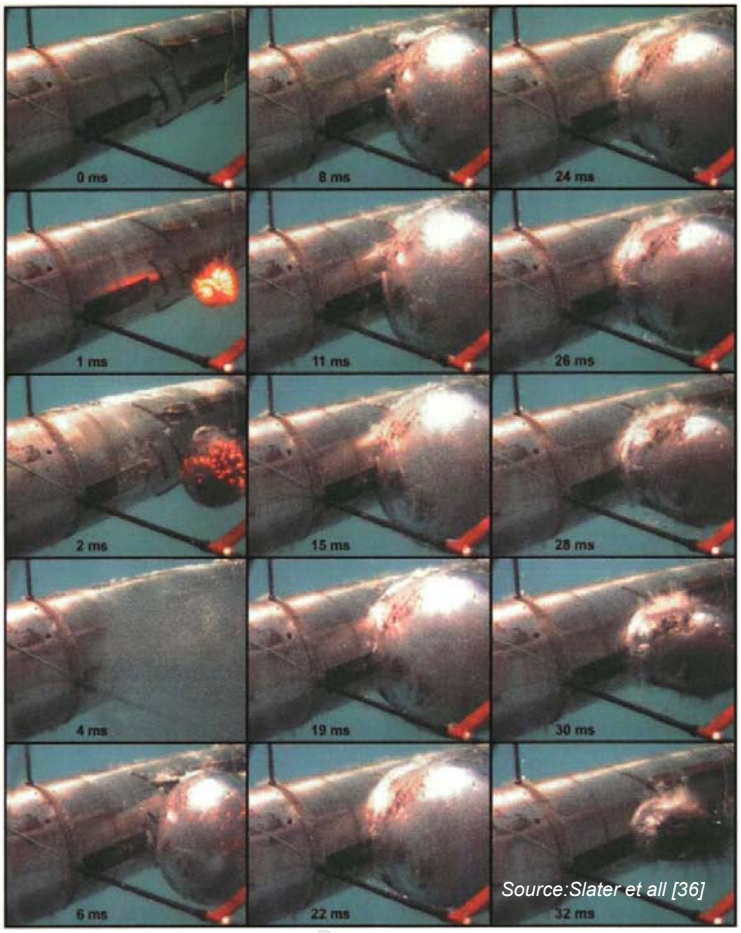

Figure 2-9: The growth and collapse of a gas bubble photographed by Slater [36]

2.2 Defining References

The publication by Cole [8] in 1948 is cited in most papers and publications by later researchers. This book addresses all aspects of an underwater explosion in both empirical as well as basic mathematical relations. This publication established a foundation that has withstood the test of time. Modern research confirmed the work as intrinsically sound and can only manage to refine the basic mathematical relations presented by them.

In1976 a compilation of contributions by various authors was edited by Swisdak [11] and published by the American NSWC (Naval Surface Weapons Centre). It addresses most aspects of underwater explosions and the phenomena associated with underwater explosions in considerable detail. A host of tabulated values and nomograms testify on the depth of the work by the contributors. Swisdak provided a number of detailed similitude constants for shockwave parameters for commonly used high explosives.

A more recent defining publication appeared in 1996 by Cooper [21]. He realised that little, if any, literature was available that ties all aspects of explosives engineering together. His publication comprises six sections, each dealing with a specific aspect related to explosives engineering. The sections include extensive treatment of explosive technologies such as chemistry, energetics of explosives, shock waves, detonation, initiation and engineering applications.

2.3 Work that is very relevant/applicable to this thesis

The ambit of this thesis entails the effects of a detonation in very close proximity of a submerged air backed target with the objective of maximising the hole by optimising the offset distance. No papers were found that treated this combination of aspects. However, a significant number of publications treated one or more of these aspects in a manner that is useful to this thesis.

Brett, Chung and Kinsey [22], [23], [24], [29], [37], [38], [39] of the Australian DSTO (Defence and Science Technology Organisation) published very useful material from 1998 to 2007. The paper by Brett and Yiannakopolous [39] is of particular importance because it addresses the effect of offset distance on the relative importance shock wave, bubble pulse and bubble collapse/jetting loads. This paper includes revealing images from high speed photography.

Brett and Yiannakopoulos [39] studied three different values of charge–target separation: $1.19xR_{bubble}$, $1.03xR_{bubble}$ and $0.89xR_{bubble}$. They report that:

> Target responses for the largest separation ($1.19R_{bubble}$) was measured to be 16m/s for the shock wave and 7 m/s for the 1st bubble pulse wave. In this case the shock wave dominated the target response.
>
> For the smaller separation of $1.03R_{bubble}$ the shock wave response remained dominant, generating a cylinder response of 19 m/s but the closer proximity of the explosion enhanced the bubble loading. During its initial pulsation the bubble remained detached from the cylinder but formed a water jet directed at the cylinder. This contributed to a total bubble collapse generated response of 8m/s. At the end of its 2nd pulsation the bubble collapsed onto the cylinder generating a similar response of 7m/s.
>
> For the smallest separation of $0.89R_{bubble}$ the situation changed dramatically with collapse of the bubble onto the target at the end of its 1st pulsation. This dominated the cylinder's response; the shock wave response was measured at 23 m/s whilst the bubble collapse response was measured as 48 m/s.
> The results show that shock wave loading generated a significant cylinder response for all values of charge–cylinder separation. Pressure wave loading from the pulsing bubble was less significant, generating a peak velocity approximately half that caused by the shock wave. However, when it occurred, the immediate collapse of the bubble onto the cylinder was clearly the most severe structural load, generating a peak velocity approximately twice that caused by the shock wave. Moreover, post trial inspection of the target cylinders showed that measurable plastic deformation occurred only for events in which the bubble immediately collapsed onto the cylinder. These results strongly suggest that bubble collapse was the dominant agent of plastic deformation for the simple and small-scale structures studied in this paper.

Rajendran and various co-authors of the Indian Institute of Technology in Bombay published a number of particularly relevant papers between 2000 and 2008 [32], [40], [41], [42], [43], [44], [45]. One of these papers dated 2005 (Rajendran and Narasimhan [40]), is an informative review of the sequence of events during an underwater explosion and the

effects on air backed plate specimens. Practical and useful relationships between various underwater explosive phenomena are given. The bibliography presented in this paper is a rich source of references. In [43] he reports on non-contact underwater explosion experiments that were carried out on air backed circular steel plates of 4 mm thickness and 290 mm diameter. He increased the magnitude of the loading until plastic deformation switched to onset of tearing. Empirical models were derived to predict the plastic deformation which was validated through a fresh set of experiments. The size of hole as a function of offset distance was not investigated.

A recent paper by Rajendran [44] gives insight into the reloading phenomenon by comparing the strain measured during experiments against the theoretical strain. This is an issue that is very relevant to this dissertation: the phenomena during the time from the initial shock pulse up to the loading due to the expanding gas bubble. Plates undergoing elastic deformation experience discrete loading by the primary shock pulse, followed by reloading pulses. The reloading pulses comprise of cavitation and gas bubble loading. According to Rajendran, closure of the cavitated space by the interaction of the *expanding* gas bubble causes major reloading on the plate, as seen in Figure 2-10 taken from [44].

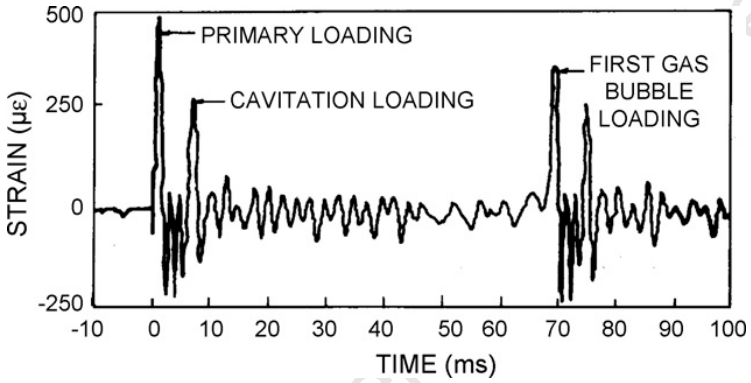

Figure 2-10: Strain-time history on a plate showing reloading response [44]

In a 2008 paper Rajendran [45] reviews the "phenomenological evolution of blast damage of plates" (sic). In this paper he briefly describes the detonation process, followed by an extensive review of work done by a host of references. Besides the valuable references, this paper reveals the difference between an explosion in an air medium versus water medium. In his conclusions he states that the significant parameters to consider for the damage process in an air medium are the peak overpressure and the impulse. In a water medium the significant parameters regarding the damage process are peak pressure, time constant, free field impulse and energy. Note: the distance between the target plate and the detonation is not mentioned as a significant parameter – it is assumed that Rajendran treats the separation distance as being included in the stated parameters.

Although not related to this dissertation, it is interesting to mention the principle differences between air and water as propagating medium. The detonation process is the same in both air and water. In the water medium a pressure pulse in transmitted to the water, initially travelling at about three times the velocity of sound in water, then slowing down to a constant velocity equal to velocity of sound in water (ca 1450m/s) at a distance of about 10

times the charge diameter [45]. The gas bubble expands (physically displacing water) at a velocity that is much slower than that of the pressure pulse. In air the shock pulse travels with the gas-air interface, slowing down to the velocity of sound in air (ca 340m/s, depending on temperature and air pressure). In other words, in air the shock pulse travels much slower than in water and no bubble is formed.

Church et al [35] was mentioned before (see Figure 2-7~~Figure 2-7~~Figure 2-7). His work contributes significantly to the understanding of the work for this dissertation. He concludes that the dynamic loading of the water is crucial and can account for 31% of the total impulse delivered to the plate. This also demonstrated that the dynamic pressure loading from the water was a major contribution to the loading. In a physical experiment a 12mm plate was subjected to a 1,5kg PE4 (contact) charge. Measurements indicated that plugging (initial hole formed) was complete in 10 μs, followed by tearing and petalling that was completed in 140 μs. This result implies that tearing and petalling was complete before the bubble collapsed. In other words, the collapsing bubble did not contribute to the damage.

3 CHAPTER 3: UNDERWATER EXPLOSIONS

3.1 The basics of an underwater explosion

3.1.1 Detonation

A detonation is, by definition, an instantaneous release of a large amount of energy. Explosive material is designed to contain as much as possible energy (Joules/kg) and to release this energy as rapidly as possible. Explosive material can be decomposed in two ways – it can burn, releasing the energy over a long period (e.g. seconds or minutes) or it can detonate, releasing the energy in an instant (typically microseconds).

The medium in which a detonation occurs (gaseous or liquid) does not alter the detonating characteristics of an explosive material. However, the phenomena resulting from the detonation is totally dependant on the medium in which the detonation occurs.

The explosive material needs to be initiated by an initiating shock pulse of sufficient energy. Usually a small amount of highly sensitive explosive is placed in contact with the main charge and then initiated electrically. The resulting shock wave triggers a chemical reaction at molecular level within the main charge. This (instantaneous) decomposition of the explosive molecules causes a shock wave that spreads out through the total body of the explosive material (Figure 3-1~~Figure 3-1~~Figure 3-1). The speed of this shock front within the explosive material is in the order of 7000 m/s (referred to as VOD, velocity of detonation). The actual value of VOD is dependant on the chemistry and density of the explosive. Typical values are 6900m/s for TNT and 8750m/s for RDX [21].

The explosive material in front of the shock front remains unaffected until the instant that the shock front reaches it. Instantaneous decomposition occurs at the shock front. Behind the shock front a gaseous region of very high pressure (ca 5 GPa) and very high temperature (ca 3000°C) exists [8].

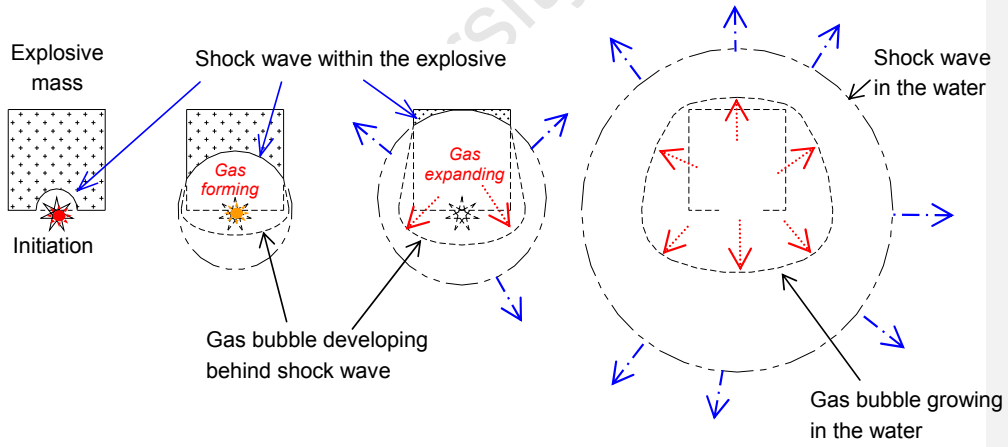

Figure 3-1 : The detonating explosive

3.1.2 The Shock wave

The shock front moves spherically from the point of initiation towards the boundaries of the explosive. When it reaches the boundary of the explosive material, the shock wave is transferred to the surrounding medium. From here the characteristics of the shock wave is determined by the medium in which it is propagating,

Figure 3-2~~Figure 3-2~~Figure 3-2 represents a typical pressure-time curve as seen at a point near the detonation.

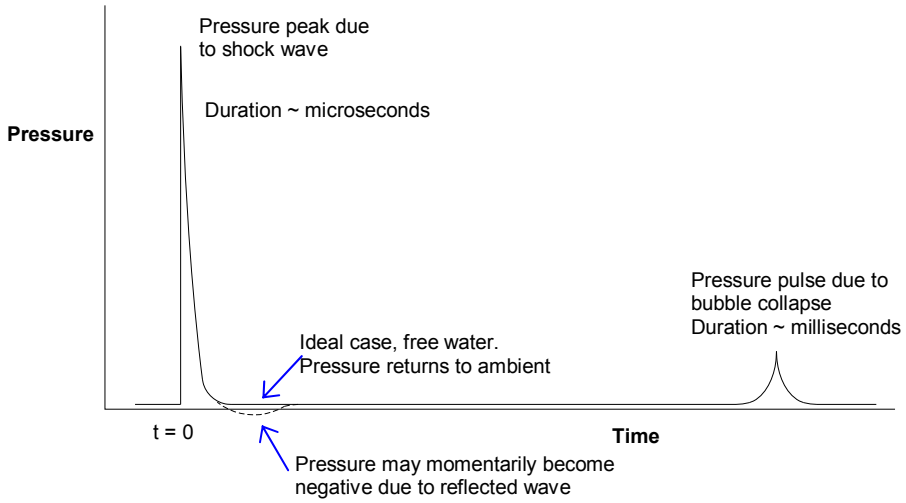

Figure 3-2 : Typical pressure – time curve in water

The detonation wave within the explosive reaches the boundary to the surrounding water at VOD of the detonating explosive. The shock wave then spreads in a spherical shape in the surrounding medium with gradually reducing velocity and exponentially reducing peak pressure. At a distance of about 5 times charge diameter, the velocity is reduced to acoustic velocity in the water (typically 1450m/s).

The pressure time history, p(t), at a fixed location starts with an instantaneous pressure increase (less than a microsecond) to a peak pressure, Pm, followed by a decay that is less rapid than the rise time.

$$p(t) = P.e^{-t/\theta}$$

The peak pressure is given by the following relation (valid for TNT equivalent mass)

$$P_m = 52.16\ (W^{1/3} / R)^{1.13}$$ (from Keil [1] and Rajendran [40]

The value θ is known as the decay constant and varies in proportion to the size (mass) of explosive as well as the distance from the detonation at which the pressure is observed. The value of θ for TNT can be approximated by a relation that is given by Keil and Rajendran.

$$\theta = 96.5\left(W^{1/3}\right)\left(\frac{W^{1/3}}{R}\right)^{-0.22}$$

The unit of P_m is MPa, θ and t is time (microseconds), W is expressed in kg of TNT and the standoff distance R, is measured in meters.

In practice, the value of θ is slightly different for different chemistries of explosives. The exact value for any particular charge can be determined by experiment if it is not available from literature.

For practical purposes the values for any given explosive composition is converted to the TNT-equivalent values (as in Table 4-1) and then used for calculation using relations that are compiled for TNT. Although these equations are calibrated for TNT, they can be used unaltered to predict the approximate values for most compositions of explosive.

These formulae apply to any size of charge, from a few grams to nuclear weapons, exploded at any depth, and describe the shock wave properly except in the immediate vicinity of the explosive charge (less than 5 times the charge diameter), where the peak pressure is higher than what the formula predicts [11].

Table 3-1~~Table 3-1~~~~Table 3-1~~ presents a number of sample calculations for the peak pressure and decay constant for four different charges and seven different offset distances.

It is general practice to convert the mass of any given explosive composition to the TNT equivalent when used in the published equations.

The mass values chosen are 100kg, 10kg, 1kg and 30grams. The latter value is presented because this is the mass of explosive used for all the field work detonations pertaining to this dissertation.

The reader will notice that the offset distance tabulated is either normal or *italic*. This is done to indicate whether the OD used for the calculation is greater than 5 times charge diameter (valid) or less than 5 times charge diameter (*not valid*).

It should be noted that depth of submersion is not represented in either of the equations.

The results are also presented as two graphs, Figure 3-3~~Figure 3-3~~~~Figure 3-3~~ and Figure 3-4~~Figure 3-4~~~~Figure 3-4~~. The region of validity is clearly indicated by the annotation on the graphs. The dashed line indicates the 5-times-charge diameter boundary. Above this line the equations are considered to be inaccurate. The region below the dashed line corresponds to an offset distance that is more than 5 times charge diameter, and therefore within the valid region of the equations.

Clearly the offset distances, used in the field work for this dissertation, ~~is~~ is in the region in which the equation for peak pressure is not accurate or is even invalid. This reinforces the decision to view the combined effect of shock impulse and bubble effect.

Table 3-1 : Illustrative calculation of Decay Constant and Peak Pressure

Mass PE4 (kg)	100	kg	Equivalent Mass TNT	120	kg		
Effective Charge sphere dia Deff	523	mm	Validity limit 5xDeff	2616	mm		
Offset Distance OD (mm)	10	100	250	500	1000	1500	2000
Equation Valid?	yes / no	yes / no	yes / no	yes / no	yes / no	yes / no	yes / no
Calculated θ (millisec) from [40]	0.56	0.92	1.13	1.31	1.53	1.67	1.78
Time constant ex Nomogram (ms)	0.47	0.81	1.00	na	na	na	na
Calc'd Peak Press. Pmx at OD (MPa)	57610	4271	1516	693	317	200	145

Mass PE4 (kg)	10	kg	Equivalent Mass TNT	12	kg		
Effective Charge sphere dia Deff	243	mm	Validity limit 5xDeff	1214	mm		
Offset Distance (mm)	10	100	250	500	1000	1500	2000
Equation Valid?	yes / no	yes / no	yes / no	yes / no	yes / no	yes / no	yes / no
Calculated θ (millisec) from [40]	0.31	0.51	0.62	0.72	0.84	0.92	0.98
Time constant ex Nomogram (ms)	0.27	0.46	0.56	0.66	0.77	na	na
Calc'd Peak Press. Pmx at OD (MPa)	24201	1794	637	291	133	84	61

Mass PE4 (kg)	1.0	kg	Equivalent Mass TNT	1.20	kg		
Effective Charge sphere dia Deff	113	mm	Validity limit 5xDeff	564	mm		
Offset Distance (mm)	10	100	250	500	1000	1500	2000
Equation Valid?	yes / no	yes / no	yes / no	yes / no	yes / no	yes / no	yes / no
Calculated θ (millisec) from [40]	0.17	0.28	0.34	0.40	0.46	0.51	0.54
Time constant ex Nomogram (ms)	0.14	0.24	0.30	0.35	0.42	na	na
Calc'd Peak Press. Pmx at OD (MPa)	10166	754	268	122	56	35	26

Mass PE4 (kg)	0.030	kg	Equivalent Mass TNT	0.036	kg		
Effective Charge sphere dia Deff	35	mm	Validity limit 5xDeff	175	mm		
Offset Distance (mm)	10	100	250	500	1000	1500	2000
Equation Valid?	yes / no	yes / no	yes / no	yes / no	yes / no	yes / no	yes / no
Calculated θ (millisec) from [40]	0.07	0.11	0.14	0.16	0.19	0.20	0.22
Time constant ex Nomogram (ms)	na	na	na	na	na	na	na
Calc'd Peak Press. Pmx at OD (MPa)	2714	201	71	33	15	9	7

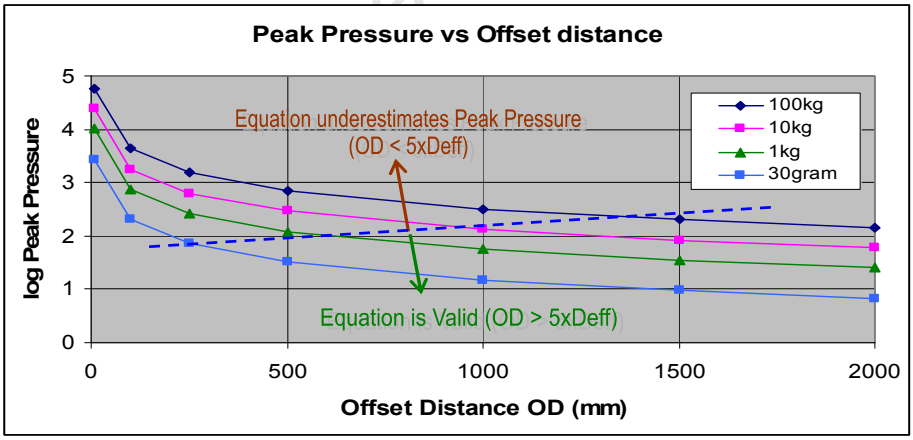

Figure 3-3: Calculated Peak Pressure vs Offset Distance

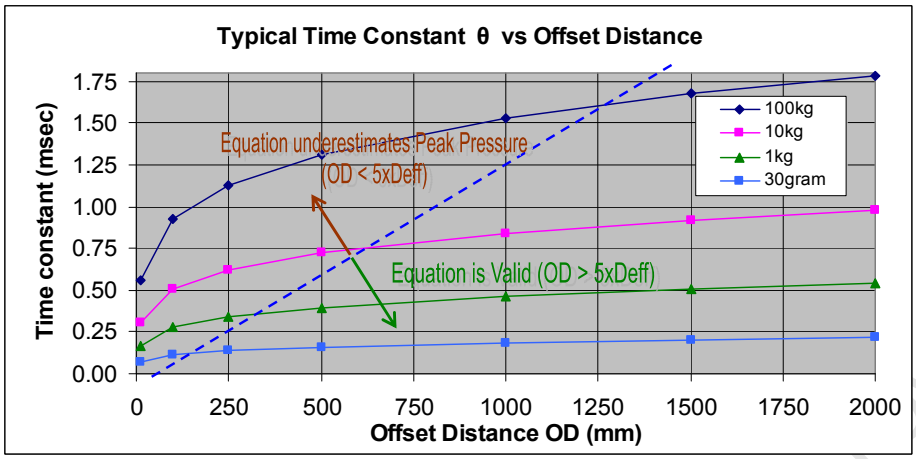

Figure 3-4: Calculated Decay constant vs Offset Distance

As the shock wave passes a fixed location, the liquid at that point is subject to a transient pressure p(t) and the liquid is simultaneously subjected to flow with a velocity v(t) in the direction of the wave. The relation between the velocity and the transient pressure is given by Keil [1]:

$$p(t) = \rho c v(t)$$

or

$$v(t) = p(t) / \rho c$$

Rajendran and Narasimhan [40] state that a correction to the velocity needs to be added for spherical flow:

$$v(t) = \frac{p(t)}{\rho c} + \frac{1}{\rho R}\int_0^t p(t)dt$$

The first term is the velocity for a plane wave and the correction term is called ‘‘after flow’’. The after flow term becomes significant in the close vicinity of the explosion (when R becomes very small) and also for large time intervals (when t becomes large). The variables are ρ (density of the medium in kg/m^3), c (speed of sound in the medium in m/s) and R is the distance from detonation (m).

The shock wave energy density E_{sh} (J/m^2) for a fully exponential shock wave is given by Rajendran and Narasimhan [40]

$$E = \frac{1}{\rho c} P_m^2 \theta$$

If J is substituted as Nm into the unit of energy density, the J/m^2 can be presented as Nm/m^2

The effectiveness of a shock wave is related to the impulse (time integral) of the pressure:

$$I = \int_0^t p(t)\,dt$$

Equations for estimating the shock energy and shock impulse (per unit area) when integrated for the whole length of the shock wave (t = 6:7xθ) are given by Cole [8]

$E_{sh} = 98000\ (W^{1/3})(W^{1/3} / S)^{2.1}$ Note: This equation is presented in imperial units

and

$I_A = 5760\ (W^{1/3})(W^{1/3} / S)^{0.891}$ Note: This equation is presented in imperial units

The unit of the impulse in metric units is Ns (product of a force and time). The impulse calculated from above two equations are~~is~~ impulse per unit area, therefore the unit of I_A is Ns/m^2.
Cole [8] states that when integrating for the full impulse a time value of t = 6.7xθ is used.
Swisdak [11] states that the integral for impulse is usually taken as 5 times θ.

It is important to note the difference between energy and impulse.

> Energy represents the amount of work that a system is capable of doing (potential work). It is a scalar entity in that it is not associated to a direction or vector. Energy and work has the same unit – Joule (or Nm). Work represents the amount of energy actually applied.
>
> Impulse is the product of a force and time. It is a vector (as opposed to energy) because force is a vector. Impulse has the unit Ns.
>
> Power is the rate at which energy is applied (alt rate of work) and is measured in watt, having the units of Nm/s). Not being associated with a direction of force, power is a scalar entity.

Knowing the value of the impulse is key to many aspects when analysing the effects of detonations. The equations given by Cole [8], Keil [1], Swisdak [11] and others are practical and reliable at offset distances beyond ten times the charge radius. Unfortunately these equations become progressively more inaccurate when the offset distance reduces from smaller than ten times the charge radius.

> *The work of this dissertation is performed at offset distances of zero to one times charge diameter. This is much smaller than the restriction of five-times-charge-diameter. Therefore the equations for peak pressure and impulse cannot be applied quantitavely.*

Likewise, the nomogram presented by Swisdak (see Figure 2-1~~Figure 2-1~~Figure 2-1) cannot be used for the offset distances of this dissertation. The smallest offset distance given is 2meters, which is far greater than the largest OD used in the field tests.

Note: The values given by the nomogram (Figure 2-1~~Figure 2-1~~Figure 2-1) are within the valid range of the equations from Cole, Swisdak and Keil.

If a straight line is drawn from the 2m mark (A) through the maximum impulse (F), a charge mass of 280 kg is found (G). The spherical volume taken up by 280kg of TNT

Formatted: English (U.K.)
Formatted: English (U.K.), Not Superscript/ Subscript
Formatted: Font: 10 pt, English (U.K.), Not Superscript/ Subscript
Formatted: Font: 10 pt
Formatted: Tab stops: 3.05", Left
Formatted: Font: 10 pt, English (U.K.), Not Superscript/ Subscript
Formatted: Font: 10 pt
Formatted: Font: 10 pt, English (U.K.), Not Superscript/ Subscript
Formatted: Font: 10 pt, English (U.K.)
Formatted: English (U.K.)
Formatted: English (U.K.)

(density 1800kg/m^3) is 0.156 m^3. This volume in a spherical shape would have a diameter of 334 mm. This diameter multiplied by five equals 1,67m, which is smaller than the 2 meters quoted on the nomogram. Therefore the nomogram conforms to the limits applicable to the equation.

3.1.3 The Gas Bubble

The gaseous region of high pressure and high temperature that develop and follow behind the shock wave expands at a very high rate (yet at much lower velocity than the shock wave) into the surrounding water, bodily displacing the water. As with the shock wave, once in the surrounding medium (water), the expanding gas volume is now affected by the surrounding medium (water).

Assuming the ideal case of free water the gas bubble generated during the detonation is spherical during the initial expansion. The hot gas under high pressure expands against the surrounding water until the pressure inside the bubble equals the pressure of the surrounding water. In actual fact, the pressure drops to slightly below the prevailing water pressure due to the momentum of the moving water that overshoots the point of pressure equilibrium. At this point the bubble starts to collapse. During the collapse of the bubble, the remains of the gas inside the bubble is rapidly re-compressed. This creates a condition of high pressure that emits a shock wave into the water and also causes another expansion into a second bubble. This pulsation will repeat itself with diminishing intensity due to energy losses.

In free water, the bubble rises towards the surface due to the buoyancy as depicted in Figure 3-5~~Figure 3-5~~~~Figure 3-5~~.

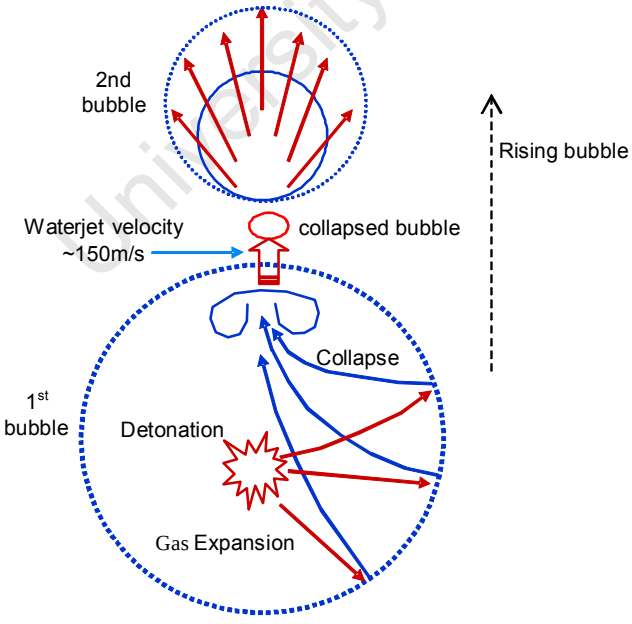

Figure 3-5 : Typical growth, collapse and rising of the gas bubble

The bubble growth (and therefore the maximum radius and time period) is affected by the close proximity of any solid object that may be within the maximum bubble radius.

In the case that a solid surface is closer than the maximum radius of the expanding bubble, the bubble tends to collapse towards the solid surface (see Figure 3-6~~Figure 3-6~~~~Figure 3-6~~). This is caused by the inflow of water that is restricted near the solid surface and unrestricted on the away-side of the bubble.

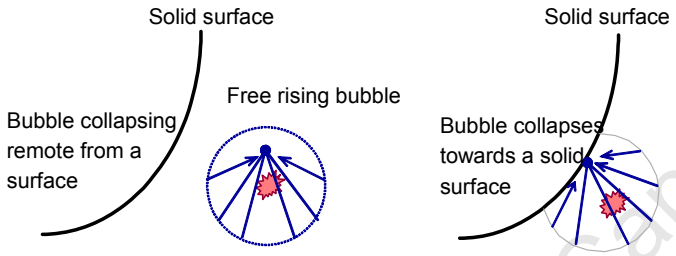

Figure 3-6 : The bubble tend to collapse towards a solid surface

The collapse of the gas bubble tends to become toroidal in that one side of the spherical boundary approaches the centre of the sphere quicker than the remaining boundary of the sphere. This effect of toroidal collapse (also referred to as jet forming) is from bottom up in free water (higher hydrostatic pressure at the bottom boundary) or towards any object that is closer than the maximum radius of the expanded bubble. The latter effect is due to restricted inflow of water due to the presence of the object (see Figure 3-6~~Figure 3-6~~~~Figure 3-6~~). A graphical representation of such toroidal collapse as illustrated in the work by Zhang [31] is shown in Figure 2-5~~Figure 2-5~~~~Figure 2-5~~.

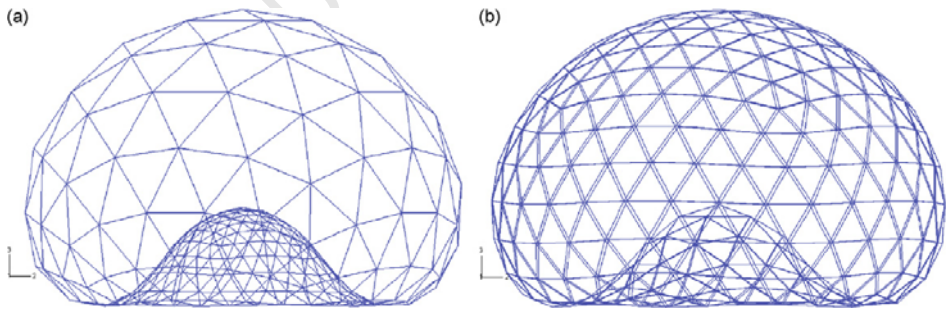

Figure 3-7 : Typical toroidal collapse of a bubble (from Zhang [31])

The two characteristic parameters of the bubble are the maximum bubble radius R_{max}, of the first pulsation and the duration T of the first pulsation (measured from the detonation until the first minimum/collapse) of the bubble. Both these parameters vary with the size of the explosion charge and the depth at which the detonation occurs. The original relations given by Cole [8] were converted to metric units by Keil [1] and is given by Rajendran [32]

The maximum radius of the gas bubble is given by

$$R_{mx} = 3.3 \{ W / (D+10) \}^{1/3}$$

and the time of pulsation T is given by

$$T = 2.08 (W^{1/3}) / (D+10)^{5/6}$$

The units are metric (*R* in meters, depth *D* in meters and *W* in TNT equivalent mass in kg).The constant '10' represents the depth of water equivalent to one atmosphere.

Using the same mass values as in paragraph 3.1.2 the calculated bubble period (from start to collapse) are calculated and presented in Table 3-2. Four depths of submersion are calculated for: 1m, 10m, 30m and 100m. As with the bubble radius, the bubble period is not mathematically affected by the standoff distance.

From Table 4.1: TNT equivalent bubble energy factor = 1.055				
Charge size PE4 =	100 kg	10 kg	1 kg	0.030 kg
Eq. mass TNT = (kg PE4 x1.2)	106 kg	11 kg	1.1 kg	0.032 kg
Depth below surface 1m	Depth below surface (meter) 1 m	1 m	1 m	1 m
	Max Bubble radius (m) 7.01 m	3.25 m	1.51 m	0.47 m
	Max Bubble radius (m) 7.32	3.40	1.58	0.49
	Bubble period (sec) 1.33 s	0.62 s	0.29 s	0.09 s
	Bubble period (sec) 1.37	0.73	0.34	0.11
Depth below surface 10m	Depth below surface (meter) 10 m	10 m	10 m	10 m
	Max Bubble radius (m) 5.74 m	2.67 m	1.24 m	0.38 m
	Max Bubble radius (m) 6.00	2.78	1.29	0.40
	Bubble period (sec) 0.81 s	0.38 s	0.17 s	0.05 s
	Bubble period (sec) 0.95	0.44	0.21	0.05
Depth below surface 30m	Depth below surface (meter) 30 m	30 m	30 m	30 m
	Max Bubble radius (m) 4.76 m	2.21 m	1.03 m	0.32 m
	Max Bubble radius (m) 4.76	2.21	1.03	0.32
	Bubble period (sec) 0.45 s	0.21 s	0.10 s	0.04 s
	Bubble period (sec) 0.54	0.25	0.12	0.04
Depth below surface 100m	Depth below surface (meter) 100 m	100 m	100 m	100 m
	Max Bubble radius (m) 3.40 m	1.58 m	0.73 m	0.23 m
	Max Bubble radius (m) 3.40	1.58	0.73	0.23
	Bubble period (sec) 0.20 s	0.09 s	0.04 s	0.01 s
	Bubble period (sec) 0.23	0.11	0.05	0.02

Table 3-2 : Illustrative calculation of Bubble Radius and Pulsation Time

The calculated bubble sizes and corresponding bubble periods are calculated for the same set of masses (100kg, 10kg, 1kg and 30gram) and are presented in graphical form in Figure 3-8. The steady decrease in maximum bubble radius with increase in depth of submersion is apparent in the graph. When the detonation occurs close to maximum bubble radius from the surface of the water, the expanding bubble will break the surface and the gas bubble will not develop. Note that at a depth of 1m, the gas bubble of only 30g charge will develop

fully.

The equation for maximum bubble radius and bubble period is valid for the field work of this dissertation because these two parameters are not related to peak pressure.

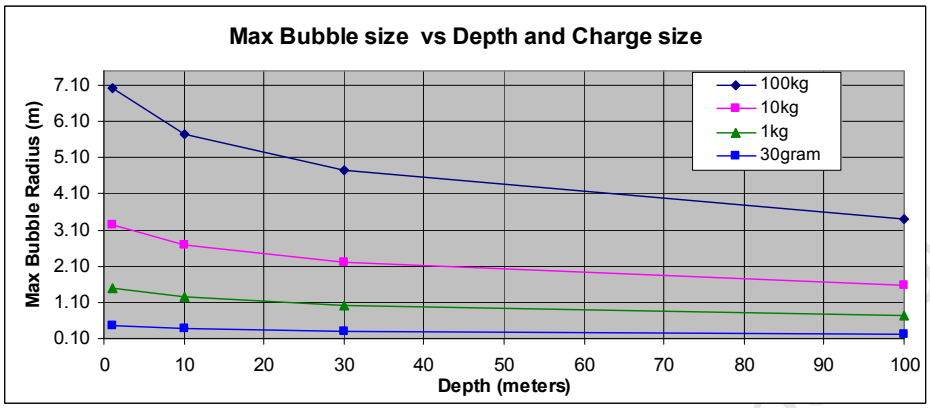

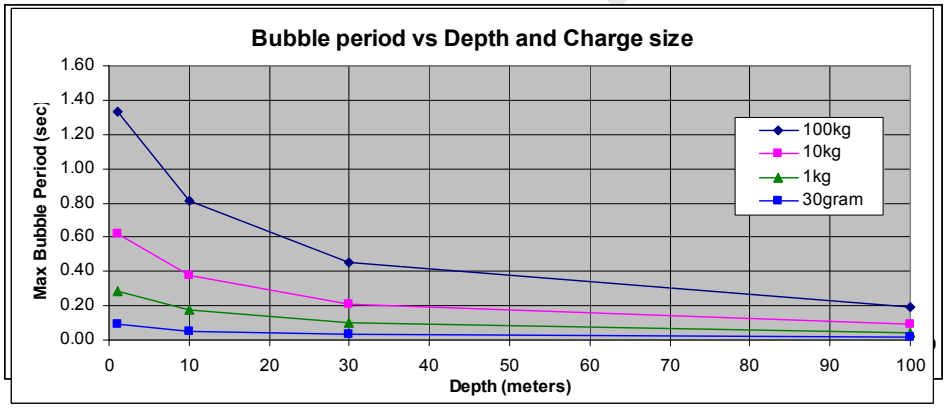

Figure 3-8: Calculated Bubble Radius vs Mass Explosive and submersion Depth

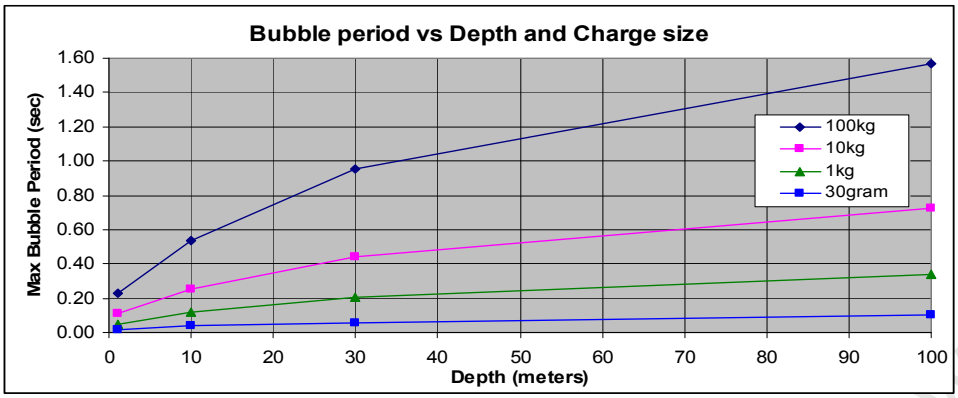

Figure 3-9: Calculated Bubble period vs Mass Explosive and submersion Depth

The general case in this dissertation is that the standoff distance is relatively small (within 5 x charge diameters) and therefore well within the radius of the fully developed bubble (~~,~~see Table 3-3).

Field Code Changed

~~A notable feature of the gas bubble is that the radius of the fully developed gas bubble is~~

From Table 4.1: TNT equivalent bubble energy factor = 1.055							
Charge size PE4 =	100	kg	10	kg	1	kg	0.03 kg
Eq. mass TNT =	106	kg	11	kg	1.1	kg	0.03 kg
Effective charge diameter if spherical	0.501	m	0.233	m	0.108	m	0.034 m
Depth below surface (meter)	1	m	1	m	1	m	1 m
Max Bubble diameter (m)	14.02	m	6.51	m	3.02	m	0.94 m
5x Charge diameter	2.51	m	1.16	m	0.54	m	0.17 m
Max bubble dia > than 5xCharge diameter	Yes		Yes		Yes		Yes

~~larger than 5 times the (spherical) charge diameter, as shown in see Table 3-3.~~

Table 3-3 : Maximum Bubble Diameter is greater than 5xcharge diameter

~~Table 3-3 : Maximum Bubble Radius is greater than 5xcharge diameter~~

~~Typical values of Bubble Radius vs 5xCharge diameter:~~

~~Charge Mass (kg)~~	~~Charge Diameter for spherical shape~~	~~5xCharge diameter~~	~~Bubble Radius~~
~~0.1kg~~	~~49mm~~	~~245mm~~	~~727mm~~
~~1 kg~~	~~106mm~~	~~530mm~~	~~1560mm~~
~~100 kg~~	~~492mm~~	~~2460mm~~	~~11600~~

Formatted Table

3.1.4 Interaction with a target plate, reflection

When reaching the target, the shock pulse is modified by the acceleration of the target plate and the shock wave is reflected back, doubling the ~~vector~~ magnitude of the shock pulse.

A principle that applies to the analysis of interaction between a body and the surrounding medium (fluid) is that the pressure is equal at adjacent points at the boundary. This also applies to a point at the boundary between two media of different density. Particle velocity is also assumed to be equal / same at adjacent points (due to incompressibility of the particles within the medium)

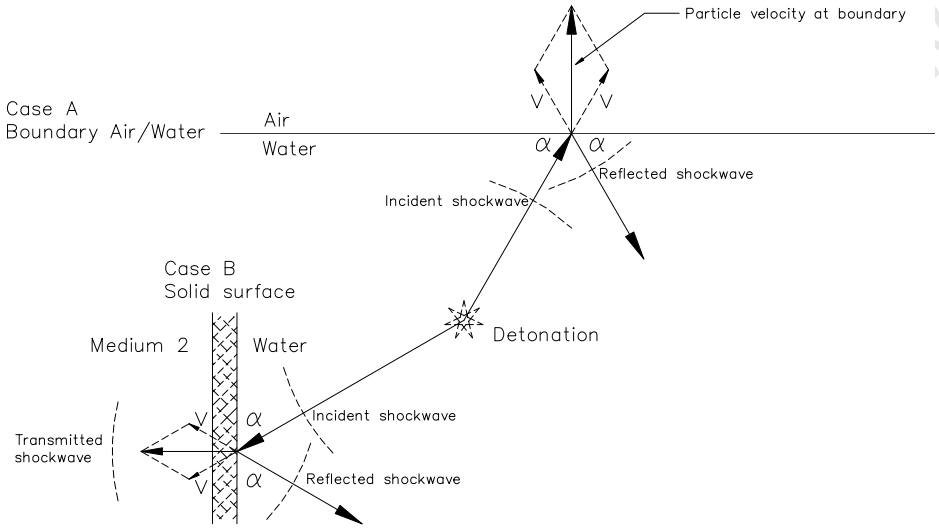

Figure 3-10 : Diagram showing a typical shock wave reflection

If the plate is initially stationary, a plane pressure wave striking it will give the plate an initial kick off velocity. As the plate accelerates, a relief wave occurs and the pressure on the struck side rapidly falls.

Rajendran [40] states (from Keil [1] and others) that the motion can be approximated from the equation

$$P_{tot} = m\frac{d^2z}{dt^2} = 2P_i - \rho c\frac{dz}{dt}$$

where m is the mass per unit area of the plate, P_{tot} is the total pressure, Pi is the incident pressure that decreases exponentially with time, dz is the displacement of each element in the direction of shock front, ρ is the density of water, c is the velocity of sound in water and t is the time which is measured from the onset of the wave.

From above equation and the pressure-time equation is

$$p(t) = P_{\cdot}e^{-t/\theta}$$

Rajendran [40] derives an equation for maximum velocity, V_{max}

$$v_{\max} = \frac{2P_m}{\rho c} x_a^{1/(1-x_a)}$$

where x_a is the inverse mass number for air backed plates, given by [40]

$$x_a = \rho c \theta / m$$

The maximum velocity V_{max} for air backed plates is reached when the resultant pressure falls to zero (the instant that the impacting pressure vector and reflected pressure vector is equal and opposite) [40].

The time to reach V_{max} is given by

$$t_{vma} = \frac{\theta \ln x_a}{x_a - 1}$$

From the equation for V_{max}, the kinetic energy or the energy transmitted per unit area E_{pa} for air backed plate is

$$E_{pa} = \frac{1}{2} m v_{mx}^2$$

$$= \frac{m}{2} \frac{4P_m^2}{\rho^2 c^2} x_a^{2/(1-x_a)}$$

$$= \frac{2(\rho_p h) P_m^2}{\rho^2 c^2} x_a^{2/(1-x_a)}$$

The mass per unit area in this equation is substituted by the product of ~~unit~~ density and thickness h of the plate, i.e. $m=\rho_p h$

Similar equations that apply to water backed plates are derived and given by Rajendran [40]. These equations will not be shown here.

3.1.5 Reloading

When a target panel is subjected to a shock impulse, the affected area is accelerated to a degree proportional to the magnitude of the impulse and inversely proportional to the mass of the target panel. Two types of reloading is prevalent – spray reloading from cavitation effects and shock reloading (often called water hammer) from the expanding bubble.

Bodily movement due to shock impulse causes reloading of the panel, as described below. Relatively thick panels are less affected due to the stiffness and therefore limited movement when struck by a shock wave.

Considering a slender (low thickness to span ratio) plate, the impact of the shockwave accelerates the panel to a high velocity within a very short time. As illustrated in Figure 3-11~~Figure 3-11~~~~Figure 3-11~~, the pressure on the impacted side decreases rapidly and cavitation sets in over the affected area of the panel. During this process, the affected water particles move towards the moving panel but fall behind due to the formation of bubbles. As the plate is retarded near the elastic limit (assuming no breeching of the panel) the water particles catch up with the panel, impart their momentum to the panel and form a layer of water that moves with the panel. This effect, called spray reloading, occurs during the first phase of the deflection. The energy from this reloading stems from the shock impulse.

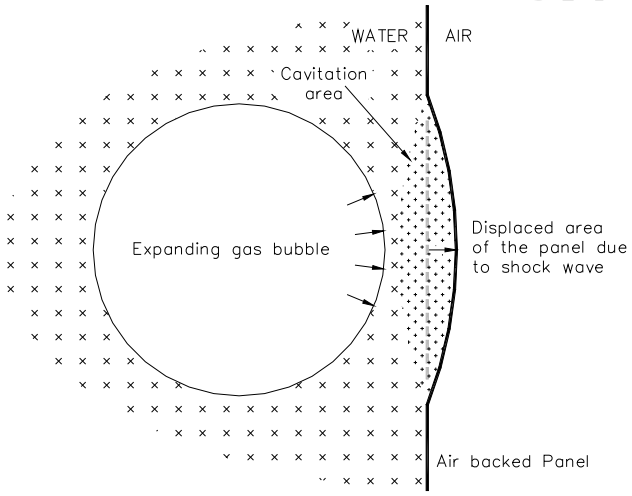

Figure 3-11 : Reloading due to cavitation collapse and bubble expansion

When the panel has slowed down and stops moving, that portion of the water that moved with the panel also stops. The water between the panel and the expanding bubble is pushed ahead towards the panel. The moving water implodes the remaining cavitation bubbles and the body of moving water impinges onto the layer of water that is stationary against the deflected panel. This second loading stems from the energy in the bubble. Snay [10] presents a graph that is shown in Figure 3-12~~Figure 3-12~~~~Figure 3-12~~.

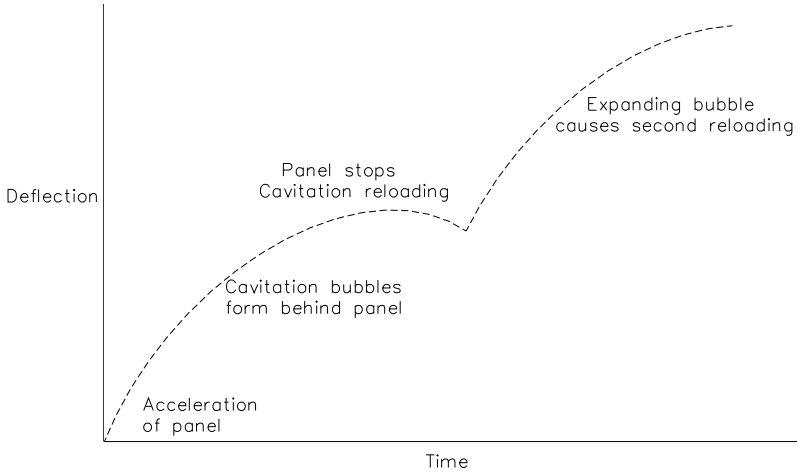

Figure 3-12 : Displacement vs time due to reloading (from Snay [10])

Closure of the cavitated space by the interaction of the expanding gas bubble causes major reloading (water hammer reloading). Snay [10] notes that cavitation is a prerequisite for liberating the energy of the bubble through water hammer reloading.

Rajendran [44] states that the pressure-time history of an air-backed plate subjected to underwater explosion shows that spray reloading is almost negligible when compared to the primary pulse whereas water hammer reloading is more intense. For reloading to occur, the water head above the charge must be greater than half the stand off distance and reloading phase delivers considerably larger amount of energy to the plate than the primary pulse. The effect of reloading reaches its maximum when the depth of explosion becomes twice the stand off.

3.1.6 Yielding behaviour and Shock Factor

For a relatively small intensity of shock impulse, the stresses developed in the plate are in the elastic range.

As the intensity of the shock impulse increases, the plate attains its limiting elastic range beyond which it undergoes plastic (permanent) deformation.

As the intensity of the shock impulse is increased even more, the plastic limit is exceeded and the plate is ruptured. The rupturing starts as tearing at a point of maximum strain, growing radially outwards or along a stiffener or support.

The prime interest of this thesis is in the domain where tearing occurs, ie beyond plastic deformation and beyond the point of yielding.

The Shock Factor (SF) is a convenient indication of shock energy. It is a dimensionless value that is used to compare the energy of different charges with different mass at different offset distances, especially at offset distances less than the 5-times-diameter limit that applies to the equations for peak shock pressure and shock impulse.

The shock factor *SF* is given by Keil [1]

$$SF = 0.445\ (W^{1/2})/S \quad \text{(imperial units)}$$

When converted to metric units the constant changes and the equation becomes

$$SF = 0.211\ (W^{1/2})/S \quad \text{(metric units)}$$

Formatted: Tab stops: 1.18", Left + 3.05", Left + Not at 0.98"

where *W* is the TNT equivalent mass (kg) of explosive and *S* is the stand-off distance (m).

The Shock Factor (SF) is a dimensionless value that is mathematically **not** restricted to a distance limitation away from the target. The SF is used by many authors, especially in cases where the detonation phenomena are viewed in the broader sense.

The value of *S* used in the equation for SF can be defined in either of two forms :

a) Offset Distance (OD) which is the physical distance from *charge face to target surface* or
b) Core Offset Distance (COD) which the physical distance from the *core (centre) of the charge* to the face of the target.

Whether the one or the other is used is not important, as long as consistency prevails in using the value of S.

However, at very small offset distances the SF based on COD has a very important advantage – division by zero is avoided when COD is used.

Consider the SF when expressed with S = OD:

$$SF_{OD} = 0.\sout{445}\ 211\ (W^{1/2})/(OD)$$

When OD becomes very small and approaches zero, the value of SF_{OD} approaches infinity.

Consider the SF when expressed with S = COD:

$$SF_{COD} = 0.\text{~~445~~}211\ (W^{1/2})/(COD)$$
$$= 0.\text{~~445~~}211\ (W^{1/2})/(OD+½D_e)$$

The value of COD equals OD plus half the effective diameter of the charge (D_e). When OD becomes very small and approaches zero, the term ½D_e ensures that division by zero is eliminated and the value of SF reaches a finite limit. This effect is illustrated in Figure 3-13.

The slope of SF_{COD} does not change significantly when the offset distance approaches zero.

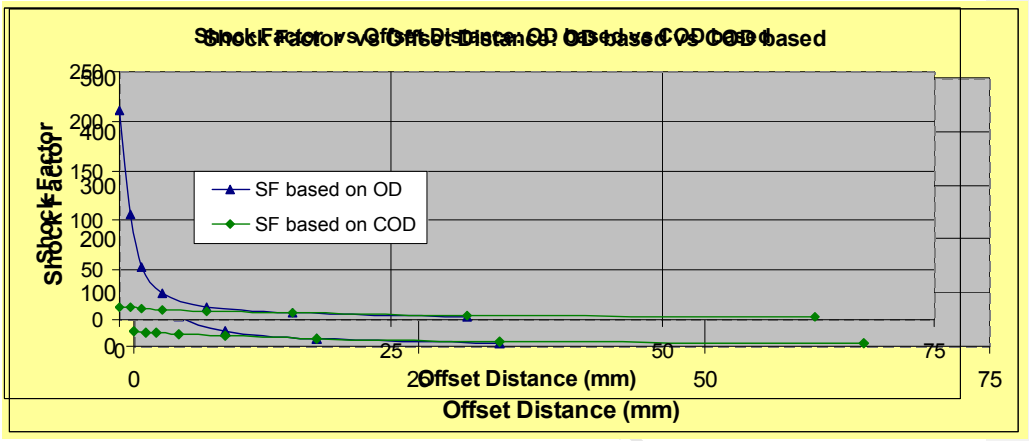

Figure 3-13: SF as a function of OD and of COD for a single mass (1kg)

When the SF for different masses is calculated as listed in Table 3-4, a set of graphs as in Figure 3-14~~Figure 3-14~~~~Figure 3-14~~ is obtained.

Table 3-4 : SF for different charge Masses and Offset Distances

From Table 4.1: TNT average equivalent factor = 1.2

Charge size PE4 (=TNTx1.2) (kg)	100	10	1	0.03
Charge size TNT (kg)	120	12	1.2	0.036
Offset Distance 10 mm	534	169	53	9.2
100	53	17	5.3	0.9
250	21	6.8	2.1	0.37
500	11	3.4	1.07	0.18
1000	5.3	1.7	0.53	0.09
1500	3.6	1.19	0.36	0.06
2000	2.7	0.84	0.27	0.05
Offset Distance (kg PE4)	231	73	23	4.0
	23	7.31	2.31	0.40
	9.2	2.92	0.92	0.16
	4.6	1.46	0.46	0.08
	2.3	0.73	0.23	0.04
	1.5	0.49	0.15	0.03
	1.2	0.37	0.12	0.02

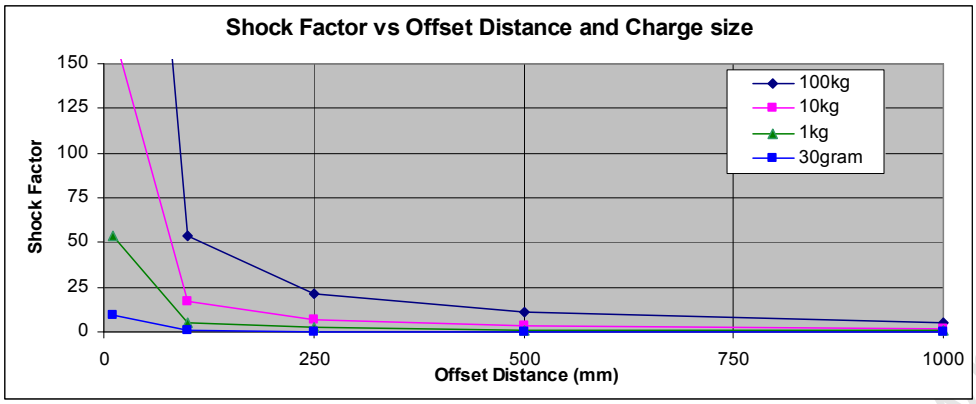

Figure 3-14: Shock Factor vs Offset distance and Charge Mass

Rajendran [40] states that the charge mass *W* in kg and stand off distance *S* in m required for generating the required shock factor for yielding at the given time constant are :

$$W = \left(\frac{SF}{0.445}\right)^{0.5946}\left(\frac{\theta}{96.6\times10^{-6}}\right)^{2.7026}$$

$$S = \left(\frac{0.445}{SF}\right)^{0.7027}\left(\frac{\theta}{96.6\times10^{-6}}\right)^{1.3513}$$

Work done by Finnie [47] has shown that the impulse per unit deformation has a linear relation with the original thickness of the plate and that the impulse required for rupture increased linearly with the original thickness.

3.1.7 Strain rate

The strain rate (deformation per unit length per time) of a metal plate has a significant effect on the extent of tearing and fracture. Keil [1] reports that the strain rate experienced during deformation process of an underwater explosion is in the range of 1to100 per second. Rajendran states that strain rates up to 500 s^{-1} have been reported.

3.1.8 Contact underwater explosion

Keil [1] reports that tests with contact charges on a discarded Japanese battleship were done in 1924. Subsequent scaled model testing by Keil indicated that the depth of submergence did not have an influence on the damage potential of a contact explosion.

This statement by him has two implications to the present work –

- Firstly, the pressure due to water depth is negligible regarding the damage (hole

size) of a target.

- Secondly, his observation could imply that the maximum size of the bubble (which is dependant on depth) is not important. What is important is the amount of energy contained in the bubble (which is not dependant on depth)

Keil [1] described a definite relation between radius of hole *R* (m), plate thickness *h* (m) and explosive weight *W* (kg) for *contact* detonations (*R* and *h* are in m and *W* is in kg)

$$R = 0{,}0704*(W/h)^{1/2}$$

He stated that the critical (minimum) mass W_{cr} of explosive above which this relation is valid, is given by

$$W_{cr} = 2.72*h$$

The basis on which the above predictions were obtained is not described. A recent analytical prediction for the radius of the hole that is bored is given by Rajendran [32]

$$R = ((2\,ή\,W_{EqTNT}\,E_{TNT}\,J)/(\pi\,h\,\sigma_y\,\varepsilon_f))^{1/2}$$

where E_{qTNT} is the TNT equivalent of the explosive , E_{TNT} is the energy of TNT in kcal/kg, *J* is the mechanical energy conversion unit, *ή* is the coupling factor which is equal to 0.1237 and ε_f is the fracture strain.

Rajendran [41] refers to the shock factor as used by other authors. He proposes an "Effective shock factor" due to incomplete transfer of energy from charge to target. He introduces a "Coupling factor" that is about 55%. He derived an equation for the total energy transferred to the plate. Only primary shock pulse is considered. Cavitation reloading and bubble pulse is not considered because these phenomena have no influence (due to time intervals).

This statement by Rajendran [41] seems to contradict the statement by Snay [10]. The only explanation is that the two authors refer to different conditions, for example [41] considers contact charges only and [10] refers to a charge with an offset distance. In references [40] and [44], Rajendran does actually state that the effect of reloading reaches its maximum when the depth of detonation becomes twice the stand off.

3.2 Current knowledge

The current understanding of the UNDEX phenomena, in approximate chronological order, as developed over the research period is summarised in the following paragraphs.

When the explosive detonates in a liquid medium, a detonation front moves from the point of initiation, through the charge and, when reaching the physical boundary of the charge body, moves spherically out beyond the charge into the surrounding medium.

During detonation, the detonation front moves as a shock wave through the explosive material at the VOD (velocity of detonation) and enters the liquid medium (eg water) at VOD (about 7000m/s). After entering the liquid medium, the shock wave slows until it reaches the speed of sound in the liquid medium (about 1450 m/s in the case of water) at a distance of about 5 times the charge diameter. From this point on the shock wave travels at the speed of sound in that particular liquid medium.

The shock wave strikes the surface of a target. This gives rise to a reflected shock wave which moves back towards the reacting explosive. A transmitted stress wave enters the target and moves at or above the speed of sound of the target material (about 6000 m/s for steel) [21].

If the target panel is relatively thin, it is physically accelerated in the direction of the shock wave. The magnitude of the acceleration and subsequent amount of movement depends on the thickness (mass per unit area) of the target panel. A thick panel will move very little, if at all.

A thin panel is subjected to spray reloading as well as water hammer due to the acceleration and movement of the panel. Tearing of a thin panel will occur if the impinging shock wave is strong enough to cause local yielding of the target panel at any point on the panel. If the yield strength is exceeded at any point on the panel, tearing occurs and a hole is breeched. Reloading due to the water hammer effect would increase the plastic deformation of the panel. If tearing has occurred, size of the hole is increased due to the water hammer effect.

In relatively thick target material, the stress wave would move to the other side of the material causing compressive loading along the way. At this second interface a reflected wave is again transmitted back into the target material and a transmitted wave moves into the adjacent air/water/medium.

The reflected wave at the end of the target material results in tensile stress on the inner surface.

a) If the reflected wave is strong enough and localised relative to the thickness of the target plate, it will break a circular hole all the way to the explosive side of the plate by tearing a ring shape, causing a piece of the target to break out and bodily move in the direction of the shock wave. This is called plugging (Figure 3-15a). The occurrence of plugging is independent of the presence of a liquid.
b) If the material is relatively thick and the stress due to the reflected shock exceeds the yield strength of the material, the material fails. A piece of the target surface would break away and move in the same direction as the shock wave. This is termed spalling (see Figure 3-15b). Note: this piece breaking away causes a shallow scar in the back (exit) surface of the target. The occurrence of spalling is

independent of the presence of a liquid.

c) Petalling occurs when tearing starts at the centre of the target due to relatively localised impact of the shock impulse. If the charge is surrounded by fluid, the shock energy is transferred to the target panel much more efficiently than in air, causing a sustained force on the circumference of the central tearing. This causes the tearing to grow radially outward while the petals are formed (Figure 3-15c). Petalling tend to form only when the detonation energy is transferred to the target in the presence of a fluid.

d) If the stress is not above the failure level, the target will either plastically or elastically deform but the material will not tear or break (Figure 3-15d). The presence of a liquid is not a prerequisite for plastic deformation to occur.

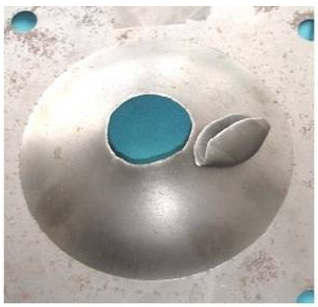

a) Plugging

b) Spalling

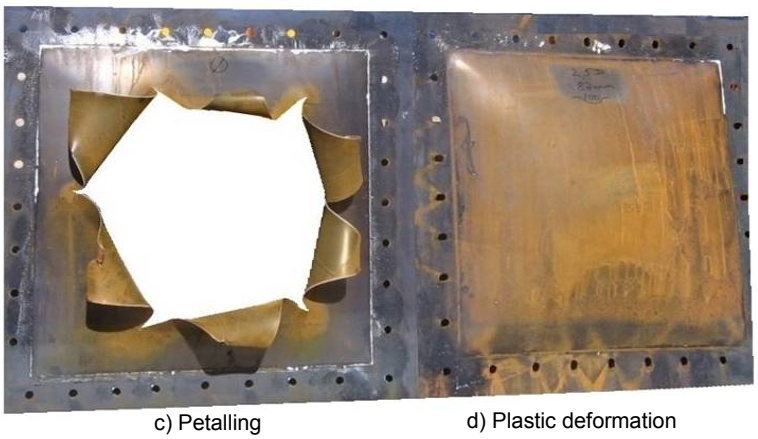

c) Petalling d) Plastic deformation

Figure 3-15 : Plugging, Spalling, Petaling and Plastic deformation

The time in which shock impulse and subsequent effects occur, is in the order of microseconds. This is followed by the rapid expansion of the explosive products that forms a gas bubble. The behaviour of the gas bubble is different in air and in water. The presence of a surface or object in the close vicinity of the detonation also influences the behaviour of the gas bubble.

In air the gas expands spherically with rapidly decreasing energy density as it moves away

from the origin and eventually dissipates. In water the gas bubble expands against the surrounding water, forming a gas bubble that is contained by the water. The gas bubble expands until the surrounding water pressure overcomes the pressure inside the bubble, causing it to collapse onto itself. This expansion and contraction occurs over a time of milliseconds, ie thousand times slower than the passage of the shock wave. The collapse of the bubble recompresses the gas and causes re-expansion into a second gas bubble.

If the expanding gas bubble in water touches a solid surface, the expansion in that direction is impeded. When the gas bubble collapses, the inflow of water on the side of the bubble towards the target is restricted. This causes the bubble to collapse towards the object surface (see Figure 3-6~~Figure 3-6~~~~Figure 3-6~~).

a) If the target has not been breeched, the water will push up against the surface and possibly deform it but is unlikely to break it (assuming the shock wave has not breeched the target).
b) If the surface is damaged but not broken, this extra load may be sufficient to plastically deform in the surface. Piercing a hole is unlikely.
c) If the shock impulse did break a hole in the target, the water will be forced into the hole and start to flow into the space beyond the target panel. This would also further the damage to the target due to momentum of the water, bending the plate into the cavity. This damage is seen as the sheet tearing into curved petals.

Provided the expanding gas bubble did not vent through the water surface to atmosphere or through the hole created by the shock impulse, the explosive gas expands to a state where the pressure inside the bubble equals the surrounding water pressure. It actually over-expands due to the momentum of the displaced water. At this point the pressure inside the bubble drops to near vacuum due to rapid cooling of the gas inside the bubble. The pressure of the surrounding water causes the bubble to contract (or collapse), and the flow of water reverses to fill this hole previously filled by gas (see Figure 3-5~~Figure 3-5~~~~Figure 3-5~~).

The collapsing bubble compresses the small amount of gas that remained within the gas bubble, generating a secondary pressure pulse that causes a jet of water into the hole (if the hole is not yet completely filled, i.e. if some air is trapped beyond the breeched surface). If no air exists into which the water jet can move, a secondary (much smaller) expansion occurs. The bubble expansion and collapse can move through a number of successive oscillations, each smaller than the previous.

3.3 Phenomena affecting the damage

The damage effect of a charge in close proximity to a target is driven by the following phenomena:

Shock wave

The charge must be close enough and/or strong enough to induce a shock impulse that is powerful enough to exceed the yield strength of the target material and initiate tearing (see par 3.1.6). A hole would develop as soon as tearing is initiated. As the distance between the exploding charge and the target is increased, the energy of the incident and therefore reflected shockwave reaching the target becomes weaker until it is too weak to result in stress that exceeds the strength of the material.

Spray reloading

Spray reloading (see par 3.1.5) is a term used to describe the reloading of the panel due to the collapse of cavitated water onto the target. The cavitated area occurs where cavitation bubbles were formed due to acceleration of the target by the shock wave. The spray reloading occurs when the cavitated water catches up with the slowing down target area. This is an important phenomenon in cases of local damage to panels, but is of lesser significance in terms of physical deformation of the target panel.

Spray reloading is different from the term cavitation as used as in general technical nomenclature, such as the sustained cavitation on a boat propeller or impeller of a pump. Spray reloading is a single occurance and then disappears.

Gas bubble

Nearly half of the energy of the detonation is carried by the first gas bubble that forms during a detonation under water. ~~Part of t~~This energy is inflicted onto the target panel by ~~spray reloading (cavitation effect),~~ water hammer (during bubble expansion) and by secondary shock impulses (during subsequent bubble collapse).

~~**Spray reloading**~~

~~Spray reloading (see par 3.1.5) is a term used to describe the collapse of a pocket of cavitated water onto the target. It occurs in areas where cavitation bubbles were formed due to a reflected shock wave. This is an important phenomenon in cases of local damage to panels, but is of lesser significance in terms of physical deformation of the target panel.~~

~~Spray reloading is different from cavitation as used as in general, such as the sustained cavitation on a boat propeller or impeller of a pump. Spray reloading is a single occurance and then disappears.~~

Water hammer

As explained in paragraph 3.1.5, water hammer does inflict major damage on panels that are relatively thin. The water hammer effect can only be effective in cases where a non-zero standoff distance exists and some water is present between the target panel and the charge.

Bubble collapse

The collapsing bubble can cause a jet of water. In the proximity of a target surface within

the bubble radius, the bubble would collapse towards the panel. A mass of water rushes towards the panel, gaining significant momentum. If the target panel was breeched by the shock impulse, then the damage due to the momentum of the water is likely to be of bending and tearing nature (versus the explosive damage being a cutting nature).

Momentum of the water

It is important to keep in mind is that the momentum of the water on its own cannot cause tearing or holing of the target. It is a prerequisite that a hole is created by the preceding shock impulse. Referring to plastic deformation, Rajendran [44 p279] states that the damage caused by the reloading component is almost equal to that of the damage caused by the primary pulse. He states that this observation is in good agreement with the experimental observation of Ezra [46].

When the bubble collapses, some water may be drawn back out of the hole. That will have the effect of reducing the size of the hole by pulling the petals inwards. However this effect is expected to be small because it is a relative slow process and involves low volume of water.

Charge shape

This could certainly have an effect on the damage to a target panel. The effect of shape was not investigated at all.

Hot detonation products

In case of a contact charge that breeches an air backed panel, the detonation product gas would vent through the breeched hole without resistance and the gas bubble will not be able to develop properly. The hot gas (~3000°C [8]) from the detonation products causes the target material to momentarily heat up. Due to the low density of the gas, it will not be able to inflict significant damage, apart from heating and temporarily softening the material.

Offset distance

The physical damage inflicted by the shock impulse is inversely proportional to the offset distance. The damage inflicted by the gas bubble and associated phenomena is the subject of investigation of this thesis. It is believed that this damage initially increases proportionally to the offset distance and then decreases when the offset distance is further increased.

3.4 Hypothesis

The damage done to a submerged target when a detonation occurs in very close proximity is caused by two phenomena – the shock impulse (very short duration, very high peak pressure) and the gas bubble (longer duration, lower peak pressure). About half of the energy of an underwater detonation is transferred to the gas bubble (see Figure A).

The impact of each of these two phenomena on the target is separated in time. In addition, the mechanism of causing damage is different. The shock impulse is most effective in contact with the target whilst the bubble requires to be separated from the target in order to develop.

It is postulated that, due to the difference in nature and timing of these two phenomena, the offset distance between the charge and target can be optimised for maximum damage (ie hole-size)

The pressure impulse is most effective when in direct contact with the target. As the distance between the detonation and the target surface increases, the effect of the shock impulse decreases due to attenuation and losses. The holing of the target gradually reduces with increasing distance. A distance is reached beyond which the target is not breached and only plastic deformation occurs.

The damage potential of the gas bubble is an opposite function of distance from the target. The development of the gas bubble is impeded close to the target. As the distance from the target increases, the gas bubble can develop more fully and therefore contribute more to the damage of the target. If it can be proven that the gas bubble contributes to enlarging the hole in the target, and that the bubble needs to have a non-zero offset distance in order to have maximum effect on the target, then it follows that it should be possible to find an optimum (non-zero) offset distance in which the combined effect is larger than having the charge in direct contact with the target.

This thesis is an attempt to prove (or disprove) that such a non-zero optimum offset distance exists.

Finding such an optimum offset distance should be possible if the effect of the shock impulse can be separated from the effect of the bubble. Each effect is then characterised and represented as a function of offset distance. The two functions could then be combined and an optimum offset distance determined.

4 Chapter 4: PLANNING OF FIELD WORK

4.1 Objective of the tests

The objective of the tests was to prove the hypothesis that the combined effect of the shock impulse and the gas bubble of an underwater detonation can be optimised for maximum hole-size and that the optimum offset distance is a non-zero value (ie charge not in direct contact with the target surface).

The initial requirement for the field testing was to physically demonstrate and quantify the contribution of the shock impulse *separate* from the contribution of the gas bubble.

It was anticipated that the effect of the shock impulse alone could be demonstrated by detonating the charge very close to the surface of the water (forcing the bubble to vent to atmosphere, thereby eliminating the effect of the gas bubble) versus detonating at a depth greater than the maximum size of the bubble (demonstrating the combined effect of shock and bubble). The results of initial tests indicated that such a separation is not a simple matter. The effects of these two phenomena (shock impulse and gas bubble) appear to be very interdependent. The holes size of the surface-detonated events and the deeply submerged events were very comparable and in some cases larger when they were expected to be smaller.

This requirement (of separating the effect of shock impulse and bubble effect) was subsequently changed to that of investigating the combined effect of the shock impulse and the bubble phenomena of a charge without separating them.

4.2 Requirement of the test equipment

The basic requirement of the testing was to subject an air-backed target surface (steel sheet) to an underwater blast. A replaceable target was required and had to be supported by a robust frame. The removable faceplate had to be subjected to a well controlled underwater blast.

The variables had to be strictly controlled in order to isolate the effect of changing specific parameters.

Three variable parameters were addressed:

- Offset distance (distance between charge and target surface)
- Depth below water surface
- Orientation of the test piece (face up/down)

Parameters that were planned to remain constant were:

- Mass, shape and orientation of the charge
- Initiation geometry and energy
- Thickness, size, material and fixing of the faceplate

Other important considerations were:

a) Multiple testing.

   It was required that the test installation had to be used repeatedly, providing a consistent base for the testing. This refers to both consistent conditions and

robustness of the test equipment.

b) Charge Mass

The size of the charge needed to be large enough to minimise scaling effects, yet small enough to suit the available demolition test ranges. The mass of the charge was chosen to be 30 grams of PE4. The reasons for this choice is that the BISRU blast chamber can accommodate this size charge in air blast and this size charge can be detonated in water very close to the quay-side in sea water.
The type of explosive chosen was PE4 due to availability and similarity to RDX (which is a practical reference compound in general literature)

c) Change as little as possible.

A principle decision was made to keep the charge and the test housing unchanged throughout the test series. The thickness of the faceplate (target) was planned to remain the same throughout testing, with the option to change if required.

d) Ruggedness of the charge housing

The ruggedness of the target housing is very important in order to ensure repeatable use.

4.3 Planning

4.3.1 Design of the Target and Test Series

4.3.1.1 Size of the Target Face

The size of the target face had to be large enough to cover most (if not all) of the gas bubble under water. For practical reasons the test depth was decided to be not more than 2 meters, being half the depth of the sea alongside the quay where the testing was to be done.

The charge used was 30gram, which would yield a gas bubble of 0.49m radius (see row 14 in Table 4-1). In practice (according to Shin [17]) the effective radius is 80% of the theoretical value. This yields a required face diameter of at least 780 x 780 mm.

The actual size chosen was 900x900mm, of which the outer perimeter of 100mm consisted of a heavy flange. The actual exposed area of the faceplate was 700x700mm.

The faceplate had to be fixed with as many bolts as practical and tightened as much as possible in order to minimise elongation of the bolt holes in the faceplate. A row of locating studs was placed in-between the bolts.

Table 4-1 : Calculation of Peak Pressure and Bubble Radius

Charge size (PE4)	**30** gm				
Charge size (PE4) Equivalent TNT	**30** gm				
Charge shape (Length = Diameter) L=D	28.8 mm	(cylinder)			
Charge shape (Length = diameter) L=D	28.8 mm	(cylinder)			
Effective Charge diameter **De**	**33.0 mm**	(sphere)			
Effective Charge diameter **De**	**33.0 mm**	(sphere)			
Distance below surface	**2.0 m**				
Dist. Charge face to Target =	0.001 m	0.010 m	0.100 m	1.000 m	10.000 m
Dist. Charge face to Target =	0.001 m	0.010 m	0.100 m	1.000 m	10.000 m
Depth below surface =	2.0 m 6.6 ft	2.0 m 6.6 ft	2.0 m 6.6 ft	2.0 m 6.6 ft	2.0 m 6.6 ft
Depth below surface =	6.6 ft	6.6 ft	6.6 ft	6.6 ft	6.6 ft
Charge size	**0.03 kg PE4**				
Charge size (PE4)	0.03 kg PE4	0.079 lb			
Equivalent TNT Charge size	0.036 kg TNT				
Equivalent TNT Charge size	0.036 kg TNT	0.079 lb			
Max Bubble Radius A	0.487 m	0.487 m	0.487 m	0.487 m	0.487 m
Max Bubble Radius A	0.779 m**	0.779 m**	0.779 m**	0.779 m**	0.779 m**
80% bubble diameter	0.779 m**	0.779 m**	0.779 m**	0.779 m**	0.779 m**
80% bubble diameter	0.0986 sec	0.0986 sec	0.0986 sec	0.0986 sec	0.0986 sec
Bubble Period	0.086 sec	0.086 sec	0.086 sec	0.086 sec	0.086 sec
Peak Pressure*	48688 Mpa*	9217 Mpa*	2137 Mpa*	1147 Mpa*	1 MPa*
Peak Pressure*	48688 Mpa*	9217 Mpa*	2137 Mpa*	1147 Mpa*	1 MPa*
Equivalent Freq.	11.7 Hz	11.7 Hz	11.7 Hz	11.7 Hz	11.7 Hz
Equivalent Freq.	11.7 Hz	11.7 Hz	11.7 Hz	11.7 Hz	11.7 Hz

* if **#value!**, then value is outside proven range of equation (250MPa)
** Green: No Venting to free surface (bubble radius < 80% depth)
** Yellow: Venting will occur to free surface (bubble radius > 80% depth)
** Yellow: Venting will occur to free surface (bubble radius > 80% depth)

Max Bubble radius (ft):	$A(mx) = K_6(W^{1/3})/(D+33)^{1/3}$
Max Bubble radius (ft):	$A(mx) = K_6(W^{1/3})/(D+33)^{1/3}$
Peak Pressure (psi):	$P(mx) = K_1((W^{1/3})/R)^{A_1}$
Peak Pressure (psi):	$P(mx) = K_1((W^{1/3})/R)^{A_1}$
Decay constant (sec):	$\theta = K_2*(W^{1/3})*((W^{1/3})/R)^{A_2}$
Decay constant (sec):	$\theta = K_2*(W^{1/3})*((W^{1/3})/R)^{A_2}$
Bubble period (1st):	$T = K_5*(W^{1/3})/(D+33)^{5/6}$
Bubble period (1st):	$T = K_5*(W^{1/3})/(D+33)^{5/6}$

W= weight explosives in lb
W= weight explosives in lb
D= depth of explosive in ft
D= depth of explosive in ft
K = konstante ex notes
K = konstante ex notes
R = standoff distance in ft
R = standoff distance in ft

[Ref: Cole RH "Underwater Explosions" page 122, 1949, Princeton University Press, Princeton, New Jersey]
[Ref: Cole RH "Underwater Explosions" 1949, Princeton University Press, Princeton, New Jersey]

		--- TNT ---
P(max)	K_1	22505
P(max)	K_1	22505
	A_1	1.18
Decay Constant	K_2	0.0058
Decay Constant	K_2	0.058
	A_2	-0.185
Impulse	K_3	1.798
Impulse	K_3	1.798
	A_3	0.98
Energy	K_4	3034.9
Energy	K_4	3034.9
	A_4	2.155
Bubble Period T	K_5	4.268
Bubble Radius A(mx)	K_6	4.268
Bubble Radius A(mx)	K_6	12.67

Material	Shock Wave energy PE4	Shock Wave energy TNT	Bubble energy PE4	Bubble energy TNT	Ave-rage
Pentolyte	1.00	1.19 g	1.00	1.06	1.13
PE4 = RDX	1.10	1.31	1.02	1.09	1.20
TNT	0.84	**1.00**	0.94	**1.00**	**1.00**
Torpex 4B	1.062	1.262	1.633?	1.737	1.5?
HBX-3	1.00	1.19 g	1.95	2.07	1.60

Approx. Equivalent energy weight ratios for u/w explosives
[Source: NSWC/WOLTR-116]

4.3.1.2 Thickness of the Faceplate

The thickness of the faceplate was chosen to be 3mm standard mild steel rolled plate. This thickness and material has been used with success in similar tests. The thickness and material of the faceplate could be changed in future, if experience indicates another thickness is required.

Most field testing was done using the 3mm faceplate. A thinner faceplate of 1,2mm was used for the final set of field tests.

4.3.1.3 Physical Design, Shape and Volume of the Test Housing

Using relatively heavy construction was imperative in order to ensure that the test housing would not be damaged by repeated blasts. The thickness of the sidewalls was chosen to be 12mm. The fixed flange with bolt holes was also made from 20mm steel plate. Twenty-four

bolts of diameter 12mm were used to fix a 20mm thick removable flange to the base flange. The faceplate was clamped between the removable flange and the fixed flange. Retaining studs were installed in-between the bolts, providing additional clamping grip to limit the inward creep of the edges of the target plate (see Figure 4-2~~Figure 4-2~~~~Figure 4-2~~)

The geometry of the test housing was calculated such that the total mass of steel had to be slightly more than the total displacement of the test assembly (see Table 4-2). The depth of the housing needed to be at least 350mm (half the face diameter) to allow free deformation of the face. An internal depth (height) of 500mm was chosen.

Table 4-2 : Calculation of the Size and Shape of the Test Housing

B (face area) =	700	mm	Input
Plate thickness h =	20	mm	Input
Overhang width w =	100	mm	
L (outside) =	900	mm	
b = crown width	80	mm	Input
Housing only			
H (height) =	500	mm	
Clamping plate thickness	20	mm	input
Volume =	6.4	liter	
Displacement =	6.56	kgf @1025kg/m3	
Total volume =	109	liter	
Displacement =	111	kgf @1025kg/m3	
Inside Volume =	83.1	liter	
Outside Volume =	109	liter	
Material volume =	25.5	liter	
Material Mass =	192	kg @7550kg/m3	
Difference =	-81	pos = float	
		neg = sink	
Faceplate thickness =	3	mm	
Length = Width =	900	mm	

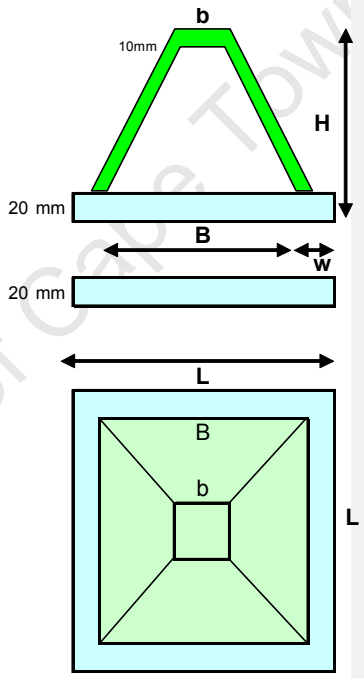

The housing needed to be fully enclosed in order to maintain an air volume behind the target face plate as the housing would be totally submerged during testing. At the same time, it had to be slightly negatively buoyant.

It transpired that the shape of the test housing had to be a truncated pyramid. If the shape approached that of a cube, the assembly becomes positively buoyant. See Figure 4-1~~Figure 4-1~~~~Figure 4-1~~ and Table 4-2 for detail.

The face of the test plate was made square (instead of circular), for ease of construction.

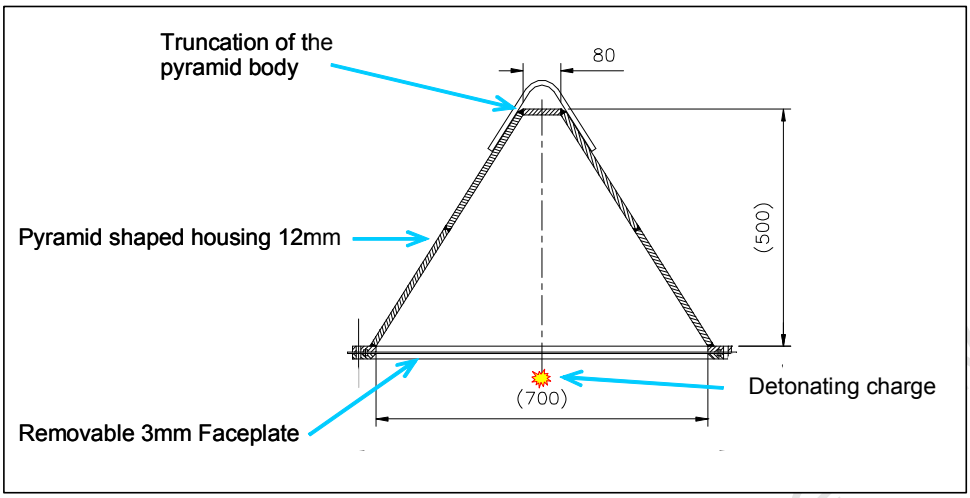

Figure 4-1: The geometry and dimensions of the target and housing

A modified version of this housing was used for a specific series of tests at the end of the field work. This modified housing is discussed together with the description of the relevant tests.

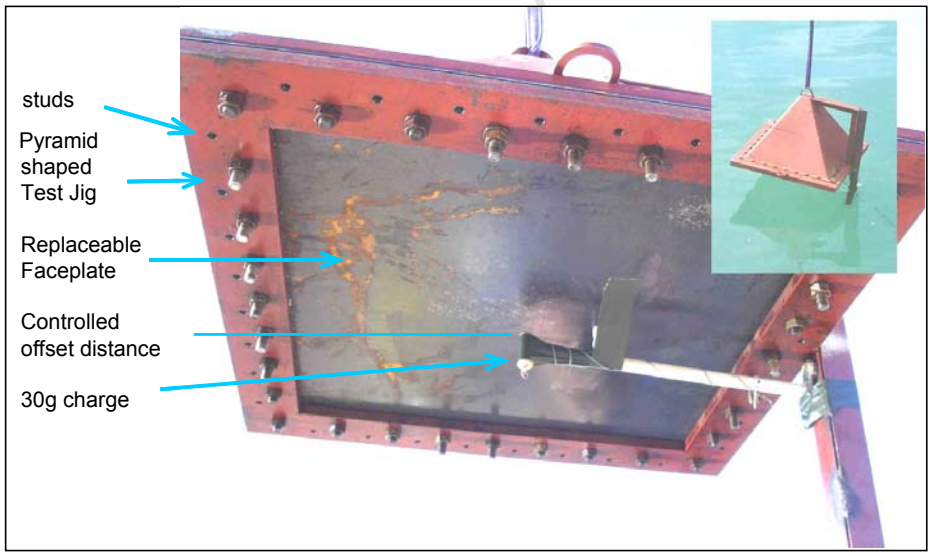

Figure 4-2: The pyramid shaped test housing and target face

4.3.1.4 Dimensions of the Charge

The ideal shape of the charge would be a sphere, but this is difficult to fabricate and initiate. The proposed shape of the charge was an approximation of a sphere by using a cylindrical charge of which the length and height is equal. A charge mass of 30 gram renders a value of Length = Diameter = 28.8 mm (see Table 4-3~~Table 4-3~~~~Table 4-3~~). Having L = D ensures that any effect due to the non-spherical charge shape used for this thesis has minimum impact.

In most literature [eg 8, 25, 35, 37, 40 etc] the distance from any point of interest to the charge is conveniently expressed as a multiple of charge diameter. This is a dimensionless parameter usually based on the diameter (or radius) of a spherical shaped charge.

Initially it was planned to mould the PE4 into an accurately machined mould. However, the charge distorted very easily when removed from the mould. It was then decided to use a rigid container to keep the charge in shape. A plastic container that had an internal diameter of 29mm was found and was used throughout (see Figure 4-4~~Figure 4-4~~~~Figure 4-4~~). The charge was weighed and then pressed into the plastic container. This ensured a consistent mass and shape of the charge.

Table 4-3 : Dimensions of the charge

Charge size (PE4)	30 gm	Container inside diameter	29.3 mm
Charge shape (L equal to dia) L=D	28.8 mm	Required Charge Mass	30 gm
Equivalent Spherical diameter D_e	33.0mm	Calculated height of filling	28 mm

4.3.2 Definitions

Figure 4-3~~Figure 4-3~~~~Figure 4-3~~ depicts the principle parameters that are referred to in this work.

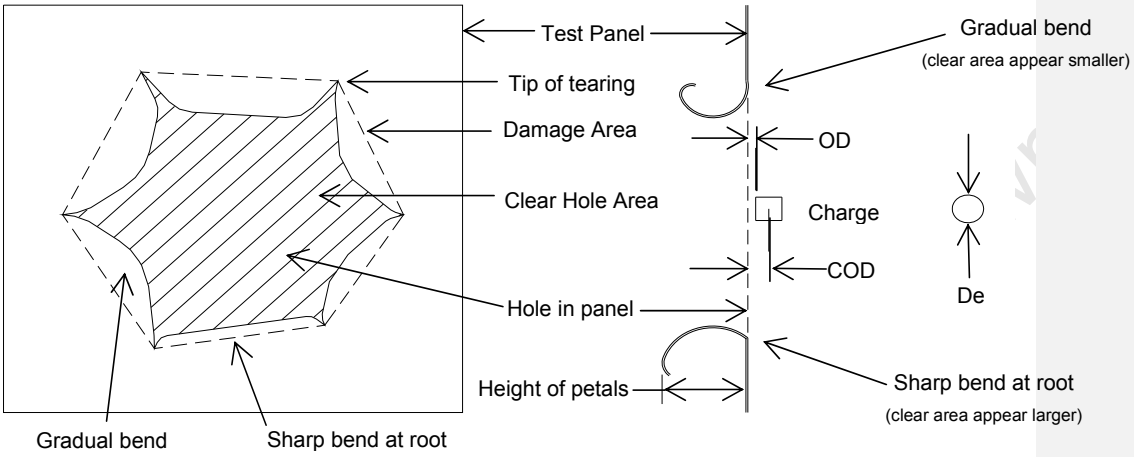

Figure 4-3: Definition of parameters

Definitions	
Clear Hole Area	the projected area of the clear hole
Damage Area	the projected area within the boundary that connects the tips of the tearing
Effective charge diameter (De)	the diameter of a spherical charge representing the same mass as the charge actually used
Offset Distance (OD)	the distance of free space (in millimetres) from the face of the charge to the surface of the target
Core Offset Distance (COD)	the distance from the centre of the charge to the surface of the target. The core offset equals the Offset Distance plus the radius of the charge, when the charge is assumed to be spherical
Offset Distance Ratio (ODR)	the Offset Distance divided by the Effective Charge Diameter (dimensionless value)
Core Offset Distance Ratio (CODR)	the Core Offset Distance divided by the Effective Charge Diameter (dimensionless value)

Notes on OD and COD

- The value of OD (and therefore the dimensionless value of ODR) is measured from the external surface of the charge. It therefore ignores the distance charge face to charge centre and subsequently does not fully take into account the physical size of the charge.
- The value of COD is referenced to the centre (core) of the charge. Therefore the

size (ie mass) of the charge is represented in the dimensionless value CODR.

- As the value of OD becomes smaller, the difference in ODR and CODR becomes greater. In the extreme case that OD = zero, then ODR equals zero as well. At the same time (when OD = zero), then COD equals the Radius of De and therefore CODR = 0,5

4.4 Physical execution of the tests

The typical steps during a test were:

a) Physical preparation of the test housing (fitting of target faceplate, handling straps, demolition wires etc).

b) Weighing the NEC mass (30gm) and moulding the explosive into the container.

c) Fitting the charge to the target and setting the offset distance from charge face to target face.

d) Fitting the detonator, laying the firing cable and testing for continuity.

e) Lowering the test housing into the water.

f) Upon the "all clear" from the demolition officer, the charge was command detonated from the quay.

g) The test housing was then lifted back onto the quay and the faceplate removed.

These steps are described in more detail in Paragraphs 4.4.1 to 4.4.5.

4.4.1 Preparation of the Charge

In order to ensure consistent shape, mass and geometry, the plastic explosive (PE4) was weighed and cast into a standard plastic container as used for 35mm photographic film (see Figure 4-4~~Figure 4-4~~~~Figure 4-4~~).

The geometry of the film container was very close to ideal shape, ie length = height (inside diameter of container was 29.3mm versus ideal diameter = height = 28.8mm).

In order to ensure consistent initiation, a HNS booster (1g) was introduced in early testing (NEC remained 30g). The booster and detonator were secured in position by a soft rubber guide (sleeve). The booster was omitted after it was established that the detonator only consistently provided enough energy for full detonation.

A 6mm hole was made in the cover, through which the M10 electric detonator was pushed against the charge inside the container. The depth of the detonator was checked (see Figure 4-5~~Figure 4-5~~~~Figure 4-5~~)

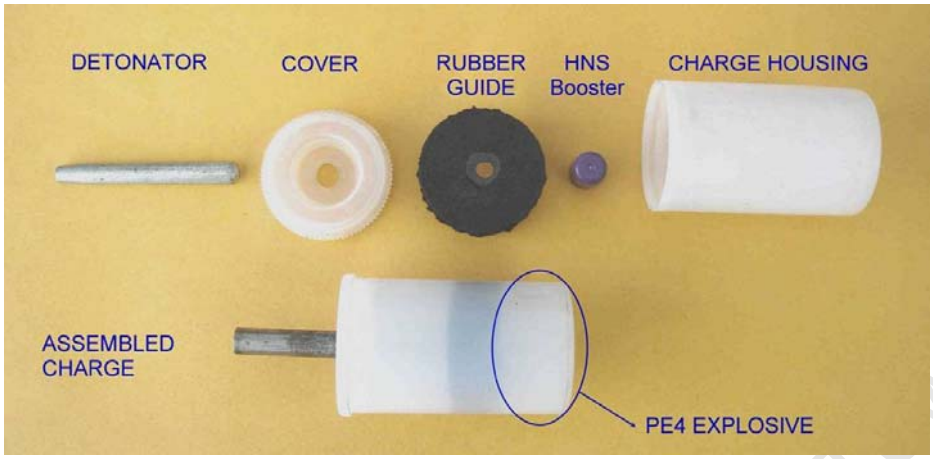

Figure 4-4 : The charge components (upper row) and charge assembly (lower row)

Figure 4-5: Checking the depth of the detonator

4.4.2 Attachment of the charge

The charge was attached to the tip of an adjustable PVC tube (Figure 4-6~~Figure 4-6~~Figure 4-6), using duct tape. The other end of the PVC tube was attached to the test housing by means of a magnet.

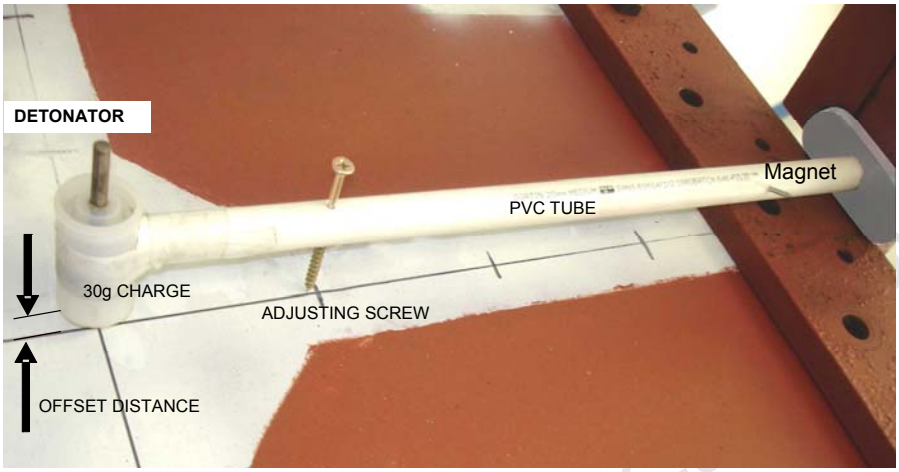

Figure 4-6 : Attachment of the charge and offset distance adjusting screw

4.4.3 Setting the offset distance

The PVC tube was secured such that the end carrying the charge tended to push towards the target faceplate. An adjusting screw (see Figure 4-6~~Figure 4-6~~Figure 4-6) was used to push the tube away from the faceplate. A set of spacers that were machined to different thicknesses were used as feeler gages to set the offset distance (Figure 4-7~~Figure 4-7~~Figure 4-7).

Figure 4-7 : Setting the OD by means of feeler gages

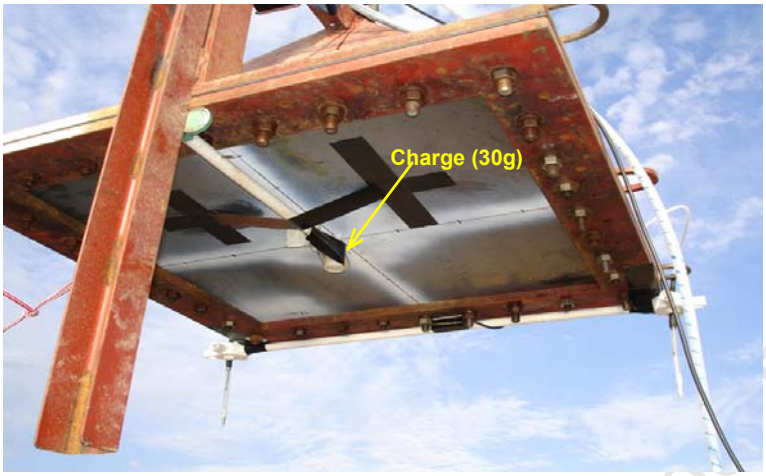

Figure 4-8: The test housing ready for submersion and detonation

4.4.4 Lowering into the water and detonation

A shore based crane was used to lower the test housing into the seawater and suspend it at the required depth. (see Figure 4-9~~Figure 4-9~~~~Figure 4-9~~).

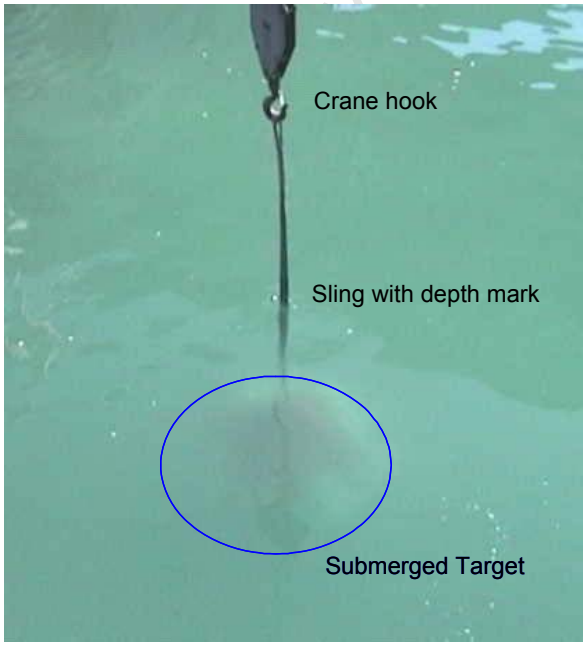

Figure 4-9 : The submerged test housing suspended from the crane

Physical detonation occurred within one minute of the housing being immersed. This ensured that very little water, if any, could leak into the housing after immersion. It should be noted that the faceplate was not fitted with a water seal, other than a tight fit onto the flange of the housing. Detonation was initiated while the test housing was hanging from the crane, at the required depth (Figure 4-10~~Figure 4-10~~~~Figure 4-10~~)

Figure 4-10 : Surface effects due to reflected shock wave

4.4.5 Recovery and Re-Preparation

The total time of immersion during each test was about one minute, from entering into the water to removal after detonation.

The clamping bolts on the test housing were loosened using a pneumatic wrench. This was required due to excessive friction by the deformed faceplate on the shanks of the bolts. (This problem was effectively solved during later tests, by using longer bolts in which the thread started beyond the edge of the face plate).

The deformed faceplate was removed and washed with fresh water.

Preparation for the next detonation cycle started.

5 Chapter 5: ACTUAL FIELD WORK

The field work was performed over a period of three years. The initial exploratory testing revealed a number of problems that were imperative to eliminate with the test equipment. Problems such as unwanted deformation of the test housing (flange was subsequently reinforced), excessive jamming of the test panel onto threads of the bolts (increase length of unthreaded shank, also studs added), accuracy of charge shape and weight (subsequent accurate weighing and use of rigid container) were encountered and solved. Test results from these initial tests are mentioned but not used in this dissertation.

After the test equipment and test procedures were finalised, a number of systematic tests were performed. The first systematic tests (Group 1 and partly Group 2) was an attempt to distinguish between the effect of the shock impulse alone, separated from the effect of the bubble. This was done by placing the target face up near the surface and face down submerged. The resulting damage to the target was very similar (less than 10%), when a difference of about 30% was expected. It was clear that the two effects are much more interdependent than anticipated. The actual difference was considered too small and proved to be impractical with the available test equipment. It was therefore decided to evaluate the combined effect.

These tests were followed by two groups of tests of different offset distances using a 3mm test panel (Group 2 and Group 3). A final set of tests (Group 4) were performed with a 1.2mm test panel.

All testing was performed at the same site and under comparable conditions. Table 5-1 provides a brief summary of the field tests. The full results are tabulated in Table 5-2.

Thumbnail photographs of the test panels are given in Appendix A. Drawings that were used to depict and compare the results of the different test panels is shown in Appendix B.

Table 5-1 : Summary of the Field Tests

Initial exploratory tests About 7 detonations, all 30g PE4 on 3mm panel. *Data not used for dissertation.* Test housing subsequently modified
Group 1 : Attempt to **distinguish** between effects of shock effect and bubble 7 detonations, all 30g PE4 on 3mm panel Achieved plastic deformation (dishing) only
Group 2 : Testing of ***combined*** effects of shock effect and bubble 5 detonations, all 30g PE4 on 3mm panel Achieved Holing & petalling
Group 3 : Testing of ***combined*** effects of shock effect and bubble 18 detonations, all 30g PE4 on 3mm panel. Detonations done in 4 sets (3a, 3b, 3c,3d) Achieved Holing & petalling
Group 4 : Testing of ***combined*** effects of shock effect and bubble 9 detonations, all 30g PE4 on 1,2mm panel Achieved Holing & petalling

Table 5-2 : Results of the Field Tests

see key on next page	1 Test Sheet Nr	2 Face up/dwn	3 Target Thickness mm	4 Submerge Depth m	5 Offset Distance OD mm	6 Core Ofst.Dist. COD mm	7 Offset/dia Ratio OD base mm/mm	8 Offset/dia Ratio COD base mm/mm	9 Damage type	10 Area of Clear Hole (clear) mm2	11 Perimeter Clear of hole mm		12 Area of Damage mm2	13 Perimeter Damage mm	14 Length of tear mm	15 Number petals	16 Height of petals mm	17 Shock Factor (on OD)	18 Shock Factor (on COD)	19 Depth of dishing mm
Group 1	#x30	dwn	3mm	1.5	30.8	47.3	0.53	1.84	dish	0.00	0		0	0	0	0	0	1.76	0.98	113
see key on next page	#x31	dwn	3mm	1.5	25.8	42.3	0.43	1.54	dish	0.00	0		0	0	0	0	0	1.76	0.98	113
	#x32	Face	Target	Submerge	Offset	Core	Offset/dia	Offset/dia	Damage	Area of	Perimeter		Area of	Perimeter	Length	Number	Height	Shock	Shock	Depth of
	#x33	up/dwn	Thickness	Depth	Distance	Ofst.Dist.	Ratio	Ratio	type	Clear	Clear		Damage	Damage	of tear	petals	of petals	Factor	Factor	dishing
1	#x34	dwn	3mm	1.5	14.8	31.3	0.25	1.04	dish	Hole (clear)	of hole							(on OD)	(on COD)	
Group 1	#x35	dwn	3mm	1.5	30.8	47.3	0.53	1.84	dish	0.00	0		0	0	0	0	0	2.53	1.65	155
1	#x36	dwn	3mm	1.5	25.8	42.3	0.43	1.54	dish	0.00	0		0	0	0	0	0	2.53	1.65	155
1	#x32	dwn	3mm	1.5	16.8	33.3	0.51	1.01	dish	0.00	0		0	0	0	0	0	4.64	2.34	123
Group 2	#x33	dwn	3mm	1.5	15.8	32.3	0.43	0.98	Petal	141124	1670		178400	1615	1370	5	230	7.22	2.86	-
2	#x34	dwn	3mm	1.5	13.8	29.3	0.45	0.95	Petal	132600	1594		155977	1580	1108	4	230	5.87	2.29	128
2	#x35	dwn	3mm	1.5	14.8	31.3	0.45	0.95	Petal	98105	1609		138450	1561	1075	4	220	5.47	2.19	94
2	#x36	up	3mm	1.5	15.8	32.3	0.48	0.98	Petal	139000	1626		167800	1600	1388	5	200	4.38	2.41	119
2	#14	up	3mm	0.250	10.8	27.3	0.33	0.83	Petal	120434	1504		145050	1471	1242	5	200	3.38	1.34	-
Group 2	#10	dwn	3mm	1.5	10.8	27.3	0.33	0.83	Petal	141124	1670		178400	1615	1370	5	230	7.22	2.86	-
Group 3a	#11	dwn	3mm	2.5	12.8	29.3	0.39	0.89	Petal	132540	1594		155977	1580	1078	4	220	46.08	2.66	-
3a	#12	dwn	3mm	2.5	9.8	26.3	0.30	0.80	Petal	105475	1389		128900	1362	1075	6	190	9.62	2.80	-
3a	#13	dwn	3mm	2.5	6.8	23.3	0.21	0.71	Petal	59910	1076		66750	1060	758	5	180	5.32	1.56	-
3a	#14	dwn	3mm	2.5	2.8	19.3	0.09	0.59	Petal	19234	574		24250	462	325	5	180	3.72	1.36	-
3a	#5	dwn	3mm	2.0	12.8	29.3	0.39	0.89	dish	0	0		0	0	0	0	0	2.86	1.25	95
Group 3a	#6	dwn	3mm	2.0	0.8	17.3	0.02	0.52	Petal	93854	1580		68075	1550	1023	4	185	46.08	2.51	-
3a	#7	dwn	3mm	2.0	3.8	20.3	0.12	0.62	Petal	105475	1389		128900	1362	1139	6	190	9.62	2.80	-
3a	#8	dwn	3mm	2.0	6.8	23.3	0.21	0.71	Petal	59910	1076		66750	1060	758	5	180	5.32	1.56	-
3a	#9	dwn	3mm	2.0	9.8	26.3	0.30	0.80	Petal	19234	574		24250	462	325	5	180	3.72	1.36	-
Group 3c	#5	dwn	3mm	2.0	12.8	29.3	0.39	0.89	Petal	136001	1726		180575	1685	1383	5	210	46.08	2.66	95
Group 3b	#6	dwn	3mm	1.5	0.8	17.3	0.02	0.52	Petal	97606	1586		68075	1550	1023	4	185	46.08	2.51	-
3b	#7	dwn	3mm	1.5	3.8	20.3	0.12	0.62	Petal	105475	1389		128900	1362	1139	6	190	9.62	2.80	-
3b	#8	dwn	3mm	1.5	6.8	23.3	0.21	0.71	Petal	59910	1076		66750	1060	758	5	180	5.32	1.56	-
3b	#9	dwn	3mm	1.5	9.8	26.3	0.30	0.80	Petal	19234	574		24250	462	325	5	180	3.72	1.36	-
3b	#5	dwn	3mm	1.5	12.8	29.3	0.39	0.89	dish	0	0		0	0	0	0	0	2.86	1.25	110
Group 3d	#6	dwn	3mm	1.5	0.8	17.3	0.02	0.52	Petal	136001	1726		180575	1685	1383	5	210	46.08	2.51	-
3d	#7	dwn	3mm	1.5	3.8	20.3	0.12	0.62	Petal	131234	1656		190851	1696	1425	5	200	9.62	2.80	-
3d	#8	dwn	3mm	1.5	6.8	23.3	0.21	0.71	Petal	97410	1604		140250	1592	1113	5	200	5.32	1.56	-
3d	#9	dwn	3mm	1.5	9.8	26.3	0.30	0.80	Petal	30566	1015		53900	948	668	4	170	3.72	1.36	-
3c	#19	dwn	3mm	1.5	12.8	29.3	0.39	0.89	dish	0	0		0	0	0	0	0	6.09	2.66	110
Group 3d	#20	dwn	3mm	1.5	0.8	17.3	0.02	0.52	Petal	137406	1732		180400	1640	1408	4	200	46.08	2.51	-
3d	#21	Group 3	3mm	1.5	3.8	20.3	0.12	0.62	Petal	131234	1656		190851	1696	1425	5	200	9.62	2.80	-
3d	#22	Averaged	3mm	1.5	6.8	23.3	0.21	0.71	Petal	97410	1604		140250	1592	1113	5	200	5.32	1.56	-
3d	#23	Values	3mm	1.5	9.8	26.3	0.30	0.80	Petal	30566	1015		53900	948	668	4	170	3.72	1.36	-
3			3mm	1.5	12.8	29.3	0.39	0.89	dish	0	0		0	0	0	0	0	2.86	1.25	155
Group 3 all			3mm	1.5	0.8	17.3	0.02	0.52	Petal	104715	1541		142170	1455	1201	4.8	201	97.43	4.51	-
Group 4	#1200	dwn	1.2mm	0.75	0.8	17.3	0.02	0.52	Petal	168428	1718		188825	1629	1629	6	*	97.43	4.51	-
4	#1203	Group 3	1.2mm	0.75	3.8	20.3	0.12	0.62	Petal	190924	2080		247650	1845	2122	7	*	20.51	3.84	-
4	#1206	Averaged	1.2mm	0.75	6.8	23.3	0.21	0.71	Petal	200567	1879		232493	1788	2056	7	*	11.46	3.55	-
4	#1209	Values	1.2mm	0.75	9.8	26.3	0.30	0.80	Petal	186473	1974		235250	1812	2082	7	*	5.37	2.96	-
4	#1212	dwn	1.2mm	0.75	12.8	29.3	0.39	0.89	Petal	165374	1975		220900	1753	1701	7	*	3.73	2.76	-
4	#1215	dwn	1.2mm	0.75	15.8	32.3	0.48	0.98	Petal	183586	1947		230438	1806	2052	6	*	2.86	1.23	-
Group 4	#1200	dwn	1.2mm	0.75	0.8	17.3	0.02	0.52	Petal	168426	1718		188825	1629	1629	6	*	97.43	4.51	-
4	#1203	dwn	1.2mm	0.75	3.8	20.3	0.12	0.62	Petal	190924	2080		247650	1845	2122	7	*	20.51	3.84	-
4	#1206	dwn	1.2mm	0.75	6.8	23.3	0.21	0.71	Petal	200567	1879		232493	1788	2056	7	*	11.46	3.55	-
4	#1209	dwn	1.2mm	0.75	9.8	26.3	0.30	0.80	Petal	186473	1974		235250	1812	2082	7	*	5.37	2.96	-
4	#1212	dwn	1.2mm	0.75	12.8	29.3	0.39	0.89	Petal	165374	1975		220900	1753	1701	7	*	3.73	2.76	-
4	#1215	dwn	1.2mm	0.75	15.8	32.3	0.48	0.98	Petal	183586	1947		230438	1806	2052	6	*	2.86	1.23	-
4	#1218	dwn	1.2mm	0.75	18.8	35.3	0.57	1.07	Petal	176475	2065		241075	1866	2133	6	*	4.15	2.21	-
4	#1224	dwn	1.2mm	0.75	24.8	41.3	0.75	1.25	Petal	90016	2177		207900	1862	1312	4	*	3.14	1.89	-
4	#1230	dwn	1.2mm	0.75	30.8	47.3	0.93	1.44	dish	0	0		0	0	0	0	*	2.53	1.65	155

* height values not comparable

Formatted Table


Face up


Face dwn

NEC Charge mass (PE4) =	30.0	gram	
Cylindrical Charge dimensions L=D=	28.8	mm	
Spherical Effective Charge diameter De=	33.0	mm	

Key: OD = Offset Distance = measured from Target surface to Charge face
i.e. OD = (free gap)+(case thickness=0.8mm)
COD = Core Offset Distance = measured from Target Surface to mass centre of the Charge
i.e. COD = (free gap)+(case thickness=0.8mm)+(33/2)
SF = Shock Factor = 0.45 x √(Mass) / Offset

Description of the columns in Table 5-2 and Table 5-3

Column 1 : Test sheet number

Column 2 : Orientation of target panel (Face Up or Face Down)

Column 3 : Thickness of target panel

Column 4 : Depth of the charge below the sea surface

Column 5 : OD (Offset distance), charge face to target face. The thickness of the plastic container is included (0,8mm).

Column 6 : COD (Core Offset Distance). Distance from charge mass centre to target face, ie OD plus half of D_e.

Column 7 : Ratio [Offset Distance (column 3)] / [D_e]. The value of D_e is 33mm (see Table 4-3~~Table 4-3~~~~Table 4-3~~)

Column 8 : Ratio [Core Offset Distance (column 4] / [D_e]

Column 9 : Damage type

Column 10 : Area of clear hole - the projected area of the hole measured in the plane of the test face.

Column 11 : Perimeter of clear hole - the circumference of the hole measured in the plane of the test face.

Column 12 : Damage area – Area within polygon joining tips of tears

Column 13 : Perimeter of Damage area – Length of polygon joining tips of tears

Column 14 : Total length of the tearing. This value is measured along the surface of the deformed petal, from the tip to the root.

Column 15 : Number of tears (number of petals)

Column 16 : Height of the petals – the vertical height of the petals measured from the plane of the test sheet

Column 17 : Shock factor based on the OD value, where SF = 0.45*(mass^{½})/OD

Column 18 : Shock factor based on the COD value

Column 19 : Depth of dishing (where applicable)

Formatted: Font: 10 pt

Formatted: Font: 10 pt

Table 5-3 : Normalised 2006/07/08 data

Worksheet: *2006+2007+2008 Normalised data*

	1	2	3	4	5	6	7	8	9	10	11		12	13	14	15	16	17	18	19	
										Normalised	Normalised		Normalised	Normalised	Normalised						
see key on previous page	Test Sheet Nr	Face up/dwn	Target Thickness mm	Submerge Depth m	Offset Distance OD mm	Core Ofst.Dist. COD mm	Offset/dia Ratio OD base mm/mm	Offset/dia Ratio COD base mm/mm	Damage type	Area of Clear Hole (clear) mm2	Perimeter Clear of hole mm	Not useful (dishing on	Area of Damage mm2	Perimeter Damage mm	Length of tear mm	Number petals	Height of petals mm	Shock Factor (on OD)	Shock Factor (on COD)	Depth of dishing mm	Depth of dishing mm
Group 1	#x30	dwn	3mm	1.5	30.8	47.3	0.93	1.44	dish	0.00	0		0	0	0	0	0	1.19	*0.77*	106	106
1	#x31	dwn	3mm	1.5	20.8	37.3	0.63	1.13	dish	0.94	0		0	0	0	0	0	1.76	*0.98*	113	113
1	#x32	dwn	3mm	1.5	16.8	33.3	0.51	1.01	dish	0.86	0		0	0	0	0	0	2.18	*1.10*	123	126
1	#x33	dwn	3mm	1.5	15.8	32.3	0.48	0.98	dish	0.84	0		0	0	0	0	0	2.31	*1.13*	126	128
1	#x34	dwn	3mm	1.5	14.8	31.3	0.45	0.95	dish	0.83	0		0	0	0	0	0	2.47	1.17	128	94
1	#x35	dwn	3mm	1.5	14.8	31.3	0.45	0.95	dish	1.13	0		0	0	0	0	0	2.47	1.17	94	*119*
1	*#x36*	*up*	3mm	*1.5*	*15.8*	*32.3*	*0.48*	*0.98*	*dish*	*0.89*	*0*		*0*	*0*	*0*	*0*	*0*	2.31	1.13	119	
Group 2	#10	dwn	3mm	1.5	10.8	27.3	0.33	0.83	Petal	1.00	1.00	Group 2	1.00	1.00	1.00	5	230	3.38	1.34	-	-
2	#11	dwn	3mm	1.5	12.8	29.3	0.39	0.89	Petal	0.94	0.95		0.87	0.98	0.82	4	230	2.86	1.25	-	-
2	#12	dwn	3mm	1.5	14.8	31.3	0.45	0.95	Petal	0.66	0.96		0.78	0.97	0.78	4	220	2.47	1.17	-	-
2	*#13*	*up*	3mm	*1.5*	*10.8*	*27.3*	*0.33*	*0.83*	*Petal*	*0.99*	0.97		*0.94*	*0.99*	*0.98*	*5*	*200*	3.38	1.34	-	-
2	*#14*	*up*	3mm	*0.250*	*10.8*	*27.3*	*0.33*	*0.83*	*Petal*	*0.85*	0.90		*0.81*	*0.91*	*0.91*	*5*	*200*	3.38	1.34	-	
Group 3a	#1	dwn	3mm	2.0	0.8	17.3	0.02	0.52	Petal	1.00	1.00	3mm Group 3a	1.00	1.00	1.00	4	205	45.68	2.11	-	-
3a	#2	dwn	3mm	2.0	3.8	20.3	0.12	0.62	Petal	1.12	0.88		0.93	0.89	1.08	6	190	9.62	1.80	-	-
3a	#3	dwn	3mm	2.0	6.8	23.3	0.21	0.71	Petal	0.54	0.69		0.47	0.70	0.69	4	180	5.37	1.57	-	-
3a	#4	dwn	3mm	2.0	9.8	26.3	0.30	0.80	Petal	0.10	0.31		0.10	0.31	0.30	4	135	3.73	1.39	-	95
3a	#5	dwn	3mm	2.0	12.8	29.3	0.39	0.89	dish	0.00	0.00		0.00	0.00	0.00	0	0	2.86	1.25	95	
Group 3b	#6	dwn	3mm	1.5	0.8	17.3	0.02	0.52	Petal	1.00	1.00	3mm Grp 3b	1.00	1.00	1.00	4	190	45.68	2.11		-
3b	#7	dwn	3mm	1.5	3.8	20.3	0.12	0.62	Petal	1.25	1.29		1.54	1.25	1.25	4	190	9.62	1.80	-	-
3b	#8	dwn	3mm	1.5	6.8	23.3	0.21	0.71	Petal	0.82	0.93		0.87	0.92	1.09	5	190	5.37	1.57	-	
3b	#9	dwn	3mm	1.5	9.8	26.3	0.30	0.80	tear	0.00	0.02		0.00	0.01	0.01	0	0	3.73	1.39		-
Group 3c	#15	dwn	3mm	1.5	0.8	17.3	0.02	0.52	Petal	1.00	1.00	3mm Group 3c	1.00	1.00	1.00	5	210	45.68	2.11	-	-
3c	#16	dwn	3mm	1.5	3.8	20.3	0.12	0.62	Petal	1.01	0.98		1.09	1.04	1.04	5	180	9.62	1.80	-	-
3c	#17	dwn	3mm	1.5	6.8	23.3	0.21	0.71	Petal	0.85	1.10		1.08	1.04	1.04	5	180	5.37	1.57	-	-
3c	#18	dwn	3mm	1.5	9.8	26.3	0.30	0.80	Petal	0.98	1.01		0.99	0.97	1.14	6	170	3.73	1.39	-	110
3c	#19	dwn	3mm	1.5	12.8	29.3	0.39	0.89	dish	0.00	0.00		0.00	0.00	0.00	0	0	2.86	1.25	110	-
Group 3d	#20	dwn	3mm	1.5	0.8	17.3	0.02	0.52	Petal	1.00	1.00	3mm Grp 3d	1.00	1.00	1.00	6	200	45.68	2.11	-	-
3d	#21	dwn	3mm	1.5	3.8	20.3	0.12	0.62	Petal	0.96	1.03		1.01	1.01	0.89	5	200	9.62	1.80	-	-
3d	#22	dwn	3mm	1.5	6.8	23.3	0.21	0.71	Petal	0.71	0.89		0.75	0.87	0.88	6	200	5.37	1.57	-	-
3d	#23	dwn	3mm	1.5	9.8	26.3	0.30	0.80	Petal	0.22	0.57		0.29	0.57	0.42	4	170	3.73	1.39	-	
Group 3 all	#300		3mm	1.5	0.8	17.3	0.02	0.52	Petal	1.00	1.00	3mm Average	1.00	1.00	1.00	4.8	201	45.68	2.11		
3	#303	Group 3	3mm	1.5	3.8	20.3	0.12	0.62	Petal	1.09	1.05		1.14	1.05	1.07	5.0	190	9.62	1.80		
3	#306	Average	3mm	1.5	6.8	23.3	0.21	0.71	Petal	0.73	0.90		0.79	0.88	0.93	5.0	188	5.37	1.57		
3	#309	Values	3mm	1.5	9.8	26.3	0.30	0.80	Petal	0.33	0.47		0.35	0.47	0.47	3.5	119	3.73	1.39		
3	#312		3mm	1.5	12.8	29.3	0.39	0.89	dish	0.00	0.00		0.00	0.00	0.00	0.0	0	2.86	1.25		
Group 4	*#1200*	dwn	1.2mm	0.75	0.8	17.3	0.02	0.52	Petal	1.00	1.00	1.2mm target. Group 4	1.00	1.00	1.00	6	*	45.68	2.11		
4	*#1203*	dwn	1.2mm	0.75	3.8	20.3	0.12	0.62	Petal	1.21	1.19		1.31	1.13	1.30	7	*	9.62	1.80		
4	*#1206*	dwn	1.2mm	0.75	6.8	23.3	0.21	0.71	Petal	1.28	1.09		1.24	1.10	1.26	7	*	5.37	1.57		
4	*#1209*	dwn	1.2mm	0.75	9.8	26.3	0.30	0.80	Petal	1.19	1.15		1.25	1.11	1.28	7	*	3.73	1.39		
4	*#1212*	dwn	1.2mm	0.75	12.8	29.3	0.39	0.89	Petal	1.06	1.15		1.17	1.08	1.04	7	*	2.86	1.25		
4	*#1215*	dwn	1.2mm	0.75	15.8	32.3	0.48	0.98	Petal	1.17	1.13		1.22	1.11	1.26	6	*	2.31	1.13		
4	*#1218*	dwn	1.2mm	0.75	18.8	35.3	0.57	1.07	Petal	1.13	1.20		1.28	1.15	1.31	6	*	1.94	1.04		
4	*#1224*	dwn	1.2mm	0.75	24.8	41.3	0.75	1.25	Petal	0.58	1.27		1.10	1.14	0.81	4	*	1.47	0.88		
4	*#1230*	dwn	1.2mm	0.75	30.8	47.3	0.93	1.44	dish	0.00	0.00		0.00	0.00	0.00	0	*	1.19	0.77		

* height values not comparable

Formatted Table

5.1 Group 1 and Group 2 Tests

5.1.1 Objective

The objective of the first two groups of tests (Group 1 and Group 2) was to establish if the effect of the bubble and the shock impulse can be separated by different orientation of the test housing. A secondary objective was to find the window of offsets in which the transition between tearing and plastic deformation occurs.

5.1.2 Test setup

The setup was in accordance with the description in paragraph 4.3.1

The test housing was suspended at a predetermined depth below the surface off a jetty, by a fixed crane (see Figure 4-9~~Figure 4-9~~~~Figure 4-9~~). The target plate was 3mm mild steel.

5.1.3 Execution

The procedure was in accordance with the description in paragraph 4.4.

Twelve detonations were performed. The offset distance started at 30mm and was incrementally reduced to 10mm. A fraction of 0.8mm representing the thickness of the casing of the explosive was added to all offsets.

Three of the detonations were facing upwards (charge above the target panel). Each of these "face-up" detonations had a comparable "face-down" test. One face-up test was close to the surface in an effort to eliminate the effect of the bubble.

5.1.4 Results

Seven detonations (Group 1) all resulted in plastic deformation (dishing only) of the test panel. Group 2 (five detonations) all resulted in holing of the target and associated petalling.

The results are tabulated in Table 5-2

5.1.5 Discussion of results from Groups 1 and 2

5.1.5.1 General trend: Damage and OD inversely proportional

From Table 5-4 can be seen that the damage increases proportionally to the decrease in OD.

Dishing in Group 1 (row A) : In this case the depth of the dishing at OD=30mm is used as reference. The dishing progressively increased to 121% (#34). The dishing of #35 is outside the trend demonstrated by all the other samples.

Holing in Group 2 (row B) : The size (area) of the hole is used as parameter of measuring damage. As expected, the size of the hole increased proportionally to the decrease in OD.

Table 5-4 : Damage and OD inversely proportional

	Comparable Parameters	Test Sheet Nr	Orientation	Submerge Depth m	Offset OD* mm	Damage type	Depth of dishing mm	Difference	Area of Clear Hole mm2	Difference	Area of Damage mm2	Difference
		#x30	down	1.5	30.8	dish	106	reference	0	n.a.	0	n.a.
A	Decreasing offset distance	#x31	down	1.5	20.8	dish	113	107%	0	n.a.	0	n.a.
	Same depth	#x32	down	1.5	16.8	dish	123	116%	0	n.a.	0	n.a.
	Same orientation (face down)	#x33	down	1.5	15.8	dish	126	119%	0	n.a.	0	n.a.
	All dishing	#x34	down	1.5	14.8	dish	128	121%	0	n.a.	0	n.a.
		#x35	down	1.5	14.8	dish	94	89%	0	n.a.	0	n.a.
	Decreasing offset distance	#12	down	1.5	14.8	Petal	n.a.	-	93175	reference	138450	reference
B	Same depth, All face down	#11	down	1.5	12.8	Petal	n.a.	-	132510	142%	155977	167%
	All holing (petalled)	#10	down	1.5	10.8	Petal	n.a.	-	141124	151%	178400	191%

*Includes thickness of charge container

5.1.5.2 Consistency of results

Within Group 1 and 2 it was found that, in certain cases, the damage to the test plate is significantly different when the OD and general test setup is the same.

Considering row C in Table 5-5, two important characteristics are clear. The difference in damage between test plate #34 and #35 is 27%. This is much more than expected. If #19 is compared to #5 (from Group 3), the difference in damage is smaller (16%).

Note: Possible causes could be inaccurate measurement of the mass of explosive, inaccurate measurement of offset or significant difference in material properties. Analysis of the circumstances indicated that inaccurate measurement of the mass of explosive is the most likely cause. In all tests that followed special attention was paid to measurement of mass.

The dishing of #32, #33 and #36 (row D) were very close to each other at 6% difference.

Note that #32 and #33 were facing down and #36 was facing up. This may influence the result, although the effect should be small (due to the depth of submersion). The reason is that the detonation was deep enough that the bubble could develop fully. The difference (as far as the bubble is concerned) is that in the face-down situation, the bubble would develop into deeper water whilst in the face-up situation it would develop into shallower water and subsequently to a slightly larger maximum diameter.

Table 5-5 : Consistency of results

	Comparable Parameters	Test Sheet Nr	Orientation	Submerge Depth m	Offset OD* mm	Damage type	Depth of dishing mm	Difference	Area of Clear Hole mm2	Difference	Area of Damage mm2	Difference
C	Dishing at similar depth same OD, all face down	#x34	down	1.5	14.8	dish	128	ref.	0	n.a.	0	n.a.
		#x35	down	1.5	14.8	dish	94	-27%	0	n.a.	0	n.a.
		#5	down	2.0	12.8	dish	95	ref.	0	n.a.	0	n.a.
		#19	down	1.5	12.8	dish	110	16%	0	n.a.	0	n.a.
D	Dishing at same Depth & OD Face Up vs Face Down	#x36	up	1.5	15.8	dish	119	ref.	0	n.a.	0	n.a.
		#x32	down	1.5	16.8	dish	123	3%	0	n.a.	0	n.a.
		#x33	down	1.5	15.8	dish	126	6%	0	n.a.	0	n.a.
E	Holing at Depth vs Surface Both Face Up	#13	up	1.5	10.8	Petal	n.a.	-	139910	ref.	167800	ref.
		#14	up	0.25	10.8	Petal	n.a.	-	120434	-14%	145050	-14%

*Includes thickness of charge container

5.1.5.3 Face Up vs Face Down, at the same depth

Considering the results tabulated in Table 5-6~~Table 5-6~~~~Table 5-6~~, the general tendency is that a face-up orientation suffers less damage than a face-down orientation. Also, near the surface the damage is less than deeply submerged (row I).

Row F: Sample #36 (face up) is dished 6% less than #33 (face down). Sample #33 and #32 (both face down) are dished to within 2% of each other.

Row G: Sample #10 (face down) vs #13 (face up) was an attempt to see if the effect of the bubble was different when the target faces up vs down. The difference was 1%, which is insignificant. Note: the energy of the detonation is split nearly 50/50 between shock impulse and bubble (see Table 5-6~~Table 5-6~~~~Table 5-6~~).

Row H: Sample #10 (submerged) vs #14 (at surface, venting) was an attempt to see if the

effect of the bubble was different when the bubble is vented (prevented from forming) vs fully developed. The damage of the near-surface sample was less than that of the submerged sample, as expected. The difference in clear hole area is 15% less and in damage area 19% less. Both values are significant, yet substantially less than expected (based on comments by [35]).

Row I: Sample #13 and #14 both faced up, one submerged and the other at the surface. As with the samples in row H, the near-surface damage is less than submerged. Both clear hole area and damage area is 14% less on the near-surface sample.

Table 5-6 : Face Up vs Face Down, at the same depth

	Comparable Parameters	Test Sheet Nr	Orientation	Submerge Depth m	Offset OD* mm	Damage type	Depth of dishing mm	Difference	Area of Clear Hole mm2	Difference	Area of Damage mm2	Difference
	Dishing at	#x33	down	1.5	15.8	dish	126	ref.	0	n.a.	0	n.a.
F	same Depth & OD	#x32	down	1.5	16.8	dish	123	-2%	0	n.a.	0	n.a.
	Face Up vs Face Down	#x36	up	1.5	15.8	dish	119	-6%	0	n.a.	0	n.a.
G	Holing at same Depth & OD	#10	down	1.5	10.8	Petal	n.a.	-	141124	ref.	178400	ref.
	Face Up vs Face Down	#13	up	1.5	10.8	Petal	n.a.	-	139910	-1%	167800	-6%
H	Holing at Depth vs Surface	#10	down	1.5	10.8	Petal	n.a.	-	141124	ref.	178400	ref.
	Face Up vs Face Down	#14	up	0.25	10.8	Petal	n.a.	-	120434	-15%	145050	-19%
I	Holing at Depth vs Surface	#13	up	1.5	10.8	Petal	n.a.	-	139910	ref.	167800	ref.
	Both Face Up	#14	up	0.25	10.8	Petal	n.a.	-	120434	-14%	145050	-14%

*Includes thickness of charge container

5.1.5.4 Shallow vs Submerged

From rows J and K in Table 5-7~~Table 5-7~~~~Table 5-7~~ it can be seen that the damage to the target is less near the surface (both clear hole area and damage area). This indicates that the proper development of the gas bubble does indeed contribute to the damage inflicted on the target panel. As mentioned before (see paragraph 5.1.5.4), the difference is less than expected. From this it can be concluded that the importance of the development and collapse of the gas bubble is ~~significant~~small~~, yet not eliminated~~ in the physical experiment.

This implies that it is not practical to isolate the effect of the bubble from the effect of the shock impulse.

Table 5-7 : Shallow vs Submerged

	Comparable Parameters	Test Sheet Nr	Orientation	Submerge Depth m	Offset OD* mm	Damage type	Depth of dishing mm	Difference	Area of Clear Hole mm2	Difference	Area of Damage mm2	Difference
J	Holing at Depth vs Surface	#10	down	1.5	10.8	Petal	n.a.	-	141124	ref.	178400	ref.
	Face Up vs Face Down	#14	up	0.25	10.8	Petal	n.a.	-	120434	-15%	145050	-19%
K	Holing at Depth vs Surface	#13	up	1.5	10.8	Petal	n.a.	-	139910	ref.	167800	ref.
	Both Face Up	#14	up	0.25	10.8	Petal	n.a.	-	120434	-14%	145050	-14%

*Includes thickness of charge container

5.1.5.5 Usefulness of the results from Group 1 and 2

It was decided not to pursue the effort to demonstrate the two separate phenomena (shock damage vs bubble damage) by way of experimenting. The two phenomena are very interwoven and the effect of the bubble entails more complex mechanism than simple development and collapse. It is clear that the development and associated reloading effects

during the development phase of the bubble cannot easily be separated from the effect of the initial shock impulse (see paragraph 3.1.5 on reloading), at least not in the present test arrangement.

It was decided that in the subsequent testing the two phenomena will be viewed in combination.

5.2 Group 3 Tests

5.2.1 Objective

The objective of the Group 3 was to determine the combined effect of shock impulse and bubble formation as a function of Offset Distance.

5.2.2 Test setup

The setup was in accordance with the description in paragraph 4.3.1

The charge was 30g PE4, contained in the plastic container as described before.

The pyramid was suspended at a predetermined depth below the surface off a jetty, by a fixed crane. The target plate was 3mm mild steel, facing down for all detonations.

5.2.3 Execution

Eighteen detonations were performed in four sub-groups. Within each subgroup the offset distance was gradually increased from 0 mm in increments of 3mm, until no penetration of the faceplate occurred. The target orientation was facedown.

One sub-group of tests was conducted at a depth of 2000mm and three sub-groups at a depth of 1500mm (see Table 5-2). In all cases the test faceplate was facing down.

5.2.4 Results

The full results of Group 3 are tabulated in Table 5-2.

Penetration and petalling occurred at offset distances less than 9mm. In two cases (3b and 3d) tearing or slight petalling occurred at 12 mm. Testing was not extended beyond 12mm because no petalling would occur beyond this offset distance.

5.2.5 Discussion of Group 3 results

5.2.5.1 General trend: Damage vs OD (Offset Distance)

Four parameters of damage are considered (see Figure 4-3~~Figure 4-3~~~~Figure 4-3~~ for the definitions):

a. Area of the clear hole
b. Perimeter of the clear hole
c. Area of the damage area
d. Perimeter of the damage area

Table 5-8~~Table 5-8~~~~Table 5-8~~ presents these parameters abstracted from Table 5-2. The parameter of the first OD (contact) is used as reference and the parameters of the following offset distances (3mm, 6mm, 9mm) are presented as a percentage increase/decrease. From the table it can be seen that each of the parameters increases at the first enlargement of OD (3mm), then decreases (6mm and beyond) until petalling ceases.

Note: The thickness of the charge container (0.8mm) is included in the OD. Therefore an OD of 0.8mm corresponds zero offset distance or contact detonation.

Table 5-8 : Combined Averaged Results from Group 3

	Offset/De Ratio OD base*	Damage type	Area of Clear Hole	% Increase	Perimeter of clear hole	% Increase	Area of Damage	% Increase	Perimeter of Damage	% Increase
			mm^2	%	mm	%	mm^2	%	mm	%
Group 3 combined average	0.02	Petal	104715	reference	1541	reference	142170	reference	1455	reference
	0.12	Petal	109728	5%	1579	2%	153758	8%	1504	3%
	0.21	Petal	76386	-26%	1397	-9%	114184	-18%	1283	-11%
	0.30	Petal	43526	-80%	812	-52%	61646	-71%	748	-55%
	0.39	dish/tear	0	n.a.	0	n.a.	0	n.a.	0	n.a.

*Includes thickness of charge container

In normalised form (see note*) a set of graphs as in Figure 5-1~~Figure 5-1~~~~Figure 5-1~~ is obtained. This clearly shows that a maximum is present at an offset distance that is non-zero.

Note*: Normalising the data values entails dividing each Y-value within a set of data by a reference value from the same set of values, typically the first Y-value. In this way the first Y-value becomes unity and all Y-values become dimensionless. This technique enables quantitative comparison to other normalised sets of data at different scales. Recognising and comparing trends is another advantage gained from the technique of normalising, because dissimilar data values can be plotted on the same graph, as in Figure 5-1~~Figure 5-1~~~~Figure 5-1~~.

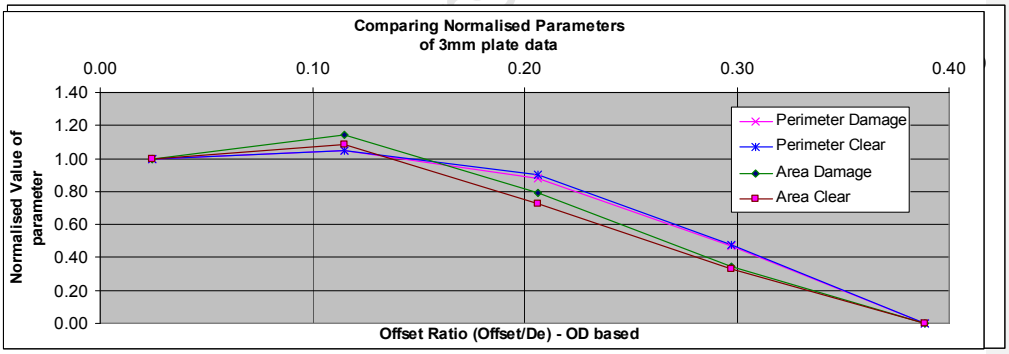

Figure 5-1: Comparing the four parameters

5.2.5.2 Effect of depth

The expected result is that more damage is inflicted at greater submergence because the

ambient pressure is higher. However, the ambient pressure of the water is insignificant compared to the peak impulse pressure and also insignificant compared to the pressure created by the expanding bubble.

Looking at the results of subgroups 3a, 3b, 3c and 3d in Table 5-2, it is clear that the damage parameters of subgroup 3a (2m submergence) are not consistently greater than the other three subgroups. Comparing the damage parameters of subgroup 3a to the Group 3 average values, the damage values are near equal or less.

Based on above results, it can be concluded that the effect of greater/smaller depth in the present test arrangement is negligible.

Note – if the target is submerged so deep that it is close to the sea bed, reflections from the seabed may have an effect. In the present test arrangement, the distance between the sea bed and test housing were more than the distance from the target to the surface.

5.3 Group 4 Tests

In conclusion of Group 3 testing, it was decided to conduct another set of tests using a thinner target plate (1.2mm instead of 3mm). The principle motivation was to enable scaling of the results. The 3mm plate was relatively thick compared to the charge – linear scaling of the charge and target plate without compensation for thickness of the 3mm plate leads to very thick panels at practical charge sizes. The 1.2mm thickness can be scaled linearly to practical charge values without mathematical correction for plate thickness.

The charge size and orientation of the target plate remained unchanged from the Group 3 tests. The test housing was modified by truncating the tip and welding a chimney-like vent to the top of the housing (Figure 5-2~~Figure 5-2~~~~Figure 5-2~~). This would allow the water and gas penetrating the target plate to escape above the water surface.

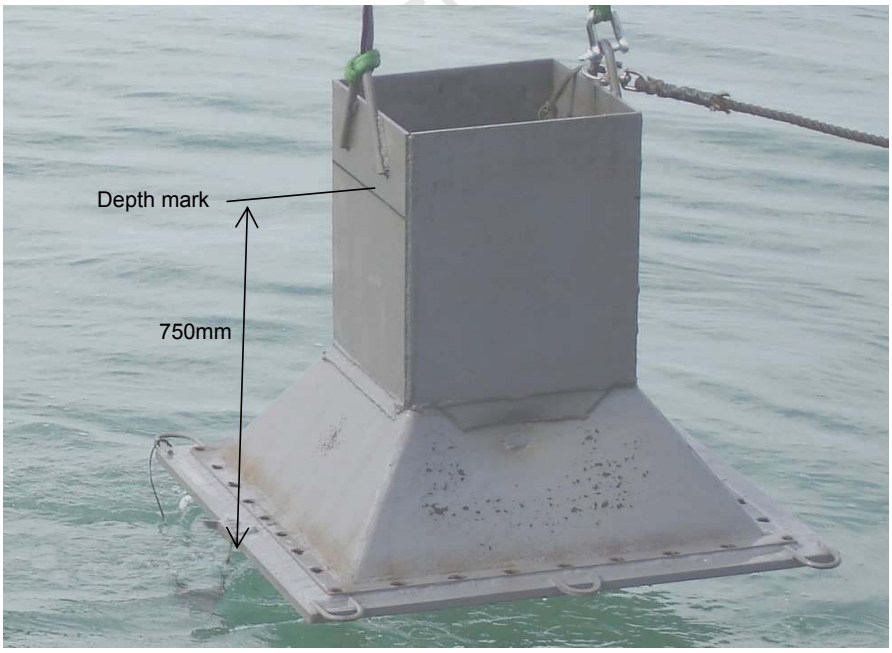

Figure 5-2: The modified housing

5.3.1 Objective

The objective of the Group 4 tests was to establish if the tendencies obtained with the 3mm target panel is evident with a target plate that is relatively thin.

5.3.2 Test setup

The housing was modified by removing part of the top and fitting a square structure akin to a chimney. This would enable the water and gas to vent to the atmosphere (see Figure 5-3~~Figure 5-3~~~~Figure 5-3~~). The length of the extension was such that the target face would be submerged to 750mm below surface. This was shallower than the Group 3 tests but deemed acceptable in view of the conclusion that physical depth does not significantly influence the resulting damage (see paragraph 5.2.5.2).

The charge size, charge attachment and adjustment of the offset distance remained unchanged from previous tests.

5.3.3 Execution

The test consisted of a series of detonations that started with the charge container in contact with the target (ie offset distance of the charge equal to the thickness of the charge container). The offset distance was increased by 3mm for each subsequent test up to 18mm, thereafter incremented by 6mm until the target plate was not penetrated anymore (ie dishing only) at an offset distance of 30mm.

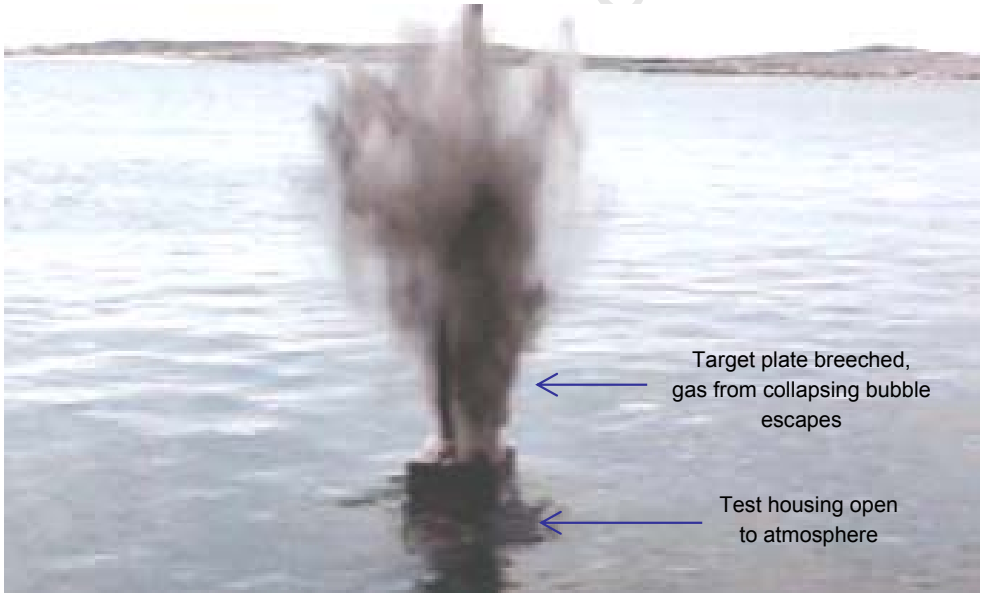

Figure 5-3: A typical detonation in Group 4

5.3.4 Results

The results of Group 4 is summarised in Table 5-9~~Table 5-9~~~~Table 5-9~~. The full results can be found in Table 5-2. As with the previous groups, four parameters are listed. Two notable trends can be seen from the values.

a) The first value (corresponding to zero offset) of all four parameters are lower than subsequent values

b) The second and subsequent values remain near the same value for most of the other offsets until dishing occurs at 30mm offset distance.

Above characteristics are illustrated in Figure 5-4~~Figure 5-4~~~~Figure 5-4~~.

Table 5-9 : Results of Group 4

Test Sheet	Face up/dwn	Offset Distance OD*	Damage type	Area of Clear Hole Value mm^2	Area of Clear Hole % Increase %	Perimeter of Clear Hole Value mm	Perimeter of Clear Hole % Increase %	Area of Damage Value mm^2	Area of Damage % Increase %	Perimeter of Damage Value mm	Perimeter of Damage % Increase %
#1200	dwn	0.8	Petal	156426	Reference	1718	Reference	188825	Reference	1629	Reference
#1203	dwn	3.8	Petal	190024	21%	2050	19%	247650	31%	1845	13%
#1206	dwn	6.8	Petal	200567	28%	1879	9%	233493	24%	1788	10%
#1209	dwn	9.8	Petal	186473	19%	1974	15%	235250	25%	1812	11%
#1212	dwn	12.8	Petal	165374	6%	1975	15%	220900	17%	1753	8%
#1215	dwn	15.8	Petal	183586	17%	1947	13%	230438	22%	1806	11%
#1218	dwn	18.8	Petal	176475	13%	2065	20%	241075	28%	1866	15%
#1224	dwn	24.8	Petal	90016	-42%	2177	27%	207900	10%	1862	14%
#1230	dwn	30.8	dish	0	n.a.	0	n.a.	0	n.a.	0	n.a.

*Includes thickness of charge container

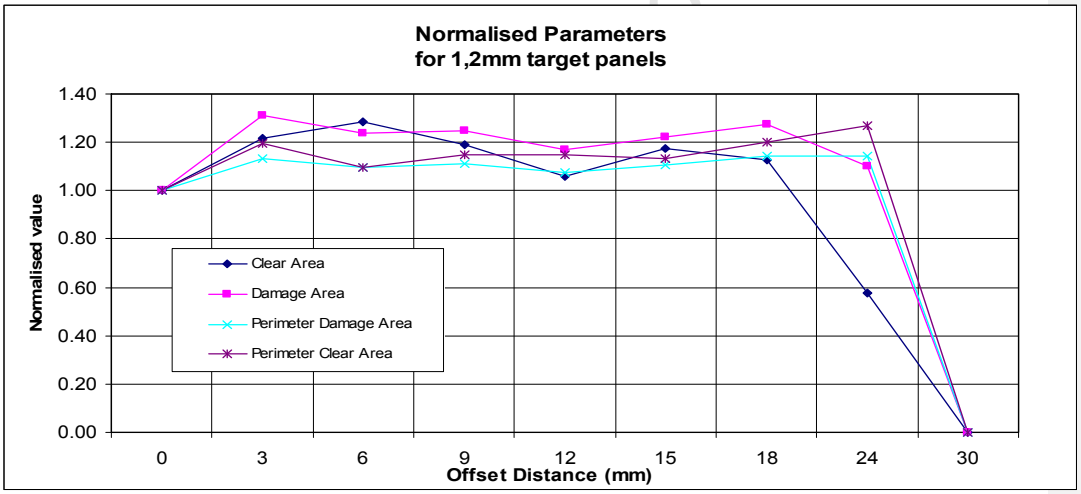

Figure 5-4: Comparing Normalised parameters of Group 4

Note the long plateau section on the graph in Figure 5-4~~Figure 5-4~~~~Figure 5-4~~ from OD=3mm to OD=24mm. This is due to the petalling of the target panels being significantly inhibited by the inner surface of the test housing. When the petalling is inhibited, then tearing will also be inhibited. This phenomenon can be seen in Figure 5-5~~Figure 5-5~~~~Figure~~

~~5-5~~, showing comparative views of a sample from Group 3 and from Group 4.

Three note-able ~~important aspects were proven~~observations is evident after ~~by~~ the Group 4 test:

i. All four parameters in Group 4 exhibits the same ~~trend~~ initial behaviour of showing an increase from zero to the following (~~at a~~ non-zero) offset distance

ii. The damage to the thinner panel (1.2mm) remains fairly constant for the next five data points, whereas the damage to the thicker panel (3mm) reduces beyond the increase with first~~The trend of increased value at~~ non-zero offset distance~~ exhibited by the 1.2mm~~

~~ii. target panel is the same as with the 3mm target panel~~

iii. The~~ increase~~ plateau of the ~~in~~ values in Group 4 ~~is~~ ~~maintained over a very long range of offset distances with the thinner panel, compared to the thicker 3mm panel.~~caused by the restriction of movement imposed on the petals by the inside surface of the housing.

Formatted: Bullets and Numbering

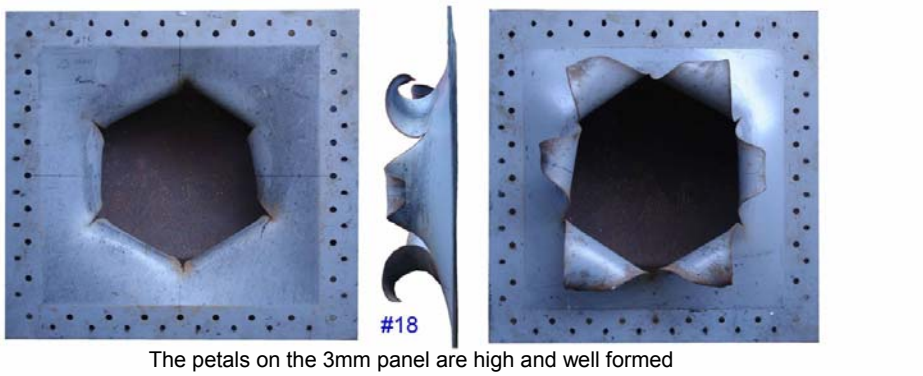

The petals on the 3mm panel are high and well formed

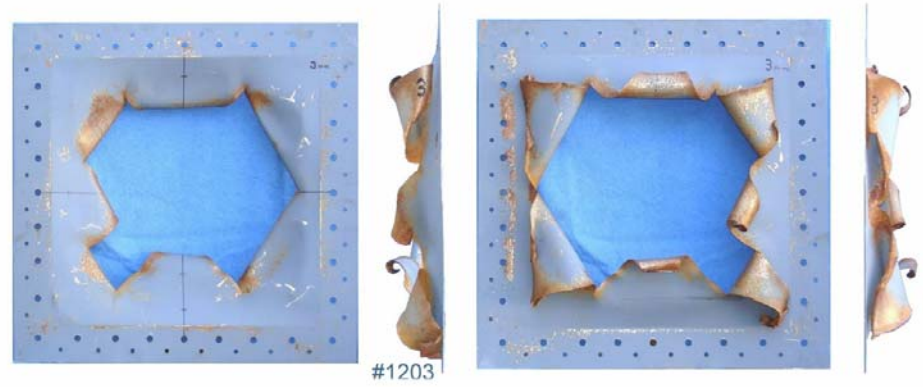

The petals on the 1.2mm panels are flattened and disfigured due to contact with the inside face of the test housing

Figure 5-5: Petaling influenced by the inside faces of the test housing

A feature of the Group 4 test housing was the addition of a "funnel" that connected the back (dry) side of the target panel with the atmosphere (see Figure 5-2~~Figure 5-2~~~~Figure 5-2~~). This enabled the water spout to be visible when rising above the test housing.

The purpose of this arrangement was to determine the relative amount of water that passes through the hole when it is breeched by the detonation. A video clip of each Group 4 detonation was made. The first four frames from selected video clips are shown in Figure 5-6~~Figure 5-6~~~~Figure 5-6~~. The frames are 0.1667 seconds apart (taken at 6 frames per second)

Four sets of frames are shown. The first row (A) shows the plume of water that rises above the surface when no target panel is present.

Row B is from the video where the 1.2mm target panel is holed by a contact charge.

Row C is from the video where the 1.2mm target panel is holed by the charge at 6mm offset distance.

Row D is from the video where the 1.2mm target panel is not holed. The offset distance in this case was 30mm. The small amount of spray that is visible originates from water that may have leaked or splashed into the air cavity.

Figure 5-6: Video frames from Group 4 tests

Some interesting features are observed from the frames.

The plume of water in row A is white, large and well shaped. A clear ring of surface cavitation (due to reflected shock wave) is visible around the base of the column.

The amount of spray rising in row C (offset distance 6mm) is visibly more than the amount of spray in row B. This is a clear indication that more water managed to pass through the hole in the target panel. The reason can be either of two:

a) The hole is larger with the non-zero offset distance,

or (if hole size is assumed equal)

b) the effect of the collapsing bubble is greater

Since it is known that the hole is 28% larger (sample #1206 Table 5-9~~Table 5-9~~~~Table 5-9~~), the increased volume of the plume should be attributed to the larger hole.

5.4 Analysis of Results of the 2006, 2007 and 2008 tests

The complete results and subsequent calculated values are tabulated in Table 5-2. The parameters listed in the column headers are defined after Table 5-2.

5.4.1 Graphs of the data

5.4.1.1 General discussion of the graphs

The offset distance (OD) is the basic parameter to be used as the X-axis of a graph. The OD can be presented in various forms. It is convenient to use the OD in a dimensionless form by dividing the OD by the equivalent diameter De (as defined in paragraphs 4.3.1.4 and 4.3.2).

This dimensionless form, the Offset Ratio (OR), can be based on either OD (Offset Distance) or COD (Core Offset Distance) as defined in paragraph 4.3.2 and Figure 4-3~~Figure 4-3~~~~Figure 4-3~~. The shape and character of the graph of any given parameter is the same whether OD or COD is used on the X-axis (see Figure 5-7). Only the scale of the X-axis is different. This is because the OD differs from the COD in that a *constant* value (De/2) is added to OD in order to obtain COD. In both cases the division is by the same

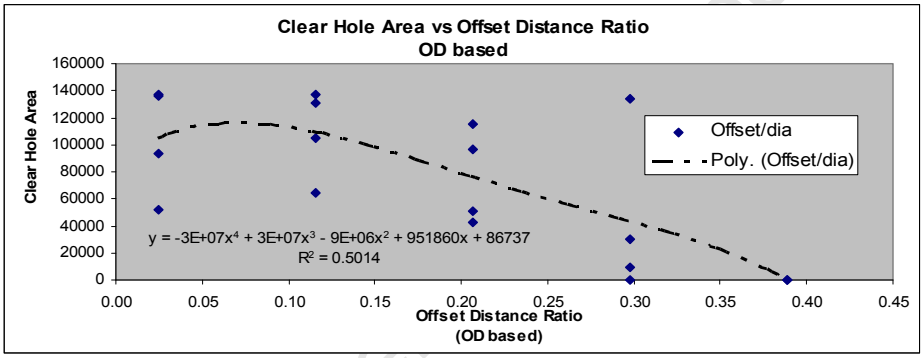

Using OD or COD on X-axis does not change the shape of graph.

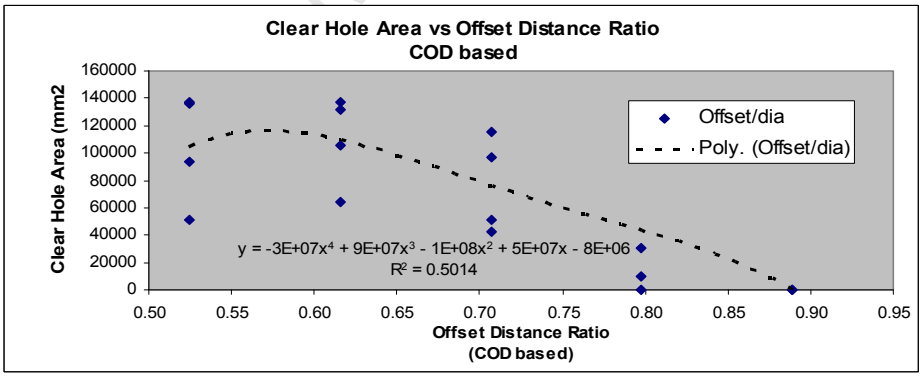

value namely De.

Figure 5-7: Curve fitted to data using OD on X-axis

The units of the Y-axis can be either the actual value of the parameter presented or the parameter can be presented in dimensionless form. The latter would enable the results of different parameters with different scales to be compared (provided the same reference is used).

A convenient technique to create a dimensionless form is normalising a set of results. This is achieved by using the first Y-value of a set of results as a reference and dividing all Y-values in that set by the first value. In this way the first value equals unity and the subsequent values are presented as a fraction of the first value.

5.4.1.2 Validity of results

Group 1

The result from Group 1 is disregarded because only dishing occurred during these tests (see column 9 in Table 5-2). Holing of the target is a required result for this thesis.

Group 2

The results from Group 2 and Group 3 are shown in Figure 5-8~~Figure 5-8~~~~Figure 5-8~~. Group 2 consisted of five detonations at various offset distances (connected triangular ticks). Group 3 consisted of seventeen detonations at various offset distances. From the figure it is clear that the values from Group 2 are not consistent with the other data. The reasons why the results from Group 2 are inconsistent to the other results is discussed in Appendix C.

The results of Group 2 are viewed in isolation, qualitatively only and is not used in conjunction with results from Group 3.

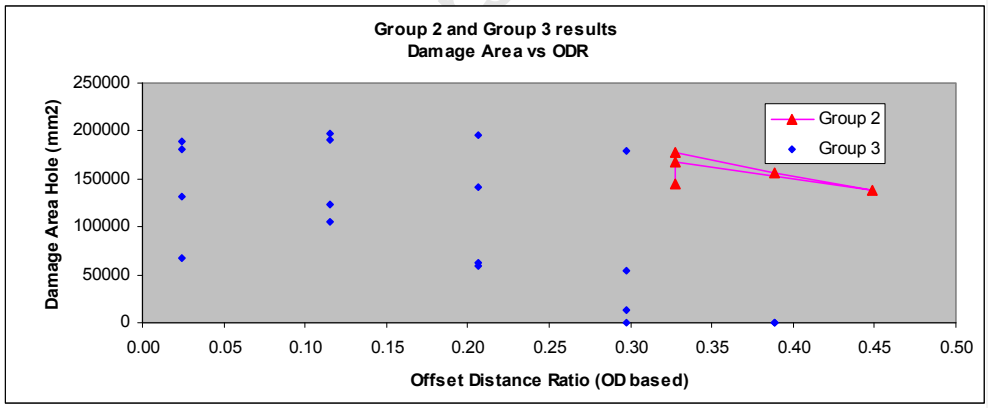

Figure 5-8: Results from Group 2 and Group 3

Group 3

The results from Group 3 appear to be widely dispersed in the Y-axis. All detonations were

done under the same conditions (albeit not done on the same day) and variables were controlled as well as practical. The vertical dispersion should therefore be accepted as a characteristic of the results from the field trials.

All measurements from Group 3 are viewed and analysed as a single group (instead of distinguishing between data obtained on different days).

Group4

The results from Group 4 were obtained by using a thinner target panel and was done in one day. Group 4 is treated as an independent set of data.

The values from this group are shown in Figure 5-9~~Figure 5-9~~~~Figure 5-9~~. Both damage area and clear area is shown in the graph. The values appear to be quite consistent.

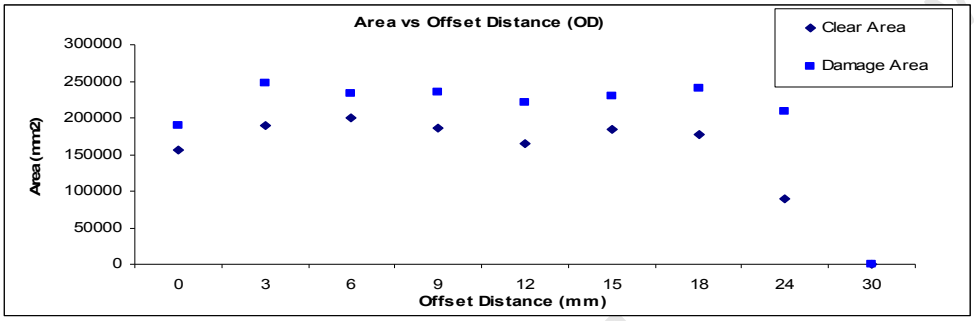

Figure 5-9: Results from Group 4

5.4.1.3 Clear Hole Area as a function of ODR

The hole size (clear area) is taken as the projected clear area opened up by the charge (see definitions Figure 4-3~~Figure 4-3~~~~Figure 4-3~~).

As seen in Figure 5-10~~Figure 5-10~~~~Figure 5-10~~, the clear hole area is spread over a wide range of Y-values at each OD. Notable is the exceptionally high value at X=0,3.

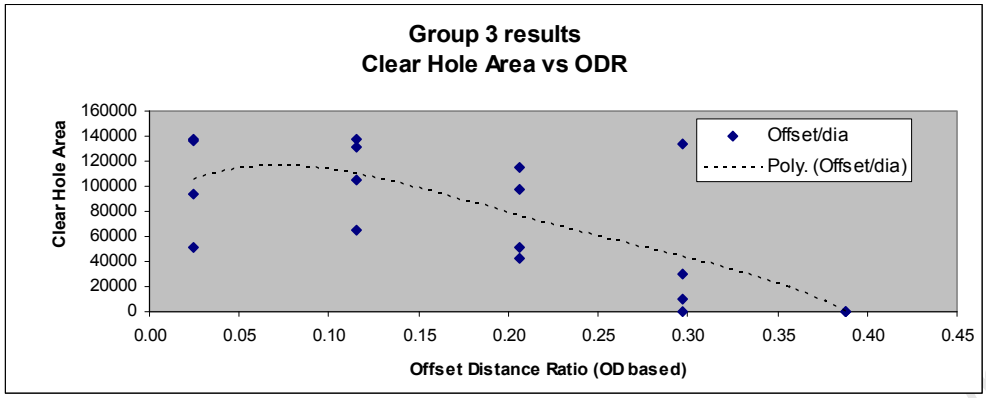

Figure 5-10: Projected clear area vs Offset Ratio, OD based

5.4.1.4 Damage area (extreme area) as a function of ODR

The damage area is the calculated area within a polygon that joins the tips of the tears (see definitions Figure 4-3~~Figure 4-3~~~~Figure 4-3~~). The damage area is considered to be a very realistic value for assessing the measure of damage to the target because the process of tearing requires significant energy. The process is associated with local heating (at crystalline level) and subsequent local weakening. In contrast to the clear hole area, the damage area is independent of the shape of the petals. The clear area of the hole is affected by the amount of bending of the petals at the root. A sharp bend would increase the clear area and a shallow bend would decrease the clear area. At the same time, the damage area is not affected.

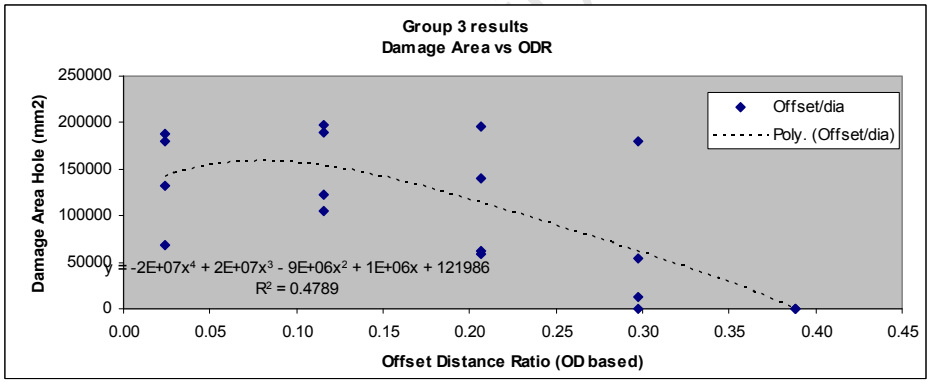

Figure 5-11: Damage Area as a function of offset ratio, OD based

Similar trends are obvious in both damage area and clear hole area. The average value exhibits a peak near the second X-value (ie OD = 6mm). The Y-value is higher at the second X-value and then decreases near linearly at X_3 and X_4

As with the clear area, the damage area also exhibits an exceptional high Y-value at X_4= 0.03.

5.4.1.5 Perimeter of the hole

The perimeter of the clear hole and damage area exhibits a similar character in that the Y-value is slightly lower at X_1 than at X_2. After X_2 the Y-value drops lower at subsequent X-values (see Figure 5-12~~Figure 5-12~~~~Figure 5-12~~ and Figure 5-13~~Figure 5-13~~~~Figure 5-13~~).

The perimeter is considered to not be very representative of the relative damage due to its dependence on the *shape* of the petals, especially the perimeter of the clear hole. Some petals bend sharply and others form a gradual curve. The contribution to perimeter length of a petal that curves sharply at the base would be less than a petal that turns less sharply and therefore partly protrudes into the hole. It is noted that petals that form a straight line at the bend at the root, contributing much more to the clear area than petals that curve gradually (see Figure 4-3~~Figure 4-3~~~~Figure 4-3~~).

Using the area parameter as in paragraph 5.4.1.4 is preferred to using the perimeter as a parameter. The reason is that the shape of the hole is very consistent and therefore the perimeter is very closely related to the area.

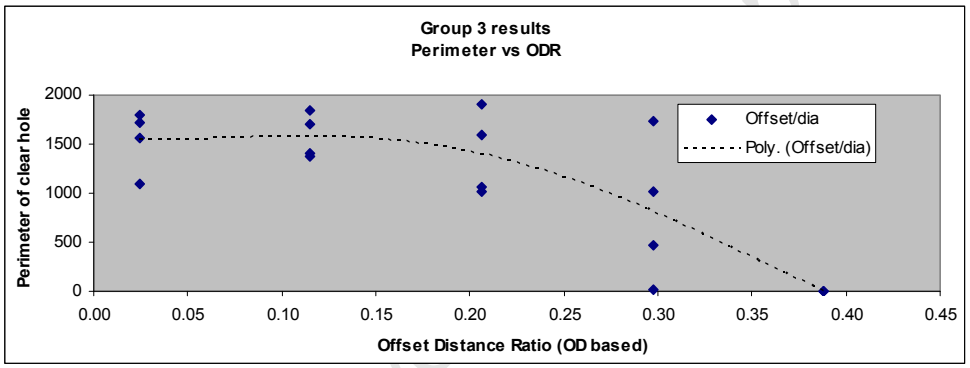

Figure 5-12: Perimeter of the clear hole as a function of ratio OD/D_e

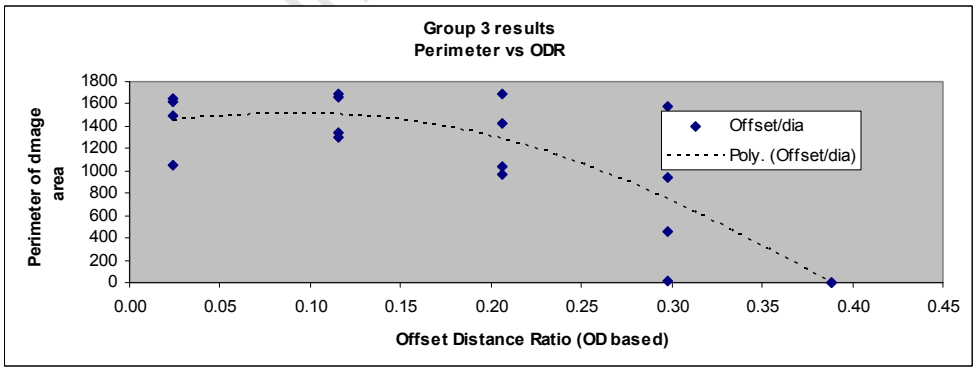

Figure 5-13: Perimeter of the damage area as a function of ratio OD/D_e

5.4.1.6 Total length of tearing as a function of ODR

The parameter *total length of tearing* versus offset distances (Figure 5-14~~Figure 5-14~~) is similar to the area-graphs. Once again, as is the case with the perimeter of the hole, the length of tearing is proportional to the area of the hole. For this reason it is sufficient to use the area parameter – the total tear length does not contribute any additional information regarding a measurement of damage.

The Y-value at the second X-value is slightly higher than at the first X-value and then drops to lower values.

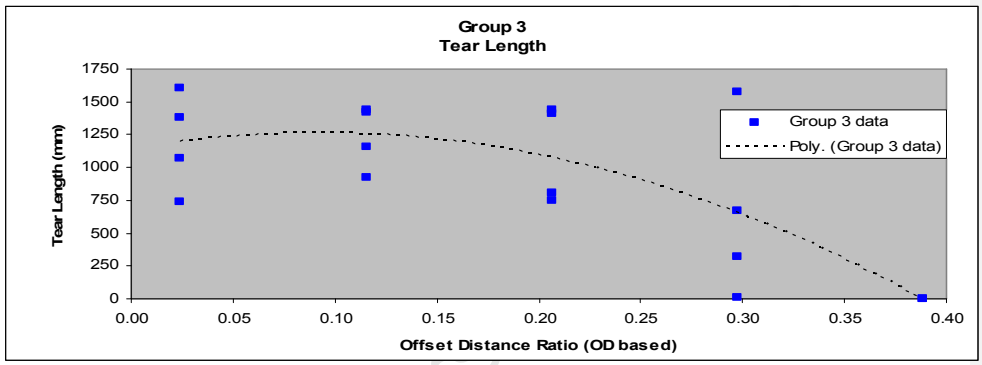

Figure 5-14: Total length of tearing as a function of offset distance ratio

5.4.1.7 Shock Factor (SF) as a function of dimensionless ratios

The Shock Factor SF is discussed in detail in paragraph 3.1.6.The equation that is based on the COD (Core Offset Distance) is used to calculate the SF that is applicable to the work in this dissertation:

$$SF = 0.\text{~~445~~}211\,(W^{1/2})/S$$

$$SF_{COD} = 0.\text{~~445~~}211\,(W^{1/2})/(COD)$$

$$= 0.\text{~~445~~}211\,(W^{1/2})/(OD+½De)$$

The applicable values for this dissertation are:

W = 30gram PE4 = 0.03*1.2 = 36gram TNT
De = 33/2 = 16,5 mm
OD ranges from 0mm to 30mm

Table 5-10 : Shock Factor based on COD (Core Offset Distance)

Mass 30g PE4 = 36g TNT equivalent					De (effective diameter if spherical) = 33mm							
Offset Distance	zero	3.8mm*	10.8mm*	15.8mm*	20.8mm*	25.8mm*	30.8mm*					
COD	17.3	20.3	27.3	32.3	37.3	42.3	47.3					
COD/De ratio	0.52	0.62	0.83	0.98	1.13	1.28	1.43					
Shock Factor SF	2.31	1.97	1.47	1.24	1.07	0.95	0.85					

* 0.8mm thickness of charge container included

The values of the Shock Factor as listed in Table 5-10~~Table 5-10~~~~Table 5-10~~ are plotted as a function of COD in Figure 5-15~~Figure 5-15~~~~Figure 5-15~~. A dash-dot line indicates the imaginary border of a spherical charge of 36g TNT.

Inspection of column 18 in Table 5-2 shows that breeching of the target occurs at a shock factor (COD based) from ~~7.9~~3.73 on the 3mm target panel and at SF greater than ~~3.1~~1.47 on the 1,2mm target panel.

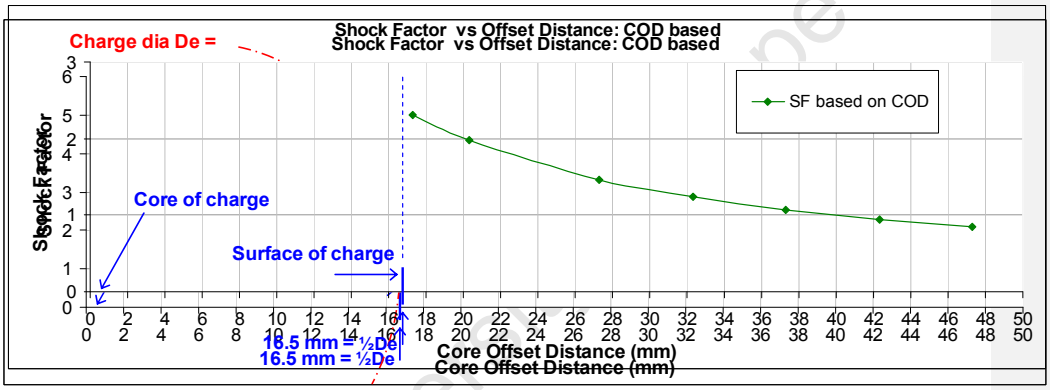

Figure 5-15: Shock Factor as a function of COD

5.4.1.8 Number of petals

The number of petals are included for completeness and for interest. The number of petals vary from four to six. The average is very close to five (see Figure 5-16~~Figure 5-16~~~~Figure~~

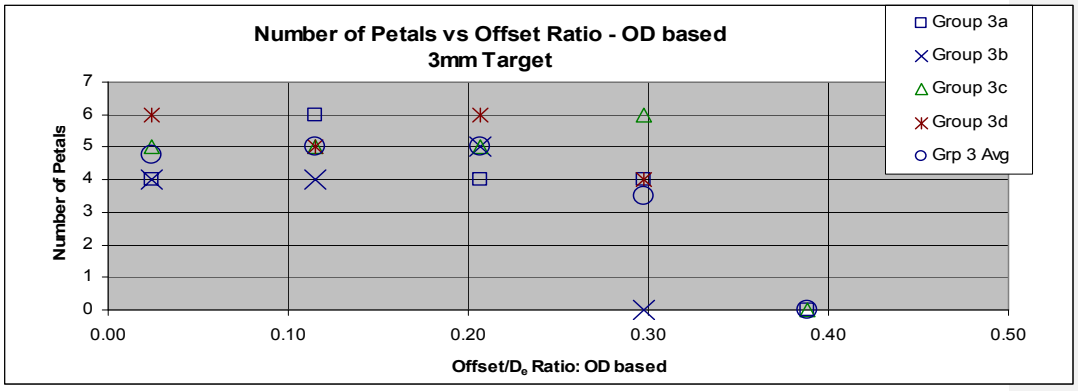

~~5-16~~).

Figure 5-16: Number of petals as a function of OD

In most cases the petals are similar in shape and size. In some instances a single petal may be partly split near the tip, forming a pair of smaller petals. Unless significantly large, such cases are counted as a single petal.

Towards the narrow ends of the petals the curvature is gradual and continuous. At the root, most petals also curve gradually into the remaining base material. However, some petals have a sharp bend at the root. This is due to straightening of the dished shape of the target plate near the root of the petal. The difference between these two types of bending is depicted in Figure 4-3~~Figure 4-3~~~~Figure 4-3~~.

5.4.1.9 Hole diameter

Refering to paragraph 3.1.8, Keil [1] presented an equation that can be used to predict the size of hole that is made by a ***contact*** charge of mass W in a target plate of thickness *h*.

$$R = 0{,}0704*(W/h)^{1/2}$$

Sample calculations using this equation are given in Table 5-11. The hole size for charge masses of 100kg, 10kg, 1kg and 30grams are calculated for plate thicknesses of 15mm, 10mm, 3mm and 1.2mm. The calculated (predicted) values are shown in the upper half of Table 5-11.

In the lower half of Table 5-11 is shown the actual hole sizes obtained for 3mm and 1,2mm target panels in the field tests.

Table 5-11 : Predicted hole diameter for different Mass and plate thickness

Predicted hole diameters		Steel Thickness h (mm)			
		15 (mm)	10 (mm)	3 (mm)	1.2 (mm)
Charge mass PE4 (contact i.e. OD=0)	100 kg	12.59	15.42	28.16	44.52
	10 kg	3.98	4.88	8.90	14.08
Predicted	1 kg	1.26	1.54	2.82	4.45
	0.03 kg	0.22	0.27	0.49	0.77
Predicted hole diameter (m) in 3mm & 1.2mm target panel				0.49	0.77
Actual measured	Measured hole diameter (m) in actual field test #1			0.35	na
	Measured hole diameter (m) in actual field test #6			0.26	na
	Measured hole diameter (m) in actual field test #15			0.42	na
	Measured hole diameter (m) in actual field test #20			0.42	na
	Measured hole diameter (m) in actual field test #1200			na	0.45
	average			0.36	0.45
Measured hole size as a percentage of Predicted hole size				73%	58%

The predicted hole size for the 3mm plate is 0.49m, which is 27% greater than the average hole size measured (0.36m from Table 5-11)

The predicted hole size for the 1.2mm plate (0.77m) is substantially greater (58%) than the hole size actually measured (0.45). This (substantial) difference can be partly explained by the fact that the petalling of the 1.2mm plate was severely restricted by the inside surfaces of the test housing, as explained in paragraph 5.3.4. As the petals were forced forward by the blast, the tips of the petals hit the inner wall of the housing, substantially reducing the freedom to continue folding and subsequently impeding the tearing that occurred. This caused the development of a smaller hole.

A common aspect is that the predicted hole size is larger than the hole size actually measured. The difference of 27% on the 3mm panel is large, but is much more acceptable

than the 58% difference found with the thinner panel. However, the hole in the thinner panel would have been much larger if the test housing did not cause the plateau effect on the petals (see 5.3.4). For this reason it is fair to assume that the percentage difference of 27% is more realistic and representative.

Keil [1] states that the critical (minimum) mass W_{cr} of explosive above which his relation for hole size is valid, is given by

$$W_{cr} = 2.72*h$$

This equation predicts that the minimum mass required to breech a hole in 3mm steel, is 8g TNT (7g PE4). The mass of explosive used in the work for this dissertation is 30g PE4 (36g TNT) which is 440% of the required minimum mass. The percentage excess is close to 1000% when calculated for the 1,2mm plate thickness.

The equation by Keil for predicting the hole size is valid for the 30g explosive and 3mm target panel as used in this dissertation.

5.4.2 Generalised offset distance

In paragraph 5.2.5 it is shown that for the 3mm panel the hole size reaches a maximum value near the second offset distance (3.8mm). This corresponds to a Core Offset Distance ratio of 0.62.

In paragraph 5.3.4 it is shown that for the 1.2mm panel the hole size forms a plateau (the reasons are explained elsewhere). If a peak/maximum is assumed to be near the ~~the~~ centre of the plateau ~~is taken as the point of maximum~~, it would correspond to about 9.8mm (Table 5-9~~Table 5-9~~~~Table 5-9~~). This ~~corresponds~~ yields~~to~~ a Core Offset Distance ratio of 0.80. It is more likely that the peak would have occurred closer to the beginning of the plateau had the petals been unimpeded. This would yield a COD ratio that is lower than 0.8.

The above value of the COD ratio for the 3mm panel can be assumed to be relatively accurate, whereas the COD ratio for the 1,2mm panel is an estimation (for previously stated reasons). However, an important aspect is that the value of COD ratio for maximum hole size is different for the thicker and the thinner panel.

An important aspect that should be borne in mind is that it has been proven that a given charge, that is known to breech a hole in a target as a contact charge, can be detonated with an increased offset distance such that the hole is actually larger than when used as a contact charge.

6 Chapter 6: CONCLUSION

6.1 General

Having described and analysed the field work, the objective and hypothesis stated in paragraphs 1.2, 3.4 and 4.1 can now be evaluated.

The stated objective was to prove or disprove that a the maximum hole size in a target panel is achieved at a non-zero offset distance.

The technique originally planned was to experimentally separate the pressure impulse from the bubble impulse, optimise each separately and then find the combined optimum.

Separating these two phenomena proved to be much more complex and interwoven than anticipated. Instead of investigating each phenomenon separately, the combined effect was investigated.

6.2 Discussion

When the value of any of the measured parameters (clear area, damage area, etc) is compared to the value of that particular parameter at zero offset distance, an increase was found when the offset distance was increased. After the initial increase, a gradual decrease followed.

Consider the graphs for the 3mm target panel in Figure-6-1 and Figure-6-2.

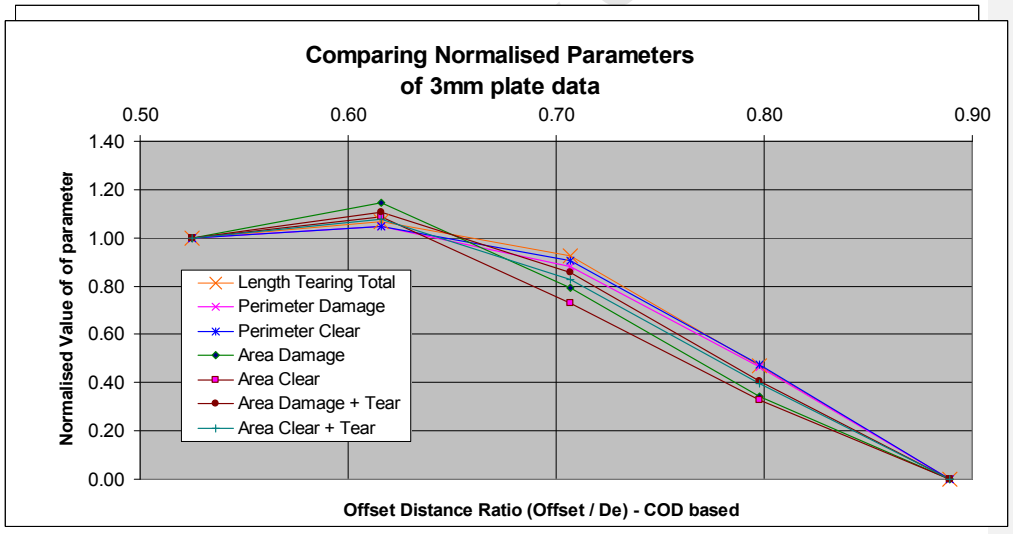

Figure-6-1 : Normalised Parameters for 3mm panel as a function of Core Offset Ratio

In Figure-6-1 (3mm panel) a maximum occurs close to a Core Offset Distance ratio of 0.62.

This maximum is evident in all the parameters listed in the annotation. Using the equation for shock factor from paragraph 5.4.1.7, the SF corresponding to this offset distance ratio is 4.16 (see Table 5-10~~Table 5-10~~~~Table 5-10~~).

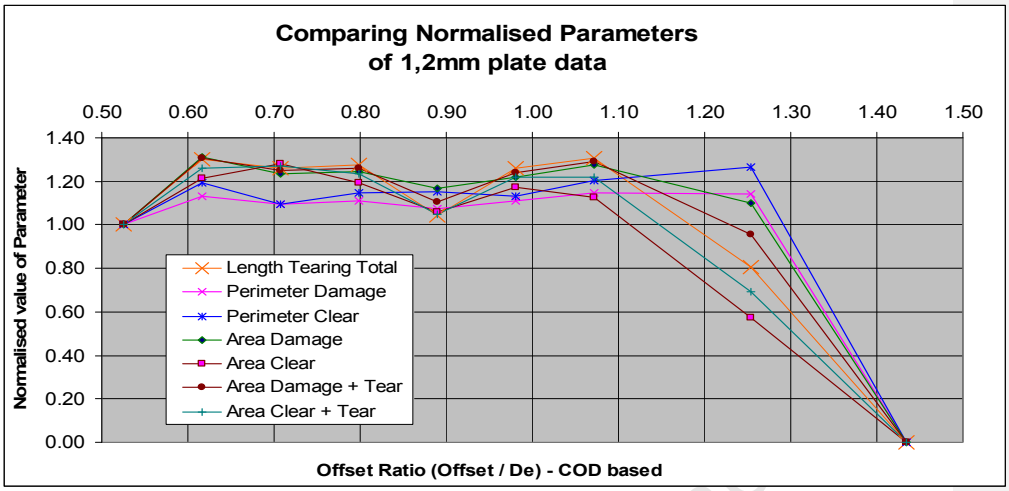

Figure-6-2 : Normalised Parameters for 1.2mm panel as a function of Core Offset Ratio

In Figure-6-2 (1,2mm panel) the second and up to seventh Y-value of all parameters are greater than the first Y-value (at zero offset distance). It was explained in paragraph 5.3.4 why the Y-values seem to form a plateau. No single maximum is evident from the data. A maximum/peak would have occurred had the~~If it is assumed that the~~ movement of the petals ~~were~~ not been restricted. Such a~~, a~~ maximum ~~may~~ would have occurred between the smallest OD and the ~~near the~~ centre of the plateau. ~~The offset ratio at the point of maximum is 0.98 and the shock factor is [redacted] (see Table 5-10)~~

Formatted: Highlight

Besides the fact that the movement of the petals were restricted by the housing, the size (area) of the test panel would also have an effect. It is conceivable that, if the area of the target panel was significantly larger, the hole size in a thinner plate (1.2mm) would be greater than that actually obtained in Group 4.

Figure-6-3 and Figure-6-4 presents the same data as before, but plotted as a function of the shock factor. The same trends as in Figure-6-1 and Figure-6-2 are evident. Note that the graphs appear reversed – this is due to the fact that the SF increases when the offset ratio decreases.

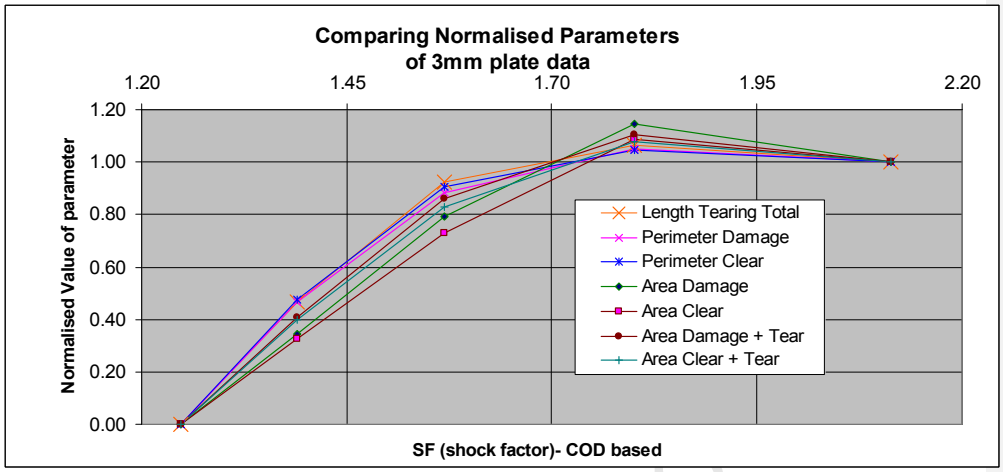

Formatted: Caption, Indent: Left: 0.39", Hanging: 0.59", Right: 0.1", Space After: 18 pt, Tab stops: 6", Left

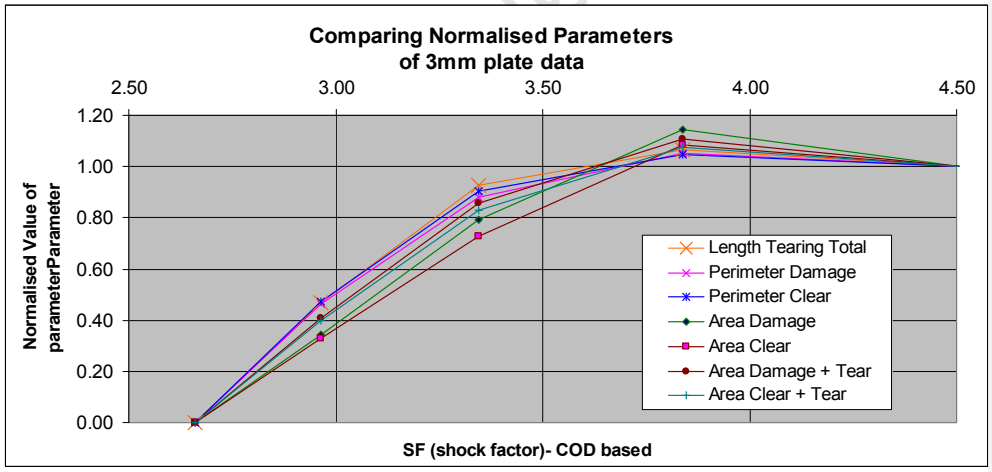

Figure-6-3 : Comparing Normalised Parameters for 3mm panel as a function of SF

Formatted: Body Text, Indent: Left: 0", First line: 0", Right: 0", Space After: 0 pt, Tab stops: Not at 6"

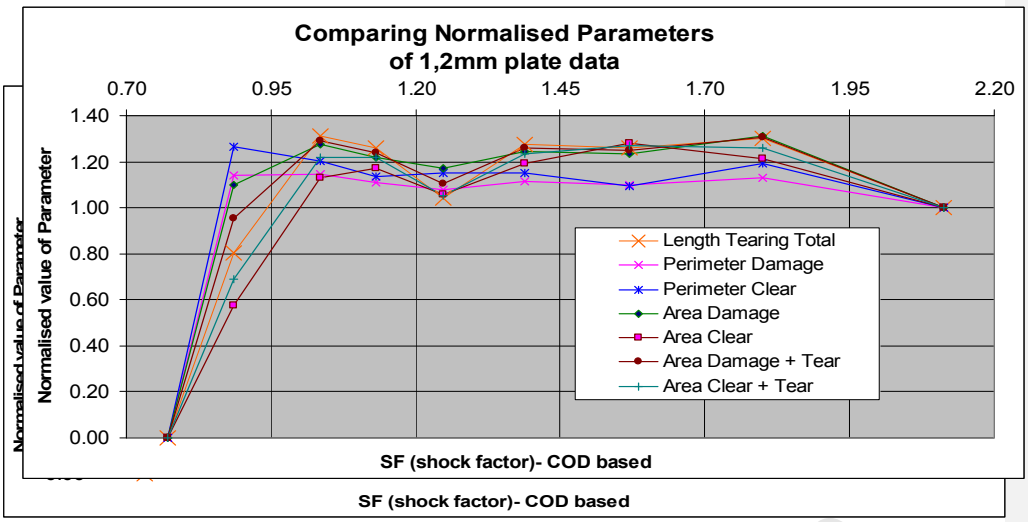

Figure-6-4 : Comparing Normalised Parameters for 1.2mm panel as a function SF

6.3 Conclusion

~~**Based on the above facts, the hypothesis was proven to be true:**~~

The effect of an underwater detonation on a submerged air-backed steel panel is increased when the offset distance is slightly increased relative to a contact detonation (zero offset distance).

The offset distance at which the maximum damage occurs is relatively small in comparison to the size (effective spherical diameter of the charge) and is ~~strongly~~ very likely to be influenced by the thickness of the panel.

For the 3mm panel the maximum occurs at about 10% of the charge diameter. For the 1,2mm panel the (estimated) maximum occurs at about 9mm, which is 27% of the charge diameter.

An important aspect that should be borne in mind is that it has been proven that a given charge that is known to breech a hole in a target as a contact charge, can be detonated with an increased offset distance such that the hole is actually larger than when used as a contact charge.

6.4 Development of a general empirical equation

It would be appropriate to develop an empirical equation that relates plate thickness, charge mass and offset distance for maximum hole size. When developing such an equation, a number of requirements should be borne in mind:

a. This equation should preferably be in a dimensionless form that enables easy scaling to different masses of explosive and different plate thicknesses.
b. The equation should be generally applicable without modification for different masses of explosive and different plate thicknesses.
c. The equation should be independent of Peak Pressure (because of the small offset distances anticipated)
d. The equation should be independent of Impulse (because of unpredictability of peak pressure at the small offset distances)

The ambit of work within this dissertation is focussed on proving that an increased hole size is obtained at a non-zero offset distance. In order to develop an equation that is generally applicable to other charge masses and plate thicknesses, requires measurement of hole size with different masses and different plate thicknesses.

The work done in this dissertation provides data on only one mass and two plate thicknesses. This limits scaling and extrapolation. Therefore development of a generally applicable equation will be discussed but not attempted.

Important factors that should be considered when developing such an equation are discussed in the following paragraphs.

6.4.1 Factors to be considered

6.4.1.1 Thickness of the target panel

The strength of a panel is directly proportional to the thickness of a panel and therefore thickness is very representative of the strength/resistance against breeching i.e.

h α strength/resistance

The **mass** of the target is calculated by the [thickness of the target] multiplied by the [area that is influenced by the shock impulse]. Therefore thickness ***h*** could be used to represent mass when viewed as 'unit mass' (or mass per unit area).

Mass = f (area, thickness)

The thickness should have **limits** beyond which the equation becomes unreliable (high end and low end)

A critical minimum value of shock impulse is required to breech a panel of given thickness. Small offset distances (less than 5x charge diameter) presents a problem …. the equation for peak pressure and for impulse do not apply at very short offset distances.

So, if offset distance is less than 5x charge diameter, then any equation that is developed should be independent of peak pressure and impulse.

An equation that relates the minimum mass of charge required to breech a panel of thickness *h* was proposed by Keil [1].

$$R = 0{,}0704*(W/h)^{1/2}$$

Note: this equation applies to contact charge (zero offset) and the equation does not contain variables of peak pressure or impulse.

This equation may be useful as the basis for a generally applicable equation to calculate the required offset distance for maximum hole size. The reason is that it has been proven that a given charge that is known to breech a hole in a target as a contact charge, can be detonated with an increased offset distance such that the hole is actually larger than when used as a contact charge.

Finney [47] reported on his work with explosive forming of dished shapes in water that the impulse per unit deformation showed linear relation with the original thickness of the plate and that the impulse required for rupture increased linearly with the original thickness.

6.4.1.2 Peak Pressure and Offset Distance

As with mass of explosive, if it is assumed that the peak pressure of the shock wave is the key parameter that causes breeching of the target panel, then it follows that the effect of offset distance should be viewed in relation to the peak pressure. However, as demonstrated in the following paragraphs, the equation for peak pressure is not valid at the very small offset distances in this dissertation.

The relation for peak pressure is an inverse power relation. The equation given by various authors are essentially the same:

$$P = K (M^{1/3}/S)^{A}$$

where K is a constant, M is mass of explosive, S is offset distance

The value of A given by different authors varies slightly – Cole [8] is the oldest work (1949) and gives A_{TNT} = 1.~~18~~3. A more recent publication by Keil [1] (1961) states A_{TNT} =1.13.

Cooper [21] (1997) state A =1.13 for both TNT and Pentolite. Cooper [21, p 412] refers to Liddiard [48] that states A_{Pent} = 1.194 for Pentolite.

The published equations for peak shock pressure and shock impulse both contain offset distance as a variable. These equations are stated to be not applicable at offset distances less than 5 times the charge diameter. This limitation dictates that the published general equations for peak pressure and pressure impulse cannot be used to quantitatively predict peak pressure at the offset distances applicable to this dissertation.

Cooper [21] presents a technique to predict the peak pressure at offset distances less than 5 times the charge diameter. By replacing the mass term in the general pressure equation with density and equivalent spherical radius, he presents an equation for pressure:

$$P_o = K \{[(4\pi\rho_o/3)^{1/3}Ro / (R-Ro)\}^{A}$$

$$= K \{[(4\pi\rho_o/3)^{1/3}] / [(R/Ro)-1]\}^{A}$$

R_o is the equivalent spherical radius of the charge. R is the distance at which the pressure is calculated. P_o is the peak pressure as calculated by the general equation for peak pressure at offset distance S or, in this instance, at distance R.

Cooper equates the pressure-velocity isentrope of the detonation products to the Hugoniot pressure-velocity isentrope for water at the surface of the charge. He then mathematically extrapolates the tangent of the pressure function obtained from above equation to an offset distance closer to the charge.

Note: Hugoniot planes are isentropes (or loci) of equilibrium states in which an explosive can exist during the detonation process. The principle variables are pressure, shock velocity, particle velocity and specific internal energy.

It can be seen that the pressure approaches infinity as the term R/R_o approaches unity, ie as the offset distance approaches the equivalent radius of the charge. He states that a ratio of R/Ro ~1.6 is the lowest practical value that can be used in this equation.

Viewing this in the context of this dissertation

– the equivalent charge diameter of 30grams of explosive is 33mm (ie radius = 16.5mm). The 5-times-charge-diameter limitation equals 165mm. Thus, the general equation for peak pressure becomes un-usable at offset distances smaller than 165mm (keep in mind that the offset distances that are important to the work in this dissertation are less than 20mm, typically single digit).

The smallest value of R that is practical using the Cooper approximation is when R approaches $1.6*R_o$, ie 26mm (1.6 x 16.5mm). Since P can be calculated using the general equation for peak pressure that is valid down to 165mm (ie 5xDe), a further pressure value P_o can be calculated at an offset distance approaching 26mm and then extrapolated to smaller values of R. This technique is illustrated in Figure 6-5

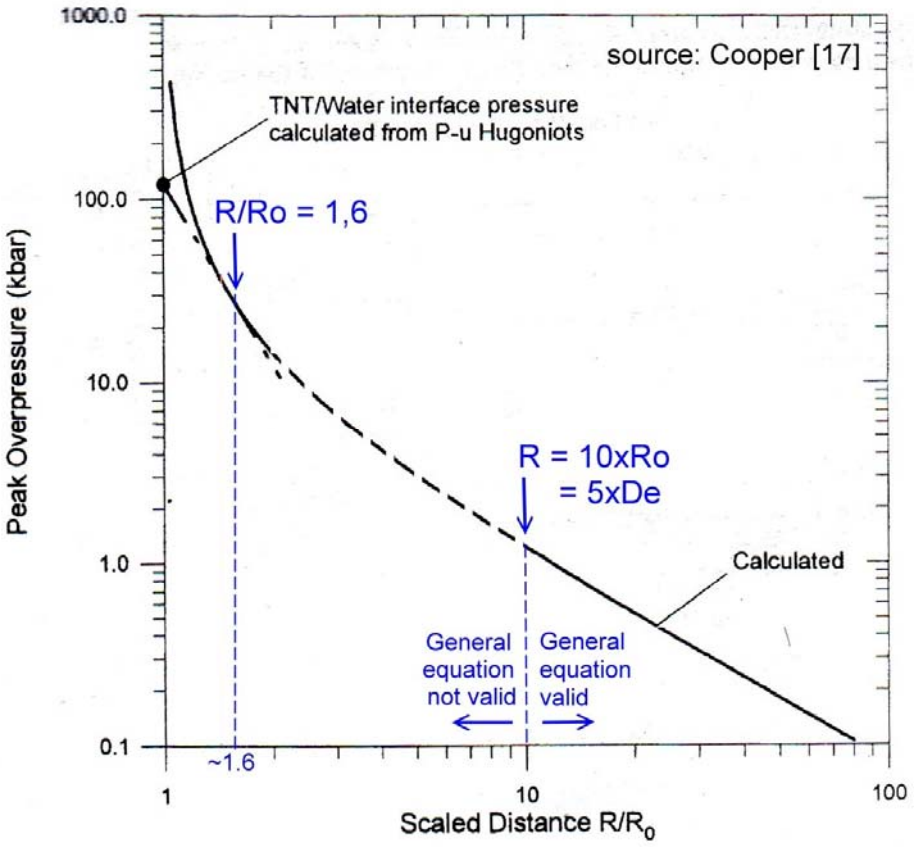

Figure 6-5: Extrapolation of calculated peak pressure (Cooper [17])

The smallest value of offset distance that is calculated by this Cooper equation is still substantially more than the offset distances at which the hole size appears to have a maximum in the field work for this dissertation.

6.4.1.3 Impulse

Paragraph 3.1.2 discusses the impulse of the shock wave.

Impulse = integral of (~~Peak~~ Pressure over Time)

In order to calculate the impulse, the function of pressure over time p(t) is required.

In the case of the field work of this dissertation, peak pressure is not known accurately and therefore impulse cannot be calculated to render reliable/accurate values.

The reason is twofold –

a) the published equations are not applicable for the very small offset distances used in the

field work for this dissertation (all offset distances are substantially closer than 5 times charge diameter).

b) no pressure measurements were taken close to the target panel

Note: Should the restriction of minimum offset distance be ignored, then values for the shock energy and shock impulse for the field work in this dissertation could be calculated, keeping in mind that the figure obtained is not correct. For this reason no calculations for peak pressure and impulse is made.

6.4.1.4 Relation between explosive mass and shock pressure

Formatted: Highlight

If it is assumed that the peak pressure of the shock wave is the key parameter that causes breeching of the target panel, then it follows that the effect of mass should ideally be viewed in relation to the peak pressure.

The published general equation for peak pressure contains the mass of explosive to a cube root. This value $M^{1/3}$ is raised to the value of A as stated in 6.4.1.2. Therefore the relation between explosive mass M and shock pressure P is to a power of between 0.377 (1/3 multiplied by A=1.13) and 0.392 (1/3 multiplied by A=1.18). This value is close to cube root since the value of A is close to unity.

6.4.1.5 Chemistry of the explosive

It is common practice to present any given equation for general application as applicable to TNT. The variables within the equation are modified as required by the user to suit the chemistry he is addressing.

This dissertation follows common practice by addressing only the case of TNT.

6.4.1.6 Shape of the explosive

The shape of the explosive is assumed to be spherical or at least symmetrical around all three axis. Examples of such symmetrical shapes are cylindrical with length equal to diameter (such as used in the field work for this dissertation) or a cube having length = height = width.

A relatively flat/wide explosive will produce a relatively uniform pressure loading on the target whereas a relatively narrow/high charge will produce a more local/focused pressure loading on the target. The aspect of effect of the shape of the charge will not be addressed in this dissertation.

6.4.1.7 Depth of the charge

The submerged depth of the charge is assumed to be deeper than the maximum gas bubble diameter. Therefore the depth of detonation will not be included in the empirical equation.

6.4.1.8 Size of the hole

For the purpose of this dissertation the initial size of the hole is not considered. The only aspect of importance is that the target is breeched (ie a hole is actually created).

This dissertation is about *enlarging* an existing/given hole created by a *given (contact) charge* by changing the offset distance.

The size of the hole will therefore not be incorporated into the proposed empirical equation.

As stated in paragraph 3.1.8, Keil [1] described a definite relation between radius of hole *R* (m), plate thickness *h* (m) and explosive weight *W* (kg) for *contact* detonations (*R* and *h* are in m and *W* is in kg)

$$R = 0{,}0704*(W/h)^{1/2}$$

He stated that the critical (minimum) mass W_{cr} of explosive above which this relation is valid, is given by

$$W_{cr} = 2.72*h$$

REFERENCES

1 Keil A.H,."The Response of Ships to Underwater Explosions (1961) Transactions of Society of Naval Architects & Marine Engineers, 1961; 69: 376-410

2. Von Neumann J, Shapiro M, "Underwater explosion of a nuclear bomb" (1946) Report LA454, US Atomic Energy Commission

3 Benjamin T.B.; Ellis A.T, "The collapse of cavitation bubbles and the pressures thereby produced against solid boundaries" (1966), Phil Trans of the Royal Society of London. Series A, Mathematical and Physical Sciences, Vol 270, No 1110, pp 221-240

4 Penney W, "The pressure-Time Curve for Underwater Explosions" (1940) Civil Defence Research Committee, England

5 Herrings C, "Theory of the Pulsations of Gas Bubble Produced by an Underwater Explosion" NDRC Report C4SR20-010 (1941) Columbia University, a Division of National Defence Research

6 Batchelor G, "The Life and Legacy of G.I.Taylor", Cambridge University Press, (1996), ISBN 0 521 46121 9

7 Penny WG, Taylor GI, "A Discussion on Detonation", Proceedings of the Royal Society of London. Series A, Mathematical and Physical Sciences, Vol. 204, No. 1076, (Nov. 22, 1950), pp. 1-33

8. Cole RH, "Underwater Explosions", 1949 Princeton University Press, Princeton, New Jersey

9. Arons AB, "Underwater Explosion Shock Wave Parameters at Large Distances from the Charge" (1954), The Journal of the Acoustical Society of America, Volume 27, No 3, May. 1954

10 Snay, HG "Hydrodynamics of Underwater Explosions (1957) Symposium on Naval Hydrodynamics, Publication 515, National Academy of Science, National Research Council, Washington DC, 335-362

11 Swisdak, M M, "Explosion effects and Properties Part II underwater" NSWC WOLTR 76-116 (1978) Report NSWC/WOL/TR-76-116, Naval Surface Weapons Center, Silver Spring, Maryland 20910

12 Hunter C, "On the collapse of an empty cavity in water" (1960), Cambridge Journals Online, Journal of Fluid Mechanics Digital Archive, 8: 241-273, Cambridge University Press

13 Marsh HW, Mellen RH, Konrad VL, "Anomalous Absorption of Pressure Waves from Explosions in Sea Water" (1965) AVCO Marine Electronics 0ffice, New London, Connecticut

14 Bjorno L, Levin P, "Underwater explosion research using small amounts of chemical explosives" (1976), ULTRASONICS. NOVEMBER 1976

15 Menkes SB, Opat HJ, "Tearing and shear failures in explosively loaded clamped beams" (1973), Explosive Mechanics 13, 480-486

16 Olson MD, Nurick GN & Fagnan JR, "Deformation and rupture of blast loaded square plates: predictions and experiments", Int. Journal of Impact Engineering 31 (1993), 279-291

17 Shin YS, Hooker DT, "Damage response of submerged imperfect cylindrical structures to underwater explosion" (1996) Computers & Structures Vol 60 No 5 pp683-693

18 Jiang J, Olson MD, "Rigid Plastic analysis of underwater blast loaded stiffened plates" (1995) International Journal of Mechanical Science Vol 37, No 8, pp 843-859

19 Librescu L, Oh SY, Hohe J, "Dynamic response of anisotropic sandwich flat panels to underwater and in-air explosions", International Journal of Solids and Structures 45 (2006) 3794-3816

20 Hammond L, "Underwater Shock Wave Characteristics of Cylindrical Charges" (1995) Aeronautical and Maritime Research Laboratory, Melbourne, Victoria 3101, Australia

21 Cooper PW, "Explosives Engineering" Wiley-VCH, Inc (1996) ISBN 0-471-18636-8

22 Chung M, Brett J, "Assessment of Underwater Blast Effects on Scaled Submerged Objects" (1997), Weapons Systems Division, Aeronautical and Maritime Laboratory, DSTO-TR-0575

23 Chung M, Kinsey T, "Investigation into the Effects of Underwater Shock Waves on Simple Structures, Shielded and Bare Explosive Materials" (1998) DSTO-RR-0134. DSTO Aeronautical and Maritime Research Laboratory, Melbourne

24 Brett J, "Numerical Modelling of Shock Wave and Pressure Pulse Generation by Underwater Explosions" (1998) DTSO-TR-0677. DSTO Aeronautical and Maritime Research Laboratory, Melbourne

25 Murata K, Takahashi K, Kato Y "Effect of Explosive Composition on the Underwater Shock and Bubble Pulse loading against Model Steel Cylinder" (1999) NOF Corporation Aichi, Japan

26 Reid WD, "The response of surface ships to underwater explosions" (1996) DSTO-GD-0109. DSTO Aeronautical and Maritime Research Laboratory, Melbourne, Australia

27 Ramajeyathilagam K, Vendhan CP, Bhujanga V, "Non-linear transient dynamic response of rectangular plates under shock loading" International Journal of Impact Engineering 24 (2000) 999-1015 & Vol 355, No 1724

28 Hammond L.D, "The structural response of submerged air-backed plates to underwater explosions" (2000) Thesis submitted for PhD at Department of Civil Engineering, Monash University

29 Brett J, Yiannakopoulos G, Van der Schaaf PJ, "Time-resolved measurement of the deformation of submerged cylinders subjected to loading from a nearby explosion", International Journal of Impact Engineering 24 (2000) 875-890

30 Zhang YL, Yeo KS, Khoo BC, Wang C, "3D Jet Impact and Toroidal Bubbles" Journal of Computational Physics 166, 336-360 (2001)

31 Zhang AM, Yao XL, Yu XB, "The dynamics of three-dimensional underwater explosion bubble", Journal of Sound and Vibration 311 (2008) 1196–1212

32 Rajendran R, Narasimhan K, "Damage prediction of clamped circular plates subjected to contact underwater explosion" International Journal of Impact Engineering 25 (2001) 373-386

33 Langdon G.S., Chung Kim Yuen S., Nurick G.N. "Experimental and Numerical studies on the response of quadrangular stiffened plates. Part II: Localised blast loading" International Journal of Impact Engineering 31 (2005) 85-111

34 Balden VH, Langdon GS, Snyman IM, Malan DF, Nurick GN, "Experimental and Numerical Response of a Scaled Hull Structure Subjected to an Underwater Blast" (2005) *BISRU, Dept of Mech Eng, University of Cape Town, South Africa*

35 Church P, Reynolds M, Huntington W, Townsley R, Sharpe K "Underwater Plate Holing Studies" (2003) QuinetiQ, Modelling and Explosives Applications, Fort Halstead, UK

36 Slater JE, Rude G, Lee JJ, "Close Proximity Blast Loading and Damage of Cylinders" (2005) Defence Research Department Canada, Suffield, TIA8K6

37 Brett JM, Buckland M, Turner T, Killoh C and Kiernan P, "An Experimental Facility for Imaging of Medium Scale Underwater Blast" (2000) DSTO-TR-1432, Maritime Platforms Division, Platforms Sciences Laboratory

38 Brett JM, Yiannakopoulos G, "An experimental study of the detonation of an explosive device in close proximity to a submerged structure" (2005) 6th Asia-Pacific Conference on Shock & Impact Loads on Structures, Dec'05, Perth, Australia

39 Brett JM, Yiannakopolous G, "A study of explosive effects in close proximity to a submerged cylinder" (2007) International Journal of Impact Engineering

40 Rajendran R, Narasimhan K, "Deformation and fracture behaviour of plate specimens subjected to underwater explosion—a review 2005" (~~2005~~2006) International Journal of Impact Engineering 32, 2006

41 Rajendran R, Narasimhan K, "A shock factor based approach for the damage assessment of plane plates subjected to underwater explosion" (2006) Journal of strain analysis Vol 41 No 6 (2006)

42 Rajendran R, Paik JN, Kim BJ, "Design of warship plates against underwater explosions" (2006) SAOS 2006 Vol 1 Nr 4 pp 347-356

43 Rajendran R, Narasimhan K, "Underwater shock response of circular HSLA steel plates" (2000) Shock and Vibration 7, 251-262

44 Rajendran R, "Reloading effects on plane plates subjected to non-contact underwater explosion" (2008) Journal of Material Processing Technology 206 (2008) 275-281

45 Rajendran R, Lee JM, "Blast loaded plates", Marine structures (2008), doi:10.1016/j.marstruc.2008.04.001

46 Ezra AA, "Principles and Practice of Explosive Metal Working, Volume 1" (1973), Industrial Newspapers Ltd., John Adams House, Adelphi, London (WC2N 6JH).

47 Finnie TM, "Explosive forming of circular diaphragms" (1962) Institution of Sheet Metal Engineering (1962) 391–398

48 Liddiard TP, Forbes JW, "Shock waves in Fresh Water generated by the detonation of Pentolite spheres" (1983), NSWC TR 82-488, Dahlgren, Virginia

APPENDICES

APPENDIX A : Photographs of the test samples

APPENDIX B : Drawings with Area and Perimeter Calculations

APPENDIX C : Possible reasons for inconsistent results in Group 2

APPENDIX D : Early test results that were disregarded

APPENDIX A : Photographs of the test samples

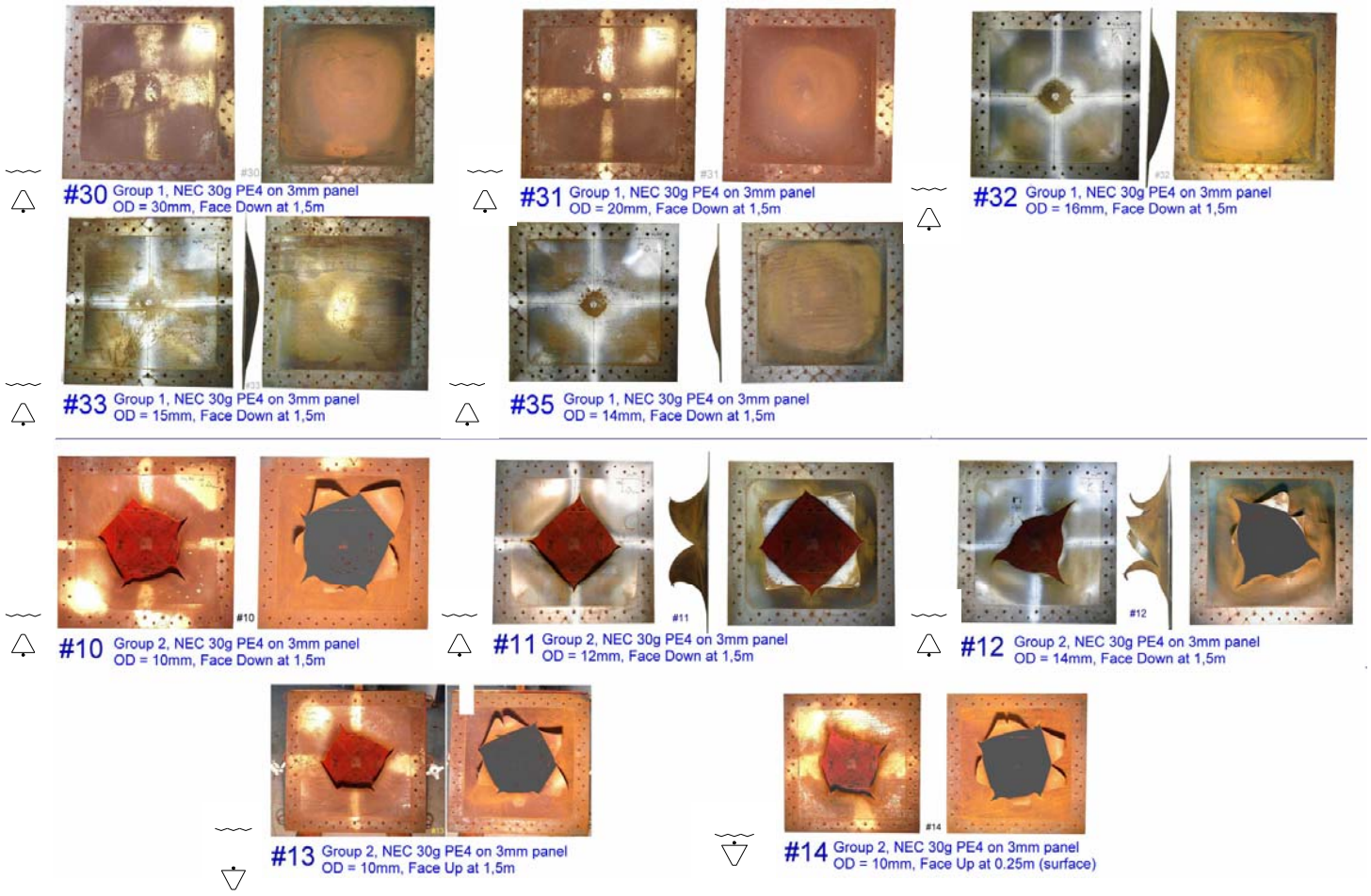

#30 Group 1, NEC 30g PE4 on 3mm panel
OD = 30mm, Face Down at 1,5m

#31 Group 1, NEC 30g PE4 on 3mm panel
OD = 20mm, Face Down at 1,5m

#32 Group 1, NEC 30g PE4 on 3mm panel
OD = 16mm, Face Down at 1,5m

#33 Group 1, NEC 30g PE4 on 3mm panel
OD = 15mm, Face Down at 1,5m

#35 Group 1, NEC 30g PE4 on 3mm panel
OD = 14mm, Face Down at 1,5m

#10 Group 2, NEC 30g PE4 on 3mm panel
OD = 10mm, Face Down at 1,5m

#11 Group 2, NEC 30g PE4 on 3mm panel
OD = 12mm, Face Down at 1,5m

#12 Group 2, NEC 30g PE4 on 3mm panel
OD = 14mm, Face Down at 1,5m

#13 Group 2, NEC 30g PE4 on 3mm panel
OD = 10mm, Face Up at 1,5m

#14 Group 2, NEC 30g PE4 on 3mm panel
OD = 10mm, Face Up at 0.25m (surface)


#01 Group 3a, NEC 30g PE4 on 3mm panel
OD = 0mm, Face Down at 2m
#02 Group 3a, NEC 30g PE4 on 3mm panel
OD = 3mm, Face Down at 2m
#03 Group 3a, NEC 30g PE4 on 3mm panel
OD = 6mm, Face Down at 2m
#04 Group 3a, NEC 30g PE4 on 3mm panel
OD = 9mm, Face Down at 2m
#05 Group 3a, NEC 30g PE4 on 3mm panel
OD = 12mm, Face Down at 2m
#06 Group 3b, NEC 30g PE4 on 3mm panel
OD = 0mm, Face Down at 1,5m
#07 Group 3b, NEC 30g PE4 on 3mm panel
OD = 3mm, Face Down at 1,5m
#08 Group 3b, NEC 30g PE4 on 3mm panel
OD = 6mm, Face Down at 1,5m
#09 Group 3b, NEC 30g PE4 on 3mm panel
OD = 9mm, Face Down at 1,5m

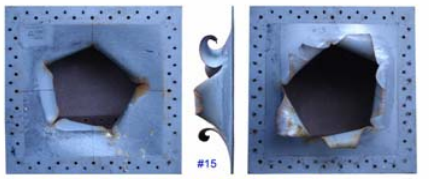

#15 Group 3c, NEC 30g PE4 on 3mm panel
OD = 0mm, Face Down at 1,5m

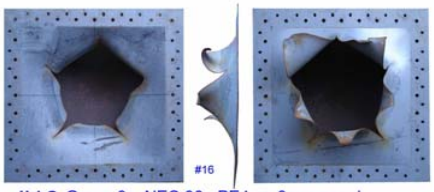

#16 Group 3c, NEC 30g PE4 on 3mm panel
OD = 3mm, Face Down at 1,5m

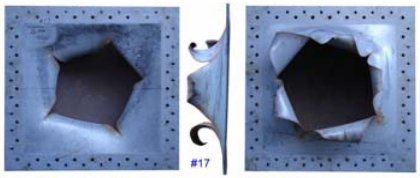

#17 Group 3c, NEC 30g PE4 on 3mm panel
OD = 6mm, Face Down at 1,5m

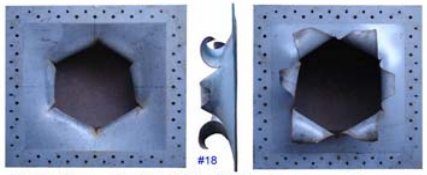

#18 Group 3c, NEC 30g PE4 on 3mm panel
OD = 9mm, Face Down at 1,5m

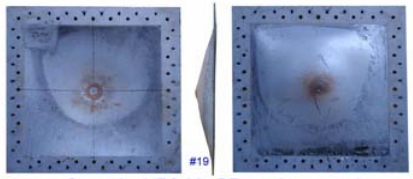

#19 Group 3c, NEC 30g PE4 on 3mm panel
OD = 12mm, Face Down at 1,5m

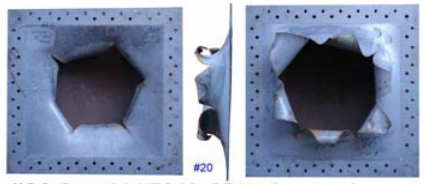

#20 Group 3d, NEC 30g PE4 on 3mm panel
OD = 0mm, Face Down at 1,5m

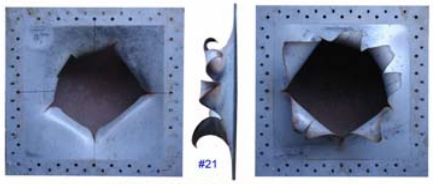

#21 Group 3d, NEC 30g PE4 on 3mm panel
OD = 3mm, Face Down at 1,5m

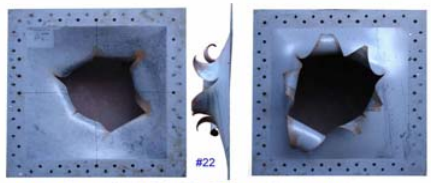

#22 Group 3d, NEC 30g PE4 on 3mm panel
OD = 6mm, Face Down at 1,5m

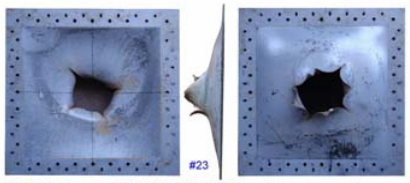

#23 Group 3d, NEC 30g PE4 on 3mm panel
OD = 9mm, Face Down at 1,5m

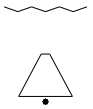

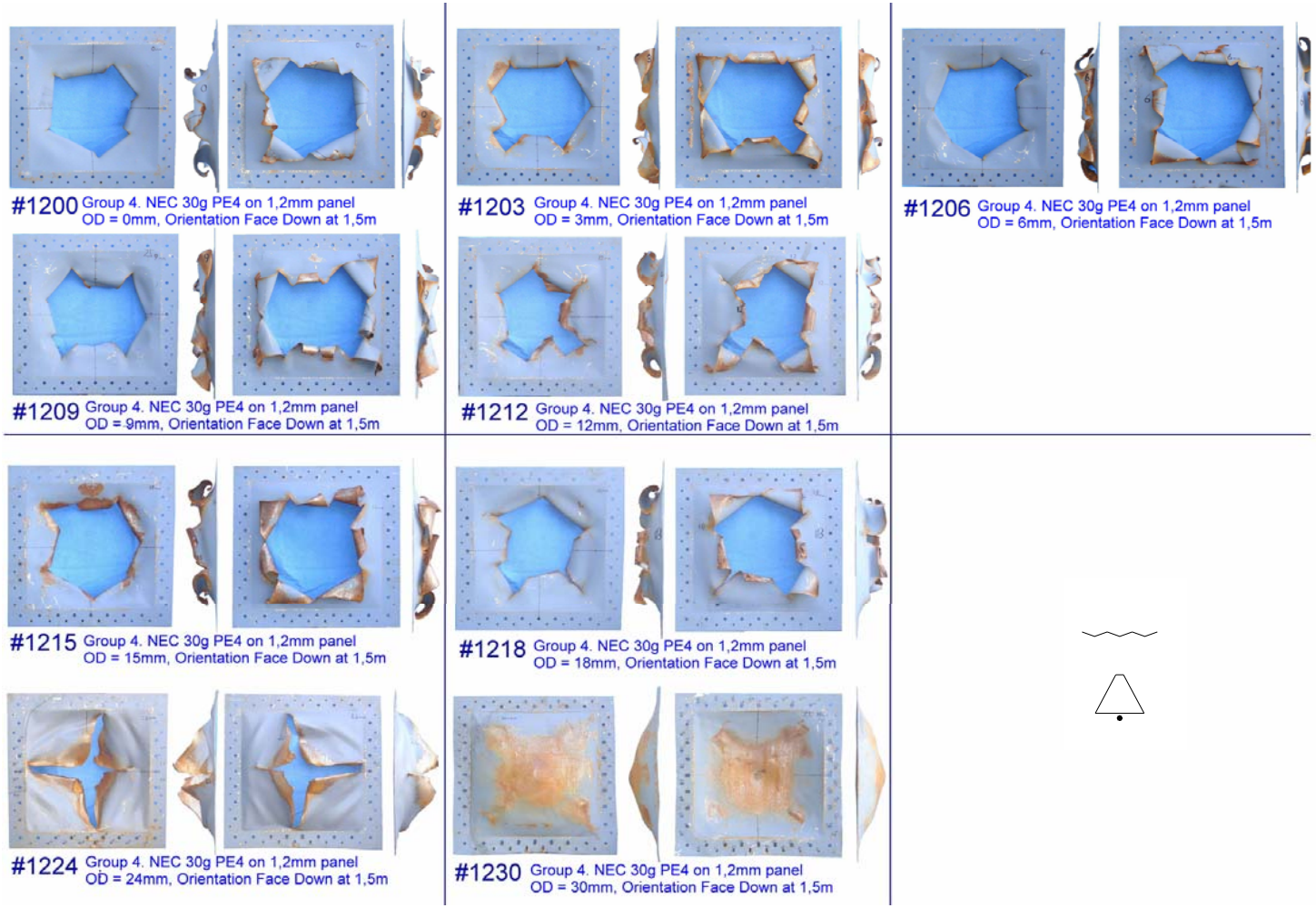
#1200 Group 4. NEC 30g PE4 on 1,2mm panel
OD = 0mm, Orientation Face Down at 1,5m
#1203 Group 4. NEC 30g PE4 on 1,2mm panel
OD = 3mm, Orientation Face Down at 1,5m
#1206 Group 4. NEC 30g PE4 on 1,2mm panel
OD = 6mm, Orientation Face Down at 1,5m
#1209 Group 4. NEC 30g PE4 on 1,2mm panel
OD = 9mm, Orientation Face Down at 1,5m
#1212 Group 4. NEC 30g PE4 on 1,2mm panel
OD = 12mm, Orientation Face Down at 1,5m
#1215 Group 4. NEC 30g PE4 on 1,2mm panel
OD = 15mm, Orientation Face Down at 1,5m
#1218 Group 4. NEC 30g PE4 on 1,2mm panel
OD = 18mm, Orientation Face Down at 1,5m
#1224 Group 4. NEC 30g PE4 on 1,2mm panel
OD = 24mm, Orientation Face Down at 1,5m
#1230 Group 4. NEC 30g PE4 on 1,2mm panel
OD = 30mm, Orientation Face Down at 1,5m

APPENDIX B : Drawings with Area and Perimeter Calculations

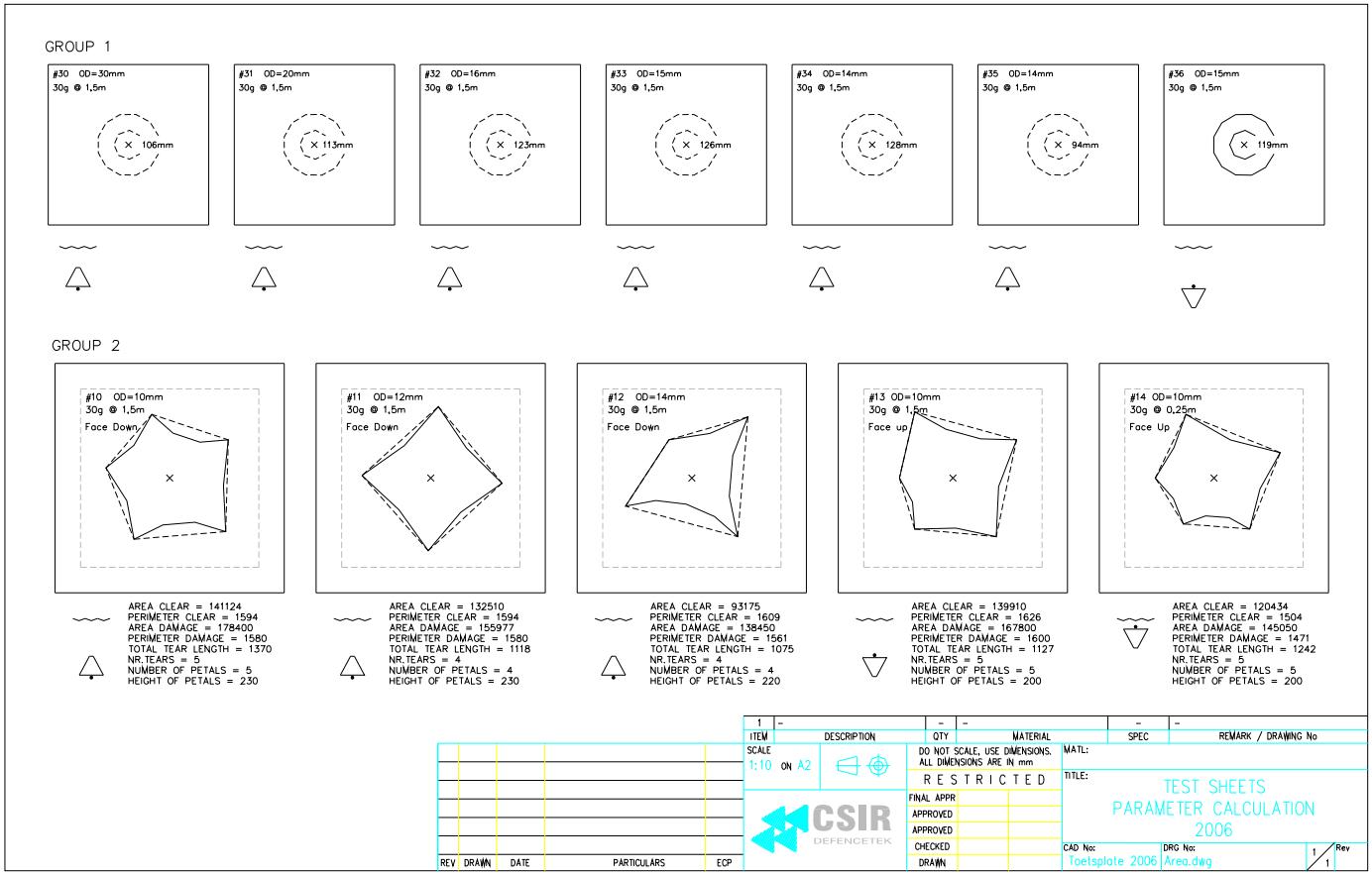

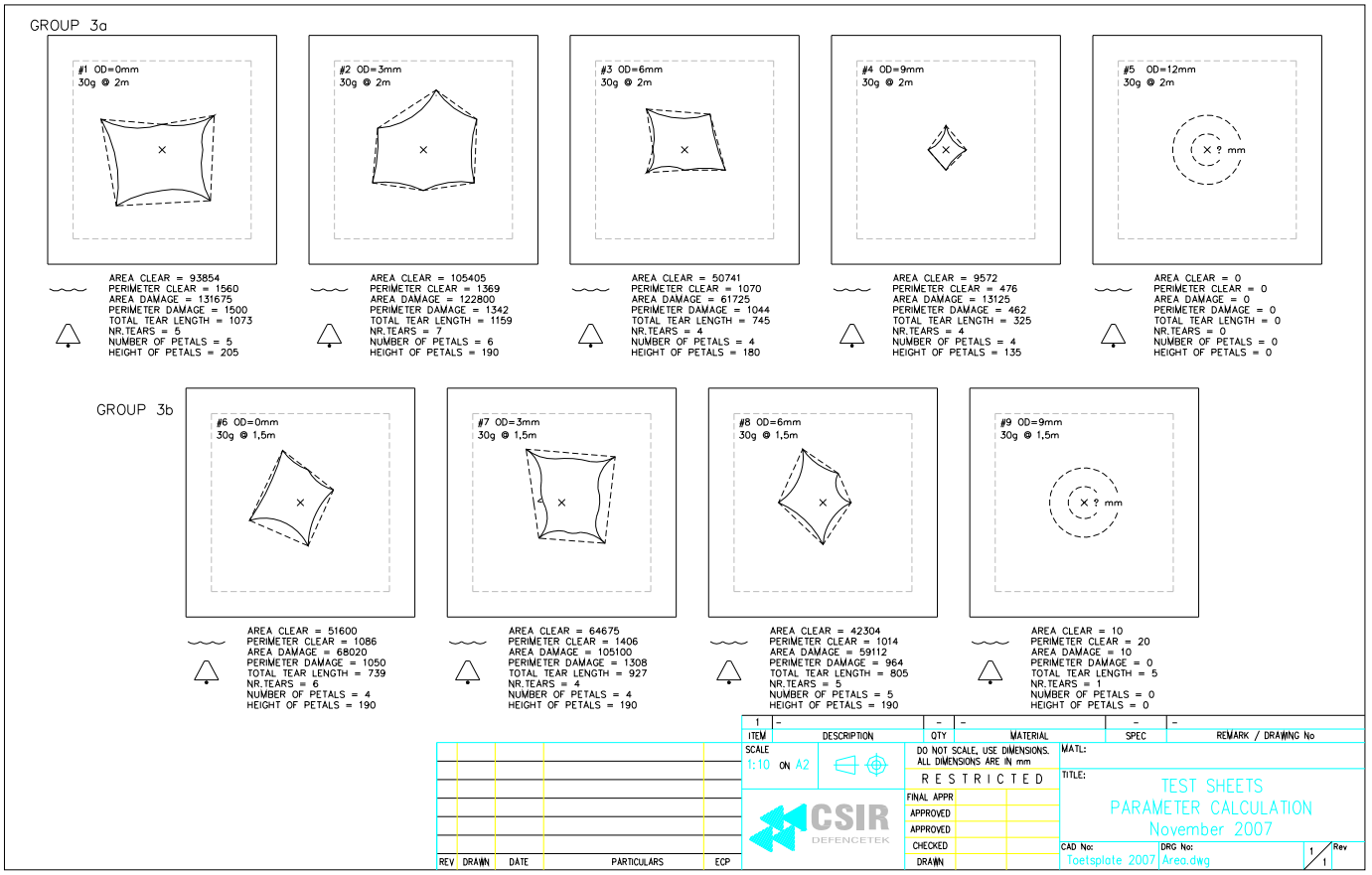
GROUP 3a
#1 OD=0mm
30g @ 2m
AREA CLEAR = 93854
PERIMETER CLEAR = 1560
AREA DAMAGE = 131675
PERIMETER DAMAGE = 1500
TOTAL TEAR LENGTH = 1073
NR.TEARS = 5
NUMBER OF PETALS = 5
HEIGHT OF PETALS = 205
#2 OD=3mm
30g @ 2m
AREA CLEAR = 105405
PERIMETER CLEAR = 1369
AREA DAMAGE = 122800
PERIMETER DAMAGE = 1342
TOTAL TEAR LENGTH = 1159
NR.TEARS = 7
NUMBER OF PETALS = 6
HEIGHT OF PETALS = 190
#3 OD=6mm
30g @ 2m
AREA CLEAR = 50741
PERIMETER CLEAR = 1070
AREA DAMAGE = 61725
PERIMETER DAMAGE = 1044
TOTAL TEAR LENGTH = 745
NR.TEARS = 4
NUMBER OF PETALS = 4
HEIGHT OF PETALS = 180
#4 OD=9mm
30g @ 2m
AREA CLEAR = 9572
PERIMETER CLEAR = 476
AREA DAMAGE = 13125
PERIMETER DAMAGE = 462
TOTAL TEAR LENGTH = 325
NR.TEARS = 4
NUMBER OF PETALS = 4
HEIGHT OF PETALS = 135
#5 OD=12mm
30g @ 2m
? mm
AREA CLEAR = 0
PERIMETER CLEAR = 0
AREA DAMAGE = 0
PERIMETER DAMAGE = 0
TOTAL TEAR LENGTH = 0
NR.TEARS = 0
NUMBER OF PETALS = 0
HEIGHT OF PETALS = 0
GROUP 3b
#6 OD=0mm
30g @ 1,5m
AREA CLEAR = 51600
PERIMETER CLEAR = 1086
AREA DAMAGE = 68020
PERIMETER DAMAGE = 1050
TOTAL TEAR LENGTH = 739
NR.TEARS = 6
NUMBER OF PETALS = 4
HEIGHT OF PETALS = 190
#7 OD=3mm
30g @ 1,5m
AREA CLEAR = 64675
PERIMETER CLEAR = 1406
AREA DAMAGE = 105100
PERIMETER DAMAGE = 1308
TOTAL TEAR LENGTH = 927
NR.TEARS = 4
NUMBER OF PETALS = 4
HEIGHT OF PETALS = 190
#8 OD=6mm
30g @ 1,5m
AREA CLEAR = 42304
PERIMETER CLEAR = 1014
AREA DAMAGE = 59112
PERIMETER DAMAGE = 964
TOTAL TEAR LENGTH = 805
NR.TEARS = 5
NUMBER OF PETALS = 5
HEIGHT OF PETALS = 190
#9 OD=9mm
30g @ 1,5m
? mm
AREA CLEAR = 10
PERIMETER CLEAR = 20
AREA DAMAGE = 10
PERIMETER DAMAGE = 0
TOTAL TEAR LENGTH = 5
NR.TEARS = 1
NUMBER OF PETALS = 0
HEIGHT OF PETALS = 0
ITEM
DESCRIPTION
QTY
MATERIAL
SPEC
REMARK / DRAWING No
SCALE
1:10 ON A2
DO NOT SCALE, USE DIMENSIONS.
ALL DIMENSIONS ARE IN mm
RESTRICTED
MATL:
TITLE:
TEST SHEETS
PARAMETER CALCULATION
November 2007
FINAL APPR
APPROVED
APPROVED
CHECKED
DRAWN
CSIR
DEFENCETEK
REV
DRAWN
DATE
PARTICULARS
ECP
CAD No:
Toetsplate 2007
DRG No:
Area.dwg
Rev

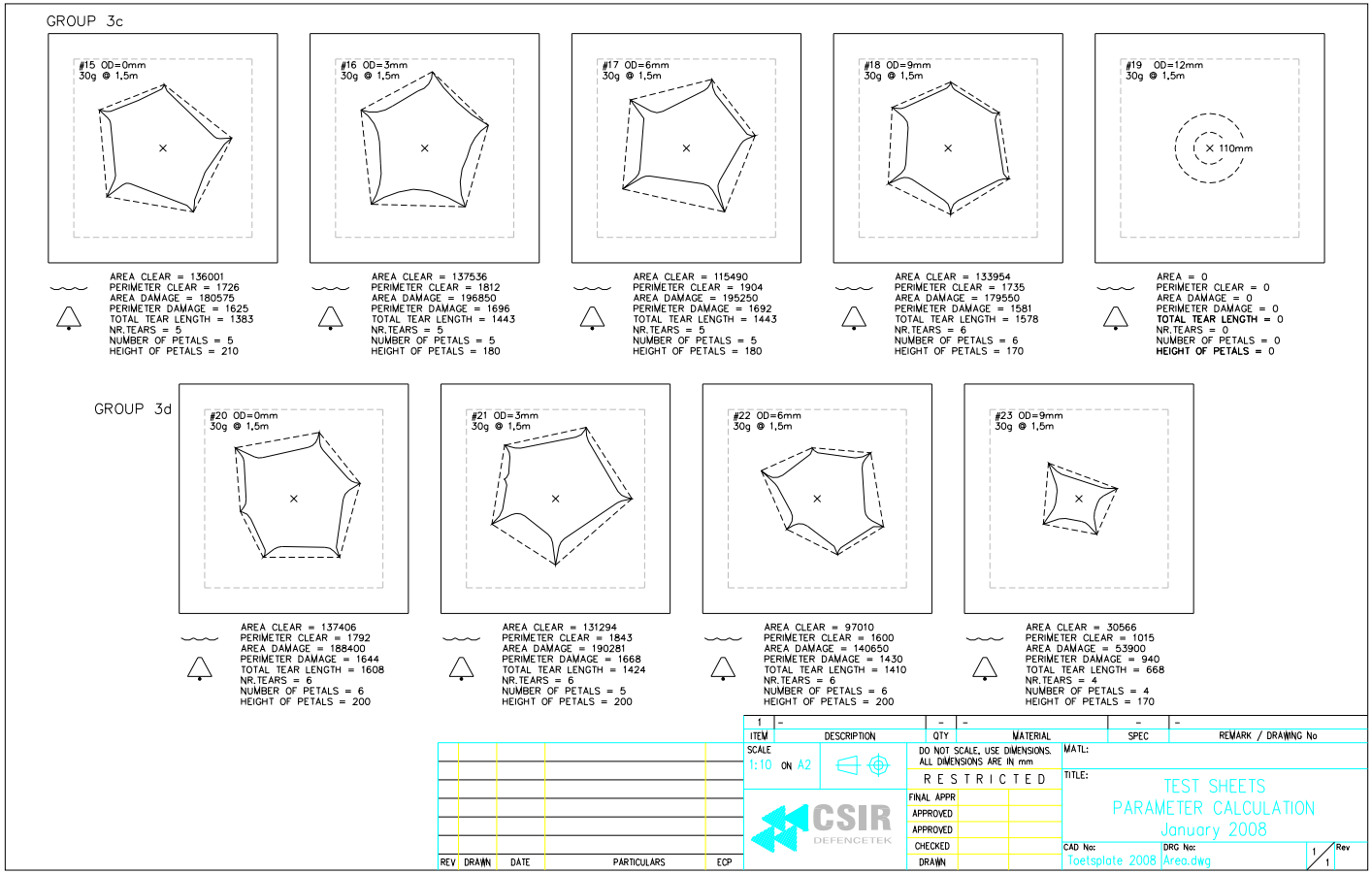
GROUP 3c
#15 OD=0mm
30g @ 1,5m
AREA CLEAR = 136001
PERIMETER CLEAR = 1726
AREA DAMAGE = 180575
PERIMETER DAMAGE = 1625
TOTAL TEAR LENGTH = 1383
NR.TEARS = 5
NUMBER OF PETALS = 5
HEIGHT OF PETALS = 210
#16 OD=3mm
30g @ 1,5m
AREA CLEAR = 137536
PERIMETER CLEAR = 1812
AREA DAMAGE = 196850
PERIMETER DAMAGE = 1696
TOTAL TEAR LENGTH = 1443
NR.TEARS = 5
NUMBER OF PETALS = 5
HEIGHT OF PETALS = 180
#17 OD=6mm
30g @ 1,5m
AREA CLEAR = 115490
PERIMETER CLEAR = 1904
AREA DAMAGE = 195250
PERIMETER DAMAGE = 1692
TOTAL TEAR LENGTH = 1443
NR.TEARS = 5
NUMBER OF PETALS = 5
HEIGHT OF PETALS = 180
#18 OD=9mm
30g @ 1,5m
AREA CLEAR = 133954
PERIMETER CLEAR = 1735
AREA DAMAGE = 179550
PERIMETER DAMAGE = 1581
TOTAL TEAR LENGTH = 1578
NR.TEARS = 6
NUMBER OF PETALS = 6
HEIGHT OF PETALS = 170
#19 OD=12mm
30g @ 1,5m
110mm
AREA = 0
PERIMETER CLEAR = 0
AREA DAMAGE = 0
PERIMETER DAMAGE = 0
TOTAL TEAR LENGTH = 0
NR.TEARS = 0
NUMBER OF PETALS = 0
HEIGHT OF PETALS = 0
GROUP 3d
#20 OD=0mm
30g @ 1,5m
AREA CLEAR = 137406
PERIMETER CLEAR = 1792
AREA DAMAGE = 188400
PERIMETER DAMAGE = 1644
TOTAL TEAR LENGTH = 1608
NR.TEARS = 6
NUMBER OF PETALS = 6
HEIGHT OF PETALS = 200
#21 OD=3mm
30g @ 1,5m
AREA CLEAR = 131294
PERIMETER CLEAR = 1843
AREA DAMAGE = 190281
PERIMETER DAMAGE = 1668
TOTAL TEAR LENGTH = 1424
NR.TEARS = 6
NUMBER OF PETALS = 5
HEIGHT OF PETALS = 200
#22 OD=6mm
30g @ 1,5m
AREA CLEAR = 97010
PERIMETER CLEAR = 1600
AREA DAMAGE = 140650
PERIMETER DAMAGE = 1430
TOTAL TEAR LENGTH = 1410
NR.TEARS = 6
NUMBER OF PETALS = 6
HEIGHT OF PETALS = 200
#23 OD=9mm
30g @ 1,5m
AREA CLEAR = 30566
PERIMETER CLEAR = 1015
AREA DAMAGE = 53900
PERIMETER DAMAGE = 940
TOTAL TEAR LENGTH = 668
NR.TEARS = 4
NUMBER OF PETALS = 4
HEIGHT OF PETALS = 170
ITEM
DESCRIPTION
QTY
MATERIAL
SPEC
REMARK / DRAWING No
SCALE
1:10 ON A2
DO NOT SCALE, USE DIMENSIONS.
ALL DIMENSIONS ARE IN mm
RESTRICTED
MATL:
TITLE:
TEST SHEETS
PARAMETER CALCULATION
January 2008
CSIR
DEFENCETEK
FINAL APPR
APPROVED
APPROVED
CHECKED
DRAWN
REV
DRAWN
DATE
PARTICULARS
ECP
CAD No:
Toetsplate 2008
DRG No:
Area.dwg
Rev

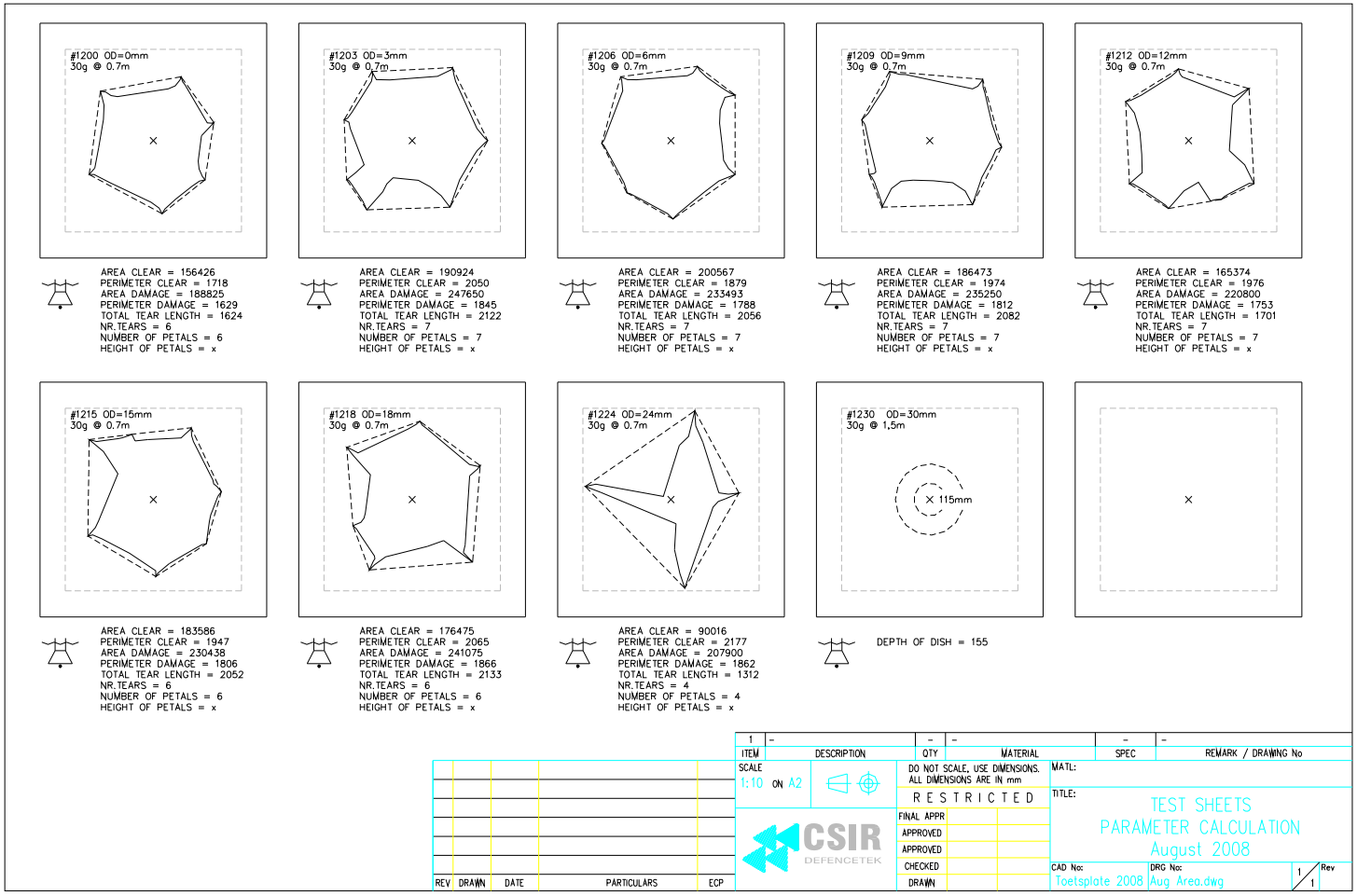
#1200 OD=0mm
30g @ 0.7m
AREA CLEAR = 156426
PERIMETER CLEAR = 1718
AREA DAMAGE = 188825
PERIMETER DAMAGE = 1629
TOTAL TEAR LENGTH = 1624
NR.TEARS = 6
NUMBER OF PETALS = 6
HEIGHT OF PETALS = x
#1203 OD=3mm
30g @ 0.7m
AREA CLEAR = 190924
PERIMETER CLEAR = 2050
AREA DAMAGE = 247650
PERIMETER DAMAGE = 1845
TOTAL TEAR LENGTH = 2122
NR.TEARS = 7
NUMBER OF PETALS = 7
HEIGHT OF PETALS = x
#1206 OD=6mm
30g @ 0.7m
AREA CLEAR = 200567
PERIMETER CLEAR = 1879
AREA DAMAGE = 233493
PERIMETER DAMAGE = 1788
TOTAL TEAR LENGTH = 2056
NR.TEARS = 7
NUMBER OF PETALS = 7
HEIGHT OF PETALS = x
#1209 OD=9mm
30g @ 0.7m
AREA CLEAR = 186473
PERIMETER CLEAR = 1974
AREA DAMAGE = 235250
PERIMETER DAMAGE = 1812
TOTAL TEAR LENGTH = 2082
NR.TEARS = 7
NUMBER OF PETALS = 7
HEIGHT OF PETALS = x
#1212 OD=12mm
30g @ 0.7m
AREA CLEAR = 165374
PERIMETER CLEAR = 1976
AREA DAMAGE = 220800
PERIMETER DAMAGE = 1753
TOTAL TEAR LENGTH = 1701
NR.TEARS = 7
NUMBER OF PETALS = 7
HEIGHT OF PETALS = x
#1215 OD=15mm
30g @ 0.7m
AREA CLEAR = 183586
PERIMETER CLEAR = 1947
AREA DAMAGE = 230438
PERIMETER DAMAGE = 1806
TOTAL TEAR LENGTH = 2052
NR.TEARS = 6
NUMBER OF PETALS = 6
HEIGHT OF PETALS = x
#1218 OD=18mm
30g @ 0.7m
AREA CLEAR = 176475
PERIMETER CLEAR = 2065
AREA DAMAGE = 241075
PERIMETER DAMAGE = 1866
TOTAL TEAR LENGTH = 2133
NR.TEARS = 6
NUMBER OF PETALS = 6
HEIGHT OF PETALS = x
#1224 OD=24mm
30g @ 0.7m
AREA CLEAR = 90016
PERIMETER CLEAR = 2177
AREA DAMAGE = 207900
PERIMETER DAMAGE = 1862
TOTAL TEAR LENGTH = 1312
NR.TEARS = 4
NUMBER OF PETALS = 4
HEIGHT OF PETALS = x
#1230 OD=30mm
30g @ 1,5m
115mm
DEPTH OF DISH = 155
ITEM
DESCRIPTION
QTY
MATERIAL
SPEC
REMARK / DRAWING No
SCALE
1:10 ON A2
DO NOT SCALE, USE DIMENSIONS.
ALL DIMENSIONS ARE IN mm
RESTRICTED
MATL:
TITLE:
TEST SHEETS
PARAMETER CALCULATION
August 2008
FINAL APPR
APPROVED
APPROVED
CHECKED
DRAWN
CSIR
DEFENCETEK
CAD No:
Toetsplate 2008
DRG No:
Aug Area.dwg
Rev
REV
DRAWN
DATE
PARTICULARS
ECP

APPENDIX C : Possible reasons for inconsistent results in Group 2

Following the clear discrepancy of the results of Group 2 versus Group 3 (see Figure 5-8~~Figure 5-8~~~~Figure 5-8~~), it was decided to investigate the reason. A number of possible factors were identified:

a) Thickness of the test panels

b) Tensile strength of the material

c) Age of the explosive

d) Geometry and environmental influences

e) Accuracy of mass measurement

f) Density/Compactness

g) Accuracy of Offset Distance

a) Thickness of the test panels

All test panels were measured individually and found to be of correct thickness (3mm)

Variation in thickness of the test panels did not cause the difference in results.

b) Tensile strength of the material

Four samples each from panel #1 (Group2) and panels #10 and #11 (Group 3) were subjected to tensile tests by Gareth Erfort at BISRU.

No extraordinary difference in Yield strength and Ultimate strength was found, as can be seen in the following three graphs.

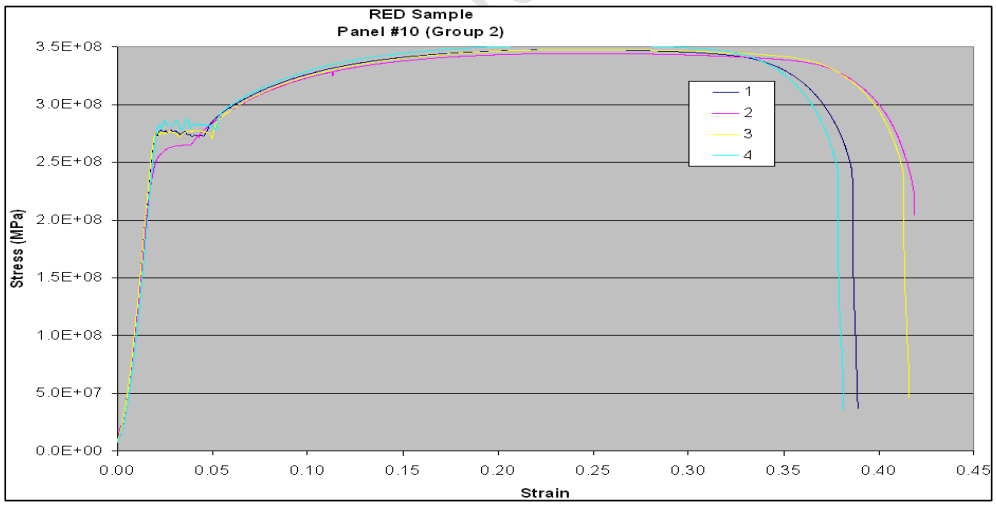

Figure 0-1: Result of tensile test on steel sample from Group 2

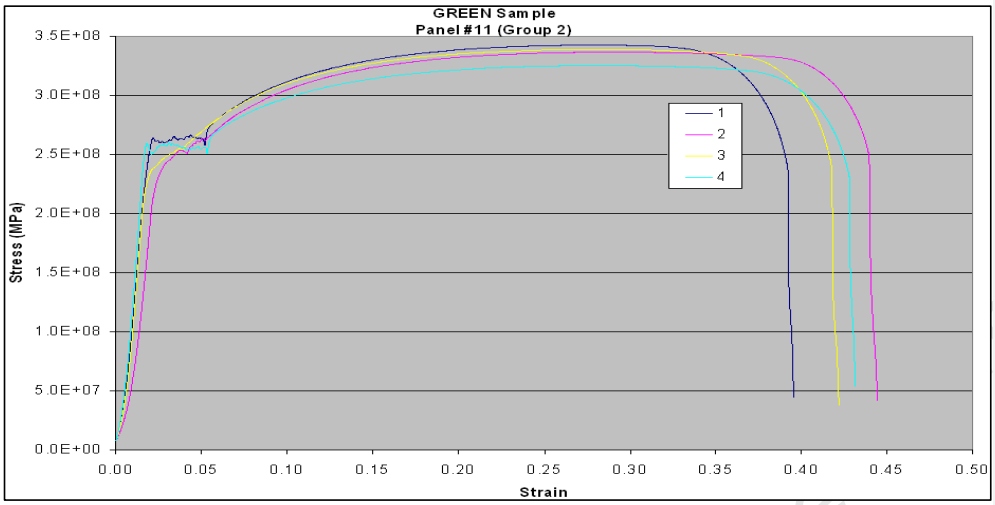

Figure 0-2: Result of tensile test on first sample from Group 3

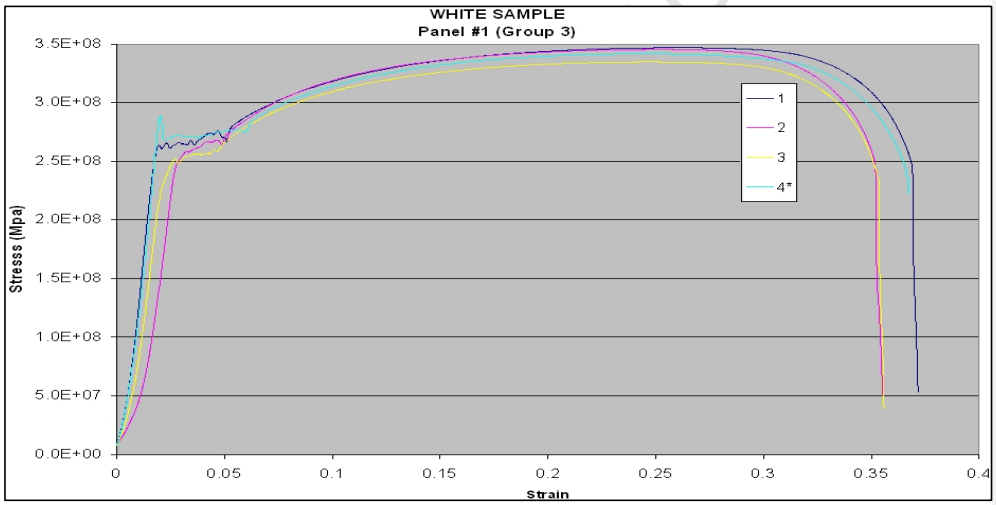

Figure 0-3: Result of tensile test on second sample from Group 3

c) Age of the explosive

Two different batches of PE4 were used for Group 2 tests and Group 3 and Group 4. The possibility that the batch/age of the explosive material could be the cause of the difference in results was investigated.

Five samples of each batch were tested by Dr Chung and Prof Nurick at BISRU. The result indicated that the energy output of both the older and the newer batch were practically indistinguishable.

The test entailed detonation of 3, 4, 5, 6 and 7grams of PE4 from each vintage at an offset distance of 10mm against a circular test panel of diameter 300mm and thickness 1,6mm

Plastic deformation (dishing) occurred with 3g, 4g and 5g charges. The larger charges (6g

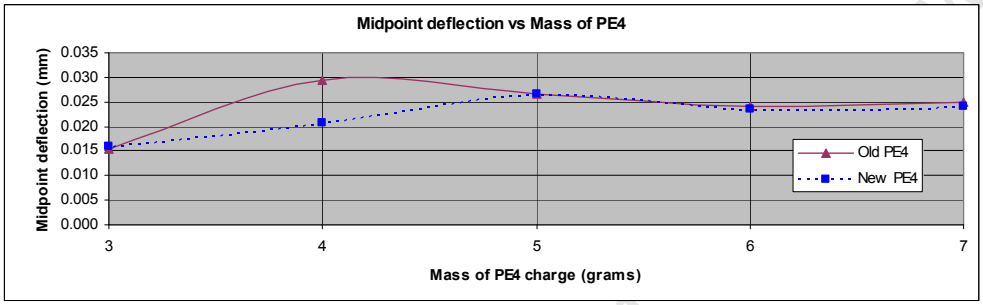

and 7g) all created a hole of diameter of 24mm to 26mm.

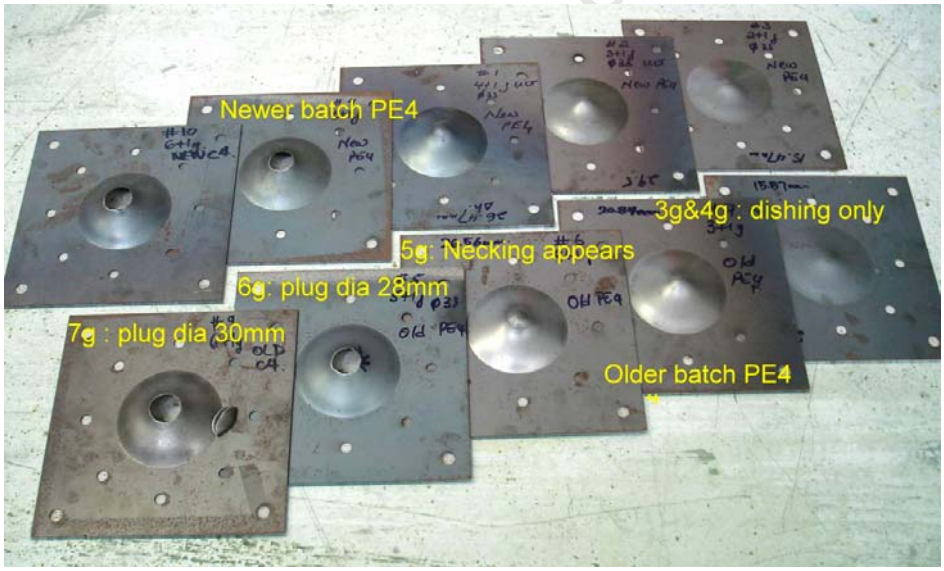

Figure 0-4: Curve fitted to the same data using COD on X-axis

The conclusion was that the difference in age of the explosive material was not the cause of

the difference in the results.

d) Geometry and environmental influences

It is unlikely that tide and water depth had any influence. All testing was done at the same spot in water that is at least twice as deep as the depth of submersion.

The depth of submersion was well controlled by virtue of a clear marker on the suspension sling.

Changes in depth due to high vs low tide amounted to no more than 20% of total water depth.

Reflection from nearby structures is unlikely to have influenced the results. The closest physical structure in the proximity of the detonation was the jetty, which was 7 meters away.

e) Accuracy of mass measurement

Upon investigating the records taken during the Group 1 and Group 2 results, it is unclear what scale was used and whether it was properly calibrated. During Group 3 and Group 4 testing the scale used was known to have been calibrated.

Therefore it is possible that the cause of the discrepancy of test results is due to inaccurate mass measurement during Group 2 testing.

Special attention was paid to mass measurement in Groups 3 and 4.

Figure 0-5: Mass measurement

f) ~~Density/Compactness~~Variation of data on different days

Variation in density/compactness of the charges may have been a greater influence than anticipated. Each charge was prepared individually by hand. Compacting the charge into the container was deemed sufficient by pressing the PE4 into the container using the thumb. No provision was made for ensuring that each charge was compacted to exactly the same density.

The field tests were done on different days. On most occasions a "complete" series of tests were performed – starting at zero offset distance and increasing the OD until breaching of the target ceased. An interesting phenomenon is observed when the test data is presented per test day (instead of all data lumped together). Although the trend is consistent for each of the four test days, the values present a large variation. ~~The graph below~~Figure 0-6 illustrates that the general shape of the graph on different days are all similar, yet displaced in the vertical axis.

This tendency could indicate that one or more characteristics (such as density/compactness or an environmental factor) may be consistent on the day, yet inconsistent from one test day to the other.

Formatted: Font: Bold

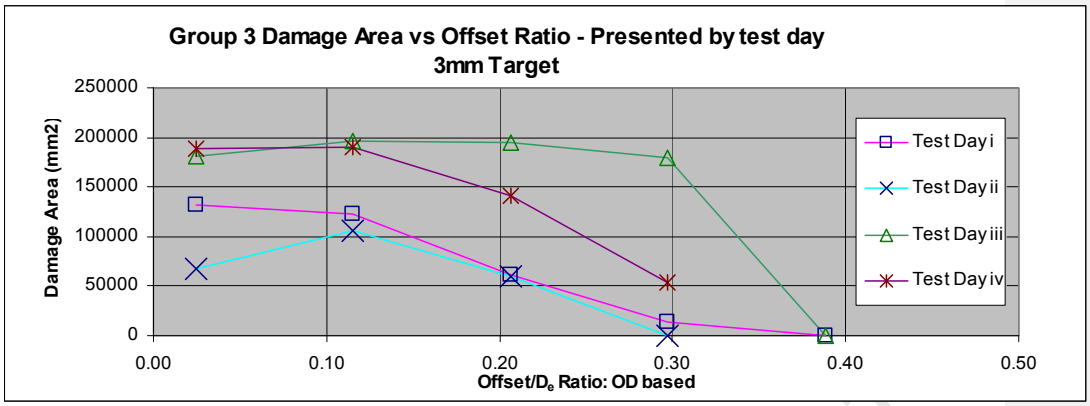

Figure 0-6: Variation of results within Group 3

Field Code Changed
Formatted: Font: Bold
Field Code Changed

~~gg~~) Accuracy of Offset Distance

Inaccurate offset distance may have contributed to the discrepancy in the results.

A vernier was used during Group 2 testing. The inaccuracy in offset distance could be as much as 1mm difference to the intended value (eg due to parallax error), however it is unlikely that it would be as much. During Groups 3 and 4 a machined feeler gage was used to set the offset distance. This ensured that the offset distance was controlled to within fractions of a millimetre.

Figure 0-~~77~~6: ~~Result of tensile test on second sample from Group 3~~Measuring offset distance

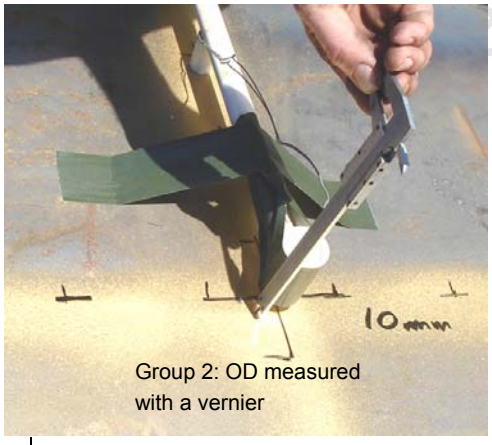

Group 2: OD measured with a vernier

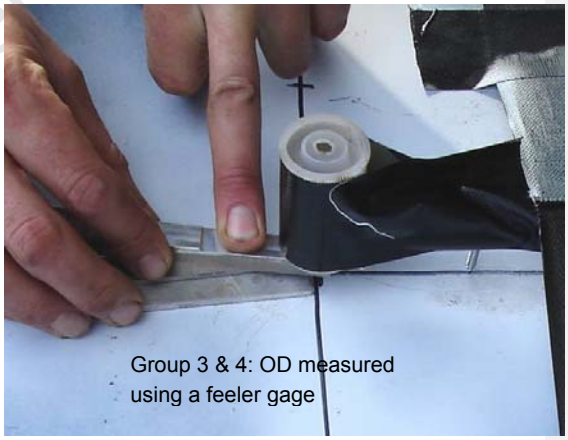

Group 3 & 4: OD measured using a feeler gage

APPENDIX D : Early test results that were disregarded

2005 Original housing with inadequate clamping

The results of this test cannot be used due to deformation and tearing of the edges because of inadequate edge clamping.

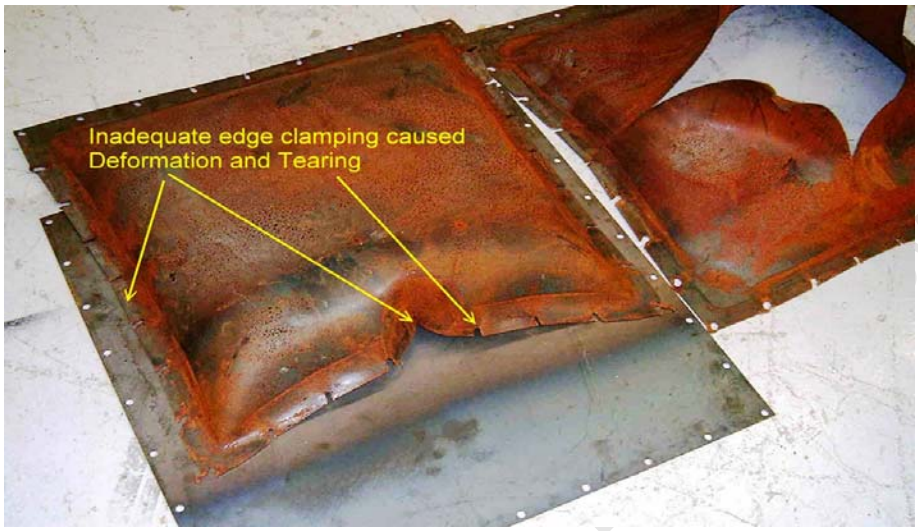

Figure 0-887: Inadequate clamping

2005 Large offset distances

These were the first tests with the reinforced housing. The aim was to determine at which offset distance holing starts to occur.

The result indicated that selected offset distances were too large.

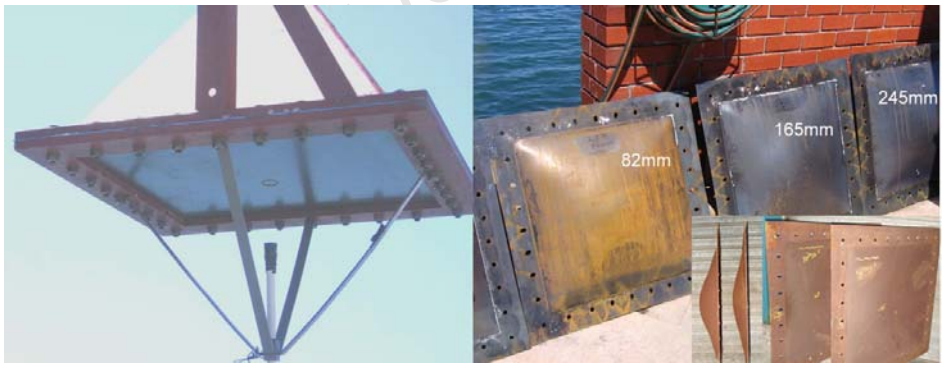

Figure 0-998: Result of Large offset distances

$E_{SH} = 98000(V$

2005 Effect of 30g in air vs in water

This test was done to see the difference in damage by the same charge in air and in water.

This is presented for interest only

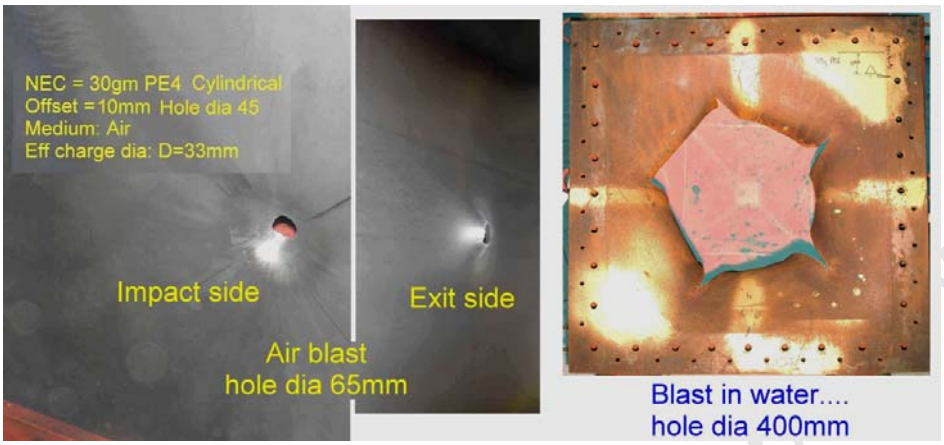

Figure 0-10109: Effect of 30g in air vs water

2005 Large charge at Large offset distance.

This test was an attempt to induce Mode II shearing (see definition in Figure 2-2Figure 2-2Figure 2-2) at the edges of the target panel. A charge of 380g was detonated at 1000mm and at 500mm offset distance. Only dishing was achieved. The creeping of material at the edges was a most likely cause that prevented shearing at the edges.

Figure 0-111110: Large charge at Large offset distance

Following this test, the clamping arrangement was improved by adding a row of retaining studs along the bolt holes. This dramatically reduced edge creeping in all subsequent tests.

No further testing using large charges were conducted.

Outeurs 20 Desember 2008	Ref	TITEL		Jaar	BRON
Arons AB	9	Underwater Explosion Shock Wave Parameters at Large Distances from the	-	1954	The Journal of the Acoustical Society of America, Volume 26, No 3, May. 1954
Balden VH, Langdon GS, Snyman IM, Malan DF, Nurick GN	34	Experimental and Numerical Response of a Scaled Hull Structure Subjected	-	2005	Proceedings of 6th Asia-Pacific conference on Shock & Impact loads on structures, December 2005, Perth, Australia
Batchelor G	6	The Life and Legacy of G.I.Taylor	-	1996	Cambridge University Press, (1996), ISBN 0 521 46121 9
Benjamin T.B.; Ellis A.T.	3	*The collapse of cavitation bubbles and the pressures thereby produced agai*	-	1966	Phil Trans of the Royal Society of London. Series A, Mathematical and Physical Sciences, Vol 260, No 1110, pp 221-240
Bjorno L, Levin P	14	Underwater explosion research using small amounts of chemical explosives	-	1976	ULTRASONICS. NOVEMBER 1976
Brett J, Yiannakopoulos G, Van der Schaaf PJ	29	Time-resolved measurement of the deformation of submerged cylinders subj	-	2000	International Journal of Impact Engineering 24 (2000) 875-890
Brett JM	24	*Numerical Modelling of Shock Wave and Pressure Pulse Generation by Und*	-	1998	DTSO-TR-0677. DSTO Aeronautical and Maritime Research Laboratory, Melbourne, Australia
Brett JM, Buckland M, Turner T, Killoh C and Kiernan P	37	An Experimental Facility for Imaging of Medium Scale Underwater Blast - DS	-	2003	Maritime Platforms Division, Platforms Sciences Laboratory, DSTO-TR-1432
Brett JM, Yiannakopolous G	39	A study of explosive effects in close proximity to a submerged cylinder	-	2007	International Journal of Impact Engineering
Brett JM, Yiannakopoulos G	38	*An experimental study of the detonation of an explosive device in close prox*	-	2005	Proceedings of 6th Asia-Pacific conference on Shock & Impact loads on structures, December 2005, Perth, Australia
Chung M, Brett J	22	DSTO-TR-0575+PR_Assessment of Underwater Blast Effects on Scaled Sul	-	1997	Weapons Systems Division, Aeronautical and Maritime Laboratory, DSTO-TR-0575
Chung M, Kinsey T	23	DSTO-RR-0134_Investigation into the Effects of Underwater Shock Waves c	-	1998	DSTO-RR-0134. DSTO Aeronautical and Maritime Research Laboratory, Melbourne, Australia
Church P, Reynolds M, Huntington W, Townsley R, Sharpe K	35	*Underwater Plate Holing Studies*	-	2003	QuinetiQ, Modelling and Explosives Applications, Fort Halstead, UK
Cole RH	8	Underwater Explosions	-	1948	Princeton University Press, Princeton, New Jersey
Cooper P.W.	21	Explosives Engineering	-	1996	Wiley-VCH, Inc (1996) ISBN 0-471-18636-8
Ezra, AA	46	*Principles and Practice of Explosive Metal Working, Volume 1*	-	1973	Industrial Newspapers Ltd., John Adams House, Adelphi, London (WC2N 6JH).
Finnie TM	47	Explosive forming of circular diaphragms	-	1962	Institution of Sheet Metal Engineering (1962) 391–398.
Hammond L	20	Underwater Shock Wave Characteristics of Cylindrical Charges	-	1995	Aeronautical and Maritime Research Laboratory, Melbourne, Victoria 3001, Australia (1995)
Hammond L.D. (PhD)	28	*The structural response of submerged air-backed plates to underwater explo*	-	2000	Thesis submitted for PhD at Department of Civil Engineering, Monash University
Herrings C	5	Theory of the Pulsations of Gas Bubble Produced by an Underwater Explosi	-	1941	NDRC Report C4SR20-010 () Columbia University, a Division of National Defence Research
Hunter C	12	On the collapse of an empty cavity in water	-	1960	Cambridge Journals Online, Journal of Fluid Mechanics Digital Archive, 8: 241-273 Cambridge University Press
Jiang J, Olson MD	18	Rigid Plastic analysis of underwater blast loaded stiffened plates	-	1995	International Journal of Mechanical Science Vol 37, No 8, pp 843-859
Keil A.H.	1	*The Response of* ***Ships*** *to Underwater Explosions*	-	1961	Department of the Navy, David Taylor Model basin Structural Mechanics Laboratory Research and development report 1576. November 1961. ook in Transactions of Society of Naval Architects & Marine Engineers, 1961; 69: 366-410
Langdon, Chung, Nurick (part II)	33	*Experimental and Numerical studies on the response of quadrangular stiffen*	-	2003	International Journal of Impact Engineering 31 (2005) 85-111
Librescu L, Oh SY, Hohe J	19	Dynamic response of anisotropic sandwich flat panels to underwater and in-a	-	2006	International Journal of Solids and Structures 45 (2006) 3794-3816
Liddiard TP, Forbes JW	48	Shock waves in Fresh Water generated by the detonation of Pentolite spher	-	1983	NSWC TR 82-488, Dahlgren, Virginia
Marsh HW, Mellen RH , Konrad VL	13	Anomalous Absorption of Pressure Waves from Explosions in Sea Water	-	1965	AVCO Marine Electronics Office, New London, Connecticut
Menkes SB, Opat HJ,	15	*Tearing and shear failures in explosively loaded clamped beams*	-	1973	Explosive Mechanics 13, 480-486
Murata K, Takahashi K, Kato Y	25	*Effect of Explosive Composition on the Underwater Shock and Bubble Pulse*	-	1999	NOF CorporationAichi, Japan
Olson M.D., Nurick G.N. & Fagnan J.R.	16	*Deformation and rupture of blast loaded square plates: predictions and expe*	-	1993	Int. Journal of Impact Engineering 31 (1993), 279-291
Penney W	4	The pressure-Time Curve for Underwater Explosions	-	1940	Civil Defense Research Committee~ England
Penny WG, Taylor G I	7	A Discussion on Detonation	-	1950	Proceedings of the Royal Society of London. Series A, Mathematical and Physical Sciences, Vol. 204, No. 1076, (Nov. 22, 1950), pp. 1-33
Rajendran R	44	Reloading effects on plane plates subjected to non-contact underwater explo	-	2008	Journal of Material Processing Technology 206 (2008) 275-281
Rajendran R, Lee JM	45	Blast loaded plates	-	2008	Marine structures (2008), doi:10.1016/j.marstruc.2008.04.001
Rajendran R, Narasimhan K	43	Underwater shock response of circular HSLA steel plates	-	2000	Shock and vibration 7 (2000) 251-262
Rajendran R, Narasimhan K	32	*Damage prediction of clamped circular plates subjected to contact underwa*	-	2001	International Journal of Impact Engineering 25 (2001) 373-386
Rajendran R, Narasimhan K	40	Deformation and tracture behaviour of plate specimens subjected to underwa	-	2005	International Journal of Impact Engineering 32 (2006) 1945-1963
Rajendran R, Narasimhan K	41	*A shock factor based approach for the damage assessment of plane plates su*	-	2006	Journal of strain analysis Vol 41 No 6 (2006)
Rajendran R, Paik JN, Kim BJ	42	Design of warship plates against underwater explosions	-	2006	SAOS (2006) Vol 1 Nr 4 pp 347-356
Ramajeyathilagam K, Vendhan CP, Bhujanga V	27	*Non-linear transient dynamic response of rectangular plates under shock loa*	-	2000	International Journal of Impact Engineering 24 (2000) 999-1015 & Vol 355, No 1724, Violent surface motion. (1997), pp 625-639
Reid WD,	26	*The response of* ***surface ships*** *to underwater explosions*	-	1996	DSTO-GD-0109. DSTO Aeronautical and Maritime Research Laboratory, Melbourne, Australia
Shin YS, Hooker DT	17	Damage response of submerged imperfect cylindrical structures to underwat	-	1996	Computers & Structures (1996) Vol 60 No 5 pp683-693
Slater JE, Rude G, Lee JJ	36	Close-Proximity Blast Loading and Damage of Cylinders	-	2005	Defence Research Department Canada, Suffield, TIA8K6
Snay, HG	10	*Hydrodynamics of Underwater Explosions*	-	1957	Symposium on Naval Hydrodynamics, Publication 515, NationalAcademy of Science, National Research Council, Washington DC, 325-352ea
Swisdak, M M	11	Explosion effects and properties: Part II - Explosion effects in water	-	1978	Report NSWC/WOL/TR-76-116, Naval Surface Weapons Center, Dahgren, Virginia 22448 0 Silver Spring, Maryland 20910
Von Neumann J, Shapiro M ,	2	Underwater explosion of a nuclear bomb	-	1946	Report LA454, US Atomic Energy Commission
Zhang AM, Yao XL, Yu XB	31	The dynamics of three-dimensional underwater explosion bubble	-	2008	Journal of Sound and Vibration 311 (2008) 1196–1212
Zhang YL, Yeo KS, Khoo BC, Wang C.	30	*3D Jet Impact and Toroidal Bubbles*	-	2001	Journal of Computational Physics 166, 336-360 (2001)
Snyman I M	X	*Report on a Theoretical Prediction - Izak Feb 2004 .pdf*	-	2007	Interne dokument
Govender R, Nurick G	X	A comparason of underwater and air-blast explosions, by numerical analysis	-	2007	BISRU MEC524Z (2007),: Structural Impact 38
anon notes		Generic approach to the damage prediction of limpet mines	-		Maritech
Balden VH, Yuen CK, Bonorchis S, Cloete D		¼ Scale Model Hulls: Consolidate Existing and Computational Results	-	2005	Blast Impact and Survivability Research Unit (BISRU), Dept of Mechanical Engineering, University of Cape Town, South Africa
Blake J.R. Hooton MC Robinson PB Tong RP		*Collapsing Cavities, toroidal bubbles and jet impact*	-	1997	Phil. Trans. Royal Soc. London A (1997) 335, 537-550
Brett, J.M. & Reid, W.D.		Modelling of Target response to underwater explosions: the response of an a	-	1995	
Byung-Wook Parka, Sang-Rai Cho		Simple design formulae for predicting the residual damage of unstiffened an	-	2005	International Journal of Impact Engineering 32 (2006) 1721–1736
Chung S, Nurick GN (part I)		*Experimental and Numerical studies on the response of quadrangular stiffen*	-	2005	International Journal of Impact Engineering 31 (2005) 55-83
Clutter JK, Stahl M		Hydrocode simulations of air and water shocks for facility vulnerability asses	-	2004	Journal of Hazardous Materials 106A (2004) 9–24
Deshpande V.S., Heaver A., Fleck N.A.		*An underwater shock simulator*	-	1993	Proc. Royal Soc. A (2006) 462: 1021-1041
Hammond L, Grzebieta R		*Structural response of submerged air-backed plates by experimental and nu*	-	2000	Shock and Vibration 7 (2000) 333-341
Held M		Similarities of shock wave damage in air and water	-	1990	Propellant, Explosives, pyrotechnics 15 (1990) 149-156
Hou W, Zhang H, Lu G, Huang X		Failure modes of circular aluminium sandwich panels with foam core under c	-	2005	Proceedings of 6th Asia-Pacific conference on Shock & Impact loads on structures, December 2005, Perth, Australia
Hung C.F. , Hsu P.Y. , Hwang-Fuu J.J.		*Elastic shock response of an air-backed plate to an underwater explosion*	-	2005	International Journal of Impact Engineering 31, 2005,151
Jacob N, Chung S, Nurick GN, Bonorhis D, Desai SA, Tait D		*Scaling aspects of quadrangular plates subjected to localised blast loads - e*	-	2005	Thesis submitted for PhD at Department of Civil Engineering, Monash University
Jones RA, Shin YS		Experimental investigation of the response and failure mechanisms of circula	-		Proceedings of 61st Shock and Vibration symposium, Pasadena, CA, USA. 1990, pp 163-178
Kalavalapally R, Penmetsa R, Grandhi R.		Configuration design of a lightweight torpedo subjected to an underwater exp	-	2008	International Journal of Impact Engineering (2008), doi: 10.1016/j.ijimpeng.2008.01.016
Kato Y, Murata K, Takahashi K		Resonse to UW explosion [slegs voorblad]	-	2005	
Kato Y, Murata K,Takahashi K.		Response of model structure to the proximity of an underwater explosion	-	2005	WIT Trans on Modelling and Simulation, Vol 40 (2005), WIT Press, ISSN 1743-355X
Kira A, Fujita M, Itoh S		Underwater explosion of spherical explosives	-	1999	Journal of Materials Processing Technology, Volume 85, Issues 1-3, 1 January 1999, Pages 64-68
Klasebo E, Khoob, Hung		Dynamics of an oscillating bubble near a floating structure	-	2005	Journal of Fluids and Structures 21 (2005) 395–412
Langdon GS, Balden VH, Nurick GN		Finite Element Modelling of a ½ Scale Hull Section Subjected to Underwater	-	2005	BISRU
Liang Cho-Chung, Tai Yuh-Shiou		*Shock responses of a surface ship subjected to noncontact underwater explo*	-	2006	DTSO-TR-0677. DSTO Aeronautical and Maritime Research Laboratory, Melbourne, Australia --- Ocean Engineering, Vol 33, Issue 5-6 (Apr 2006) pp 748-772
Librescu S, Oh SY, Hohe J		Dynamic response of anisotropic sandwich flat panels to underwater and in-a	-	2006	International Journal of Solids and Structures 43 (2006) 3794–3816
MacLean M, Steyn D		Dimensional Analysis - Some basics	-	2004	Science One Program, UBC
Masimo		Ship Survivability	-	2006	
McCoy RW, Sun CT		Fluid-structure interaction analysis of a thick section composite cylinder subje	-	1997	Composite Structures Vol. 37, No. 1, pp. 45-55, 1997, Elsevier Science Ltd.
Murata K, Takahashi K, Kato Y		Precise measurements of underwater explosion phenomena by pressure sen	-	1999	
Nourgaliev RR , Sushchikh, Dinh, Theofanous		Shock wave refraction patterns at interfaces - Nourgalief	-	2005	International Journal of Multiphase Flow 31 (2005) 969–995
Nurick, G.N & Martin, J.B		*Deformation of thin plates subjected to impulsive loading - a review Part 2: e*	-		Int. Journal of Impact Engineering 8 (1989), 170-186
O'Daniel J, Krauthammer T, Koudela K, Strait L		An UNDEX response validation methodology	-	2002	International Journal of Impact Engineering 27 (2002) 919–937
Olson MD, Nurick GN, Fagnan JR		Deformation and rupture of blast loaded square plates—predictions and exp	-	1993	Int.J Impact Eng 1993;13:279–91.
Peng LI, Gengguang XU, Lin Z		Study of the Underwater Explosion Energy Output of Aluminized Explosive	-	2000?	State Key Laboratory of Explosion Science and Technology, Beijing Institute of Technology, Beijing 100081, China (2000?)
Poche		Underwater Shock-Wave Pressures from Small Detonators	-	1971	Naval Research Laboratory, Underwater Sound Reference Division, Orlando, Florida 32806
Radovitzky		*Compressibility effects in the interaction of shock wave and plates*	-		
Rajendran R, Narasimhan K		Linear elastic shock response of plane plates subjected to underwater explo	-	2001	International Journal of Impact Engineering 25 (2001) 493-506
Rajendran R, Paik JK, Lee JM		Of Underwater Explosion Experiments on Plane Plates	-	2007	Experimental Techniques, Ja-Feb 2007, pp 18-24
Rajendran, R.		Numerical simulation of response of plane plates subjected to uniform prima	-	2008	Materials and Design (2008), doi: 10.1016/j.matdes.2008.06.054
Ramajeyathilagam,Vendhan, Bhujanga		Experimental and numerical investigations on deformation of cylindrical shell	-	2001	Shock and Vibration 8 (2001) 253–270, ISSN 1070-9622
Roux A		Experimental Response of an optical - A Roux 2007	-	2007	MSc
Rudrapatna NS, Vaziri R, Olson MD		Deformation and failure of blast loaded SQUARE plates"	-		Int J Impact Eng 1999; 22: 449-467
Rudrapatna NS, Vaziri R, Olson MD		Deformation and failure of blast loaded **stiffened** plates"	-		Int J Impact Eng 2000; 24: 457-474
Slater J.E. & Rude G.		Experimental study of fluid-structure interaction during close-proximity under	-		Proceedings of ASME Pressure vessels and piping conference, Structures under extreme loading conditions PVP vol 325, Montreal, Quebec, Canada 1996
Swift, E. & Decius, J.C.		*Measurements of Bubble Pulse Phenomena, III*	-	1950	Underwater explosion research: A compendium of British and American reports, Vol 2, Office of Naval Research, Department of the Navy, Washington DC, 553-599
Swisdak, M M		Explosion effects and Properties - Part **1** -Explosion effects in **air**	-	1975	Report NSWC/WOL/TR-75-116, Naval Surface Weapons Center, Dahgren, Virginia 22448 0 Silver Spring, Maryland 20910
Taylor GI		Compendium of Scientific papers of GI Taylor	-	1963	Scientific papers of GI Taylor Vol III, No 4, Cambridge University Press, Cambridge , MA, 1963
Taylor GI		The Formation of a Blast Wave by a Very Intense Explosion. I. Theoretical D	-	1950	Proceedings of the Royal Society of London. Series A, Mathematical and Physical Sciences, Vol. 201, No. 1065, (Mar. 22, 1950), pp. 159-174
Taylor GI		The Formation of a Blast Wave by a Very Intense Explosion. II. The Atomic E	-	1950	Proceedings of the Royal Society of London. Series A, Mathematical and Physical Sciences, Vol. 201, No. 1065, (Mar. 22, 1950), pp. 175-186
Taylor GI		The Air Wave Surrounding an Expanding Sphere	-	1946	Proceedings of the Royal Society of London. Series A, Mathematical and Physical Sciences, Vol. 186, No. 1006, (Sep. 24, 1946), pp. 273-292
Taylor GI		The Mechanics of Large Bubbles Rising through Extended Liquids and throu	-	1950	Proceedings of the Royal Society of London. Series A, Mathematical and Physical Sciences, Vol. 200, No. 1062, (Feb. 7, 1950), pp. 375-390
Taylor GI		The pressure and impulse of submarine explosion waves on plates	-	1950	Compendium Underwater Explosion Res ONR 1950; 1:1155-74
Thomas, B.M. , Nurick, G.N.		The effect of boundary conditions on thin plates subjected to impulsive loads	-	1995	Dept of Mechanical Engineering, UCT, CTN
Venter FA		*Prediction of behaviour of structures subjected to underwater explosions anc*	-	2005	In-house report
Wadley H, Dharmasena K, Chen Y, Dudt P, Knight D, Charette R, Kiddy K		Compressive response of multilayered pyramidal lattices during underwater	-	2008	International Journal of Impact Engineering 35 (2008) 1102–1114
Wang		*Deformation and rupture of thin rectangular plates subjected to underwater s*	-	2004	Journal of Computational Physics 194 (2004) 451–480
Wang		Strong Interaction Between a Buoyancy Bubble and a free surface	-	2004	
Wang C, Khoo B.C		An indirect boundary element method for three-dimensional explosion bubble	-	2004	Journal of Computational Physics 194 (2004) 451–480
Wartlaw			-		
Wilkinson C. R. Anderson J. G.		DSTO-TN-0526 An Introduction to Detonation and Blast for the Non-Speciali	-	2003	Weapons Systems Division Systems Sciences Laboratory
Zong Z		A hydroplastic analysis of a free–free beam floating on water subjected to an	-	2005	Journal of Fluids and Structures 20 (2005) 359–372
Zyskowski, Sochet, Mavrot, Bailly, Renard		Study of the explosion process in a small scale experiment	-	2006	Int Journal of Impact Engineering 32 (2006) 1721-1736
McCoy RW, Sun CT		Fluid-structure interaction analysis of a thicksection composite cylinder subje	-	1997	Composite Structures (1997) Vol. 37, No. 1, pp. 45-55,
Mouritz		The effect of underwater explosion shock loading on the flexural properties c	-	?	?